HYDROMETRIC AND GEOCHEMICAL EVIDENCE OF STREAMFLOW SOURCES IN THE UPPER DRY CREEK EXPERIMENTAL WATERSHED, SOUTHWESTERN IDAHO

by

Melissa K. Yenko

A thesis

submitted in partial fulfillment

of the requirements for the degree of

Master of Science in Geology

Boise State University

December, 2003

The thesis presented by Melissa K. Yenko entitled Hydrometric and Geochemical Evidence of Streamflow Sources in the Upper Dry Creek Experimental Watershed, Southwestern Idaho is hereby approved:

Advisor

Committee Member

Committee Member

Graduate Dean

ACKNOWLEDGEMENTS

Without the technical, financial, and emotional support of many individuals and organizations, this project would not have been possible. For technical guidance, I would like to thank Dr. Spencer Wood, Dr. Shiva Achet, Dr. David Chandler, Dr. Richard P. Hooper, and most importantly Dr. James McNamara, who played an influential role in this project from its inception to the production of this thesis.

Numerous individuals provided assistance with data collection and analysis for this project. People who contributed to the field effort in project include Dr. McNamara, Dr. Chandler, Patty Jones, Sara Smith, John Wirt, Heather Best, Laura Grant, and Eric Rothwell. Data analysis assistance was provided by the Utah State University Analytic Laboratory, Dr. Hooper, and Ed Reboulet. Ed Reboulet's assistance with data analysis was indispensable and very much appreciated.

Funding for this project was provided by several sources; the National Aeronautic and Space Administration (Grant Number NAG5-7537), the Agriculture Research Service (Grant Number 2001-35102-11031), and a Boise State University – Will Burnham Geosciences Research Grant.

Last but not least, I would like to thank my family for their constant support and inspiration. I could not have done this without all of you. To my parents and grandparents, thank you for always believing in me and teaching me to finish what I start. To Scott, Benny, and Kanawa Yenko, thank you for your patience, support,

companionship, field instrument design and construction, physical labor, and field assistance during what seemed like an endless process to complete this project. You are my inspiration.

ABSTRACT

In order to investigate the sources contributing to streamflow in the Upper Dry Creek Experimental Watershed (UDCEW), hydrometric and geochemical data were collected in the 2000/2001 cold-season in a highly instrumented 0.02 km^2 headwater catchment within the semi-arid Dry Creek Watershed (DCW). Data collected included precipitation, snowmelt, streamflow, meteorological data, and basin water samples. This data was used to evaluate the concentration-discharge (C-Q) relationships, hydrograph separation, and to complete End-Member Mixing Analysis (EMMA) for the two major snowmelt events occurring in the 2000/2001 cold-season.

The flow sources considered in this study include precipitation, regional groundwater, and soilwaters. The hydrometric and geochemical data provided evidence that all water contributing to streamflow in UDCEW can be accounted for by cold-season precipitation occurring in the basin and that there is no contribution to streamflow by a regional groundwater source. The EMMA analysis showed that three end-members including snowmelt, and two soilwater sources, contribute to cold-season streamflow. The sampled soilwater end-members did not explain the observed streamwater chemistry, so a hypothesized soilwater end-member was suggested. Both EMMA and the two-component hydrograph separation indicate that the major flow source area contributing to streamflow is direct interception of snowmelt.

TABLE OF CONTENTS

LIST OF FIGURES

LIST OF TABLES

1. INTRODUCTION

Many hydrologic studies have been conducted to try and answer the question of how water moves through small catchments. There has been considerable progress in hydrologic science to explain the physical mechanisms controlling streamflow generation and stream water chemistry (Bishop, Grip, and O'Neill, 1990; Mulholland, Wilson, and Jardine, 1990; Puigdefabregas, del Barrio, Boer, Gutierrez, and Sole, 1998; Brown, McDonnell, Burns, and Kendall, 1999; Kendal, Shanley, and McDonnell, 1999; and Burns et al., 2001). In many cases, the flow pathways that occur during precipitation events, rain or snowmelt, determine the resulting surface water chemistry during and after the event (Bonell, 1993). The physical mechanisms that transport water from the hillslope to the stream channel are a function of many physical properties of the landscape such as the antecedent moisture conditions, event timing and magnitude, soil depth, topography, and underlying bedrock topography (Elsenbeer, West, and Bonnell, 1994, McDonnell, 1990; Ross, Bartlett, Magdoff, and Walsh, 1994; and Brammer and McDonnell, 1996). Many of these studies were completed in humid temperate environments, where antecedent moisture conditions are high, moisture deficits are low, precipitation exceeds evapotranspiration, and a wide variety of hydrologic processes occur such as infiltration excess, saturation overland flow, saturated and unsaturated subsurface flow, return flow, groundwater flow to transport water downhill.

The physical mechanisms that govern the delivery of precipitation and soilwater during dry conditions are not well documented. The hydrologic behavior in semi-arid environments is difficult to quantify due to low antecedent moisture condition, highly variable soil moisture conditions, evapotranspiration exceeds precipitation for much of the year, and the lack of saturated subsurface layers (Puigdefabregas et al., 1998). Water delivery in these regions occurs most often by unsaturated subsurface flow and occasionally by overland flow (McCord and Stephens, 1987).

Streamflow or flow sources are defined as the precipitation and/or hillslope areas contributing to streamflow. Flow sources may include precipitation, groundwater, soilwater, and overland flow. Identification of flow sources and runoff generation mechanisms will provide a more comprehensive understanding of the hydrologic processes occurring in semi-arid environments.

1.1 Project Description

The goal of this study is to quantify the streamflow sources in the Upper Dry Creek Experimental Watershed (UDCEW) in the cold season using hydrometric and geochemical data. In order to meet the study's goal the following hypotheses were tested in the UDCEW: 1) there is no regional groundwater input into the UDCEW system during the cold-season flow period; 2) all discharge within the UDCEW originates from the cold-season precipitation (rain and snowmelt events) and soilwaters originating within the basin. These hypotheses were addressed by completing a hydrologic characterization of the UDCEW using hydrometric and geochemical data. Both hydrometric and geochemical data were used to complete concentration-discharge (C-Q) analysis, hydrograph separation, and end-member mixing analysis (EMMA) for the UDCEW. The relationship between concentration and discharge was used to make inferences about the mixing patterns of the waters contributing to cold-season streamflow. Hydrograph separation was used to identify the proportion of event and pre-event water contributing to cold-season streamflow. The EMMA analysis was completed as an attempt to explain the streamwater as a mixture of snowmelt and soilwater components.

1.2 Scientific Background

1.2.1 Semi-Arid Watershed Processes

The hydrologic processes generating streamflow in semi-arid environments are not fully understood. Investigations of hydrologic processes in semi-arid regions have been found to be challenging due to highly variable moisture conditions and most streams are ephemeral in nature. Hydrologic studies in semi-arid watersheds have shown that the precipitation duration and intensity, combined with the infiltration capacity of the soil, controls the runoff generation and flow (Blackburn, 1975; Schumm and Lusby, 1963; Osborn and Lane, 1969; Lane, Diskin, and Renard, 1971; and Branson, Gifford, Renard, and Hadley, 1981). Research at a semi-arid research watershed in New Mexico showed that soil moisture conditions control the generation of both matric and macropore flow (Newman, Campbell, and Wilcox, 1998). Wilcox, Newman, Brandes, Davenport, and Reid (1997) found that lateral subsurface flow is a major runoff mechanism in semi-arid watersheds particularly during snowmelt events. These lateral subsurface flows can occur under either unsaturated or saturated conditions if the vertical flux of water into the soil exceeds the hydraulic conductivity near the wetting front. Studies in the Reynolds Creek experimental watershed (RCEW) in Southwestern Idaho, demonstrated that the spatial distribution of snowcover, the presence of frozen soil, and the extent of frozen soil control the cold-season runoff generation mechanisms operating in the basin (Johnson and McArthur, 1973; Flerchinger, Cooley, and Ralston, 1992; and Seyfried and Wilcox, 1995). The spatial organization of flow paths, the dynamic nature of near stream saturated areas in response to drift snowmelt, and the controls on stream groundwater linkages at the catchment scale were evaluated at RCEW. The primary run off generation mechanism in RCEW was identified to be variable source areas within the fractured basalt bedrock zone as evidenced by the development of multiple saturated zones during snowmelt with different isotopic signatures (Unnikrishna, McDonnell, Tarboton, Kendall and Flerchinger, unpublished).

1.2.2 Concentration-Discharge Relationships

Dissolved solute concentrations in streamflow vary as streamflow rises and falls through an event, and are influenced by the source of water that is contributing to streamflow (precipitation, soil water, and deep groundwater for example). Numerous studies have observed hysteresis in the concentration-discharge (C-Q) relationships, where solute concentrations at given discharges on the rising and falling limbs of an event hydrograph are different, indicating that different sources become important during different phases of the hydrograph (Evans and Davies, 1998; Oxley, 1974; Johnson and

East, 1982; Walling and Webb, 1986; Miller and Drever, 1977; Swistock, DeWalle, and Sharpe, 1989; Hooper and Christopherson., 1992; Shanley and Peters, 1993; Scanlon, Raffensperger, and Hornberger, 2001, and Hornberger, Scanlon, and Raffensperger, 2001).

Hydrochemical response in small forested catchments have been analyzed with respect to (C-Q) plots to infer how flow components such as precipitation, including rain and snowmelt, soil water, and groundwater, mix to produce streamflow (Chanat, Rice, and Hornberger, 2002). Construction of C-Q plots requires stream discharge (Q) data and stream chemistry at the catchment outlet where the concentration is typically plotted against the $\log_{10}$ Q data. These plots can range from simple to complex shapes and patterns have been used to describe runoff processes and pathways (Evans and Davies, 1998). The hysteresis loop rotational pattern can be described as either clockwise or counter-clockwise. A clockwise hysteresis loop is defined by higher solute concentrations on the rising limb than on the falling limb of the hydrograph. Clockwise hysteresis rotation is produced when a concentrate solute source contributes to streamflow at the onset of an event and becomes more dilute as the event progresses. In a counter-clockwise hysteresis loop the solute concentrations are higher on the falling limb than on the rising limb of the hydrograph (Walling and Webb, 1986). Counter-clockwise hysteresis rotation is produced when the streamwater becomes more concentrated with respect to a solute as an event progresses, i.e. activation of a more concentrate source later in the event. Figure 1.1 provides schematics of the clockwise and the counter-clockwise hysteresis loop patterns. Evans and Davies, 1998 found that three and two component mixing models are capable of producing a wide range of C-Q looping patterns using fixed concentrations. EMMA can also be used to identify and analyze mixing and C-Q relationships (Hooper, Christopherson, and Peters, 1990; Scanlon et al., 2001; and Brown et al., 1999).

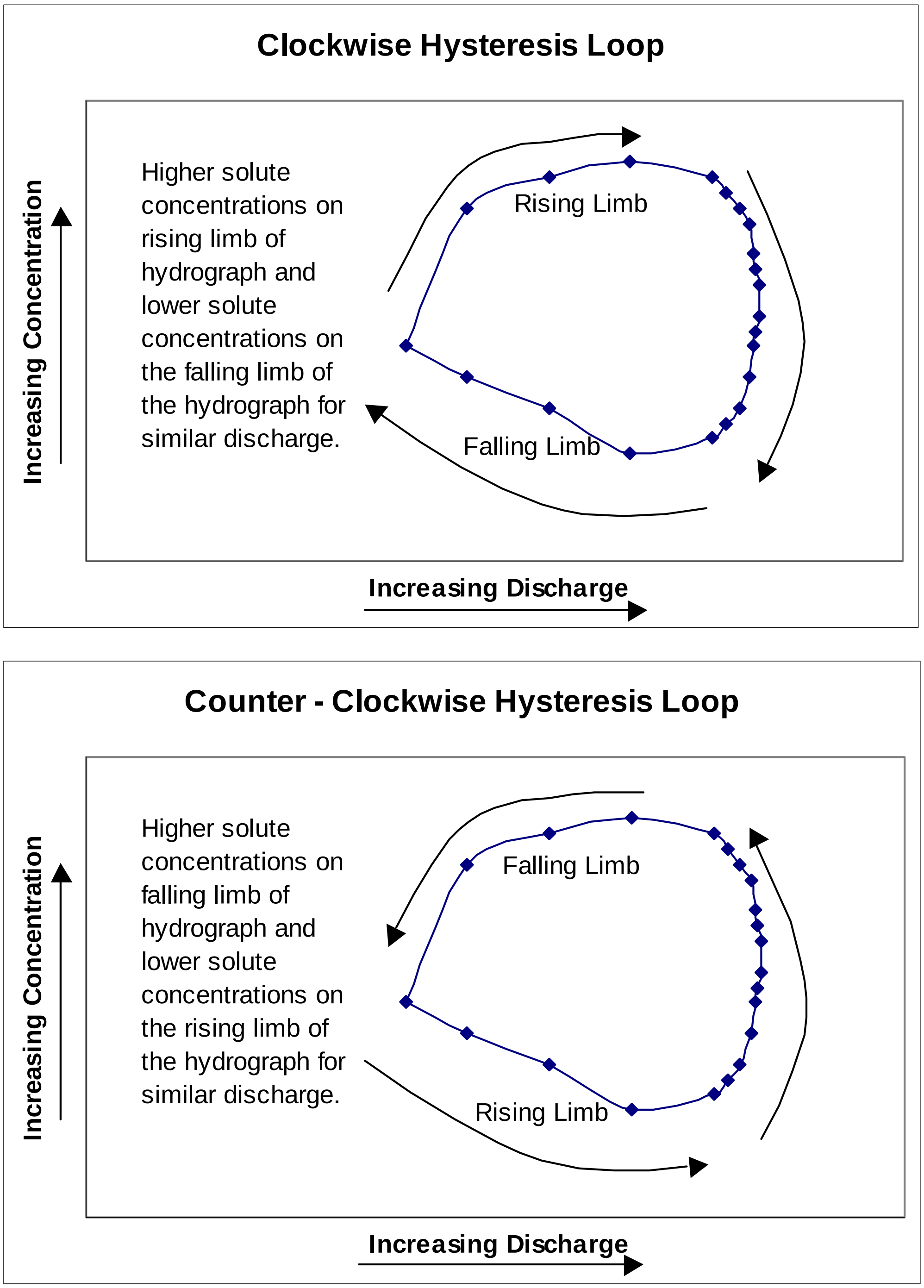

Figure 1.1. Examples of clockwise and counter-clockwise hysteresis loop diagrams.

1.2.3 Hydrograph Separation

Hydrograph separations based on chemical mass balance equations are commonly used to determine the relative contributions of event and pre-event water as sources of streamflow during runoff events (Hooper and Shoemaker, 1986; McNamara, Kane, and Hinzman, 1997; Hinton, Schiff, and English, 1994; Pinder and Jones, 1969; Pilgrim, Huff, and Steele, 1979; Sklash and Farvolden, 1979; and Wels, Cornett, and LaZerte, 1991). Event water is the water input into a catchment during a precipitation event. Pre-event water is defined as the water stored in the catchment prior to a precipitation event. Equation 1.1 represents the simple mixing equation used to complete a two- component hydrograph separation:

$$C_oQ_o + C_nQ_n = C_tQ_t \tag{1.1}$$

where C represents the concentration of each solution, Q is the discharge, and the subscripts o, n, and t refer to the old (or pre-event) water, the new (or event water) and the total water, respectively (Pinder and Jones, 1969). This technique requires that the chemical tracers used be conservative or unchanging through an event. Many case studies have found that old or pre-event water generally dominated the event hydrograph (Buttle and Sami, 1992; Dincer, Payne, and Florkowski, 1970; McNamara et al., 1997, McDonnell, Owens, and Stewart, 1991; and Peters, Buttle, Taylor, and LaZerte, 1995). The dominance of pre-event water in these studies raised the question of how does groundwater or soilwater, which travels at low velocities, contribute water rapidly and continuously to streams during storm events. Hydrograph separation techniques tell us nothing about how the water reaches the stream, only where the water comes from (Sklash, 1990). To obtain a complete understanding of the hydrologic pathways in a watershed, source area studies must be combined with hillslope runoff generation mechanism studies (Scanlon, Raffensperger, and Hornberger, 2000).

1.2.4 End-Member Mixing Analysis

Variations in stream water chemistry have been explained as dynamic mixtures of sources such as precipitation and groundwater, event and pre-event water, direct inception, or soil-water solutions (Sklash and Farvolden, 1979; Pilgrim et al., 1979; Dewalle, Swistock, and Sharpe, 1988; and Christopherson, Neal, Hooper, Vogt, and Andersen, 1990; Hooper et al., 1990; and Hooper and Christophersen, 1992). The end-member mixing analysis (EMMA) approach can be used to explain stream water as a mixture of soil water end-members, which bound the observed stream water chemistry. EMMA was developed as a method to include soil water quality in hydrochemical models. This approach is based on observations that the chemical variations of stream water can be linked to differences in soil water chemistry across soil horizons (Christopherson, Seip, and Wright, 1982; and Neal, Smith, Walls, and Dunn, 1986). The changing proportions of each end-member contribution to streamflow explain episodic chemical variations in the stream water (Hooper and Christophersen, 1992). Studies at Panola Mountain Research Watershed in Georgia, USA, have shown that a mixture of three soil water solutions can explain variations in stream water chemistry (Hooper, et al., 1990). EMMA was developed to use a least-square method to determine the contribution of each end-member to the stream using stream water chemistry. This method allows the stream water chemistry to not only provide information on proportion of end-members, but also information on hydrological pathways (Christopherson et al., 1990).

Christopherson and Hooper (1992) explored combining elements of EMMA and factor analysis for analyzing chemistry observations. Multivariate analysis, including Principal Component Analysis (PCA) and its application to the earth science, was examined by Joreskog, Klovan, and Reyment, (1976). PCA is used to reduce the dimensionality of data (Christopherson and Hooper, 1992).

2. STUDY SITE

2.1 Geographic Description

The Dry Creek Watershed (DCW) is located in southwestern Idaho, approximately 16 km north of Boise, Idaho, and falling within both Ada and Boise counties (Figure 2.1). The foothills that the DCW is located in are called the Boise Front.

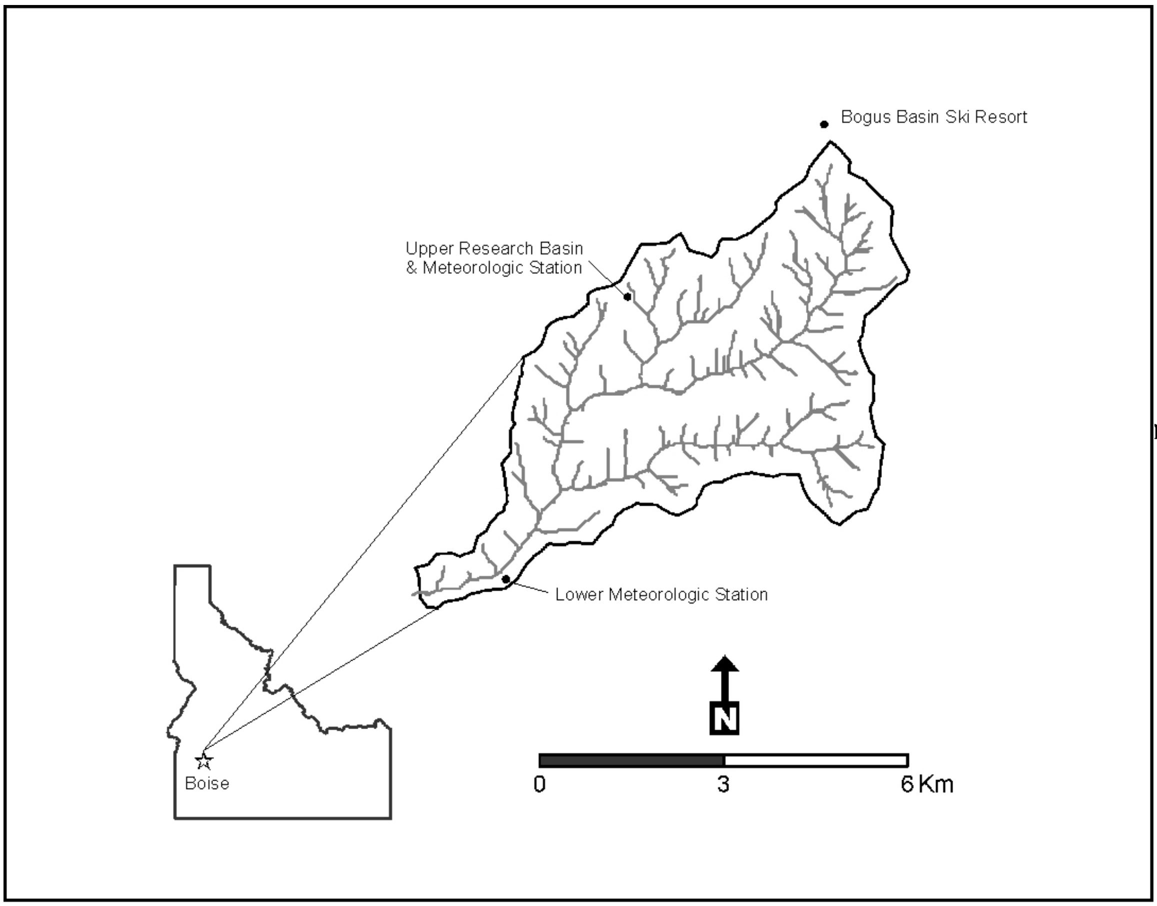

Figure 2.1. Dry Creek Watershed and regional location map.

The headwaters of the Dry Creek originate at approximately the 2,100 m elevation in the upper granitic region of the Boise Front in the Boise National Forest and extend south-southwest to its confluence with the Boise River. The DCW is delineated from the 1,000 m elevation where Dry Creek crosses Bogus Basin Road trending north-northeastward, encompassing an area of 28 km^2 including the upper 11 km of Dry Creek. Dry Creek is a perennial stream within the DCW with one perennial tributary, Shingle Creek, and numerous unnamed intermittent tributaries.

2.2.2 Climate

The DCW has extremely variable climatic conditions resulting from the considerable variation in elevation, aspect, and configuration of the lands. The climate of southwestern Idaho is typified by winters that are moderately-cold to cold with abundant precipitation falling predominantly snow; springs that are rainy and cool changing to sunny and warm; summers are hot with occasional thunderstorms; autumns are clear and warm changing to cold and moist (USDA, 1974).

The climate system in this region is the result of two opposing weather systems: the Aleutian Low and the Pacific High. The Aleutian Low is a low-pressure system centered near the Aleutian Islands, Alaska. This low-pressure system is a moisture-laden air mass that reaches its southern-most position in the winter months, bringing generally cool moist air into the southwestern Idaho. As summer approaches, the Pacific High begins to dominate the weather in southwestern Idaho. The Pacific High is a high-pressure system dry air mass centered in the Pacific Ocean (USDA, 1974).

There are three meteorological stations located in the DCW region, one at the Lower Dry Creek Research Site, the second at DCEW and the third is located just outside the watershed boundary at the Bogus Basin Ski Resort. The stations represent the climate in the basin's lower elevation (1,100m), intermediate elevation (1,650 m) and upper elevation (1,930 m). The period of record for each station is as follows:

- Lower Dry Creek Research Site – 1998 - Present
- Upper Dry Creek Experimental Watershed – 1998 – Present
- Bogus Basin Snotel Site – 1999 – Present

Average monthly temperatures are greatest in July and lowest in January and the wettest months are December through February. The average annual precipitation at the Lower Dry Creek Research Site, Upper Dry Creek Experimental Watershed, and Bogus Basin are 37.25 cm, 57 cm, and 100 cm, respectively.

2.2.3 Geology

The geology of the DCW is dominated by the Idaho Batholith, a Cretaceous age granitic intrusion ranging in age from 75 to 85 million years. The Idaho Batholith is one of the large batholiths associated with the Mesozoic subduction zone located along the western margin of North America. It extends over 485 km in a north-south direction and is 130 km wide. The batholith is divided into two lobes, the northern Bitterroot Lobe and the southern Atlanta Lobe. DCW is located in the Atlanta Lobe of the Idaho Batholith. The Atlanta Lobe is approximately 275 km long and 130 km wide and consists of six main rock types: tonalite, horneblend-biotite granodiorite, porphyritic granodiorite, biotite granodiroite, muscovite-biotite granite and leucocratic granite (Johnson, Lewis, Bennett, and Kiilsgaard, 1988). The most common unit in the Altanta lobe is the biotite granodiorite ranging in age from 75 to 85 million years old based on K-Ar radiometric age dates (Lewis, Kiilsgaard, Bennett, and Hall, 1987 and Johnson et al., 1988). Biotite granodiorite outcrops in the higher elevations of the Boise Front (Othberg and Gillerman, 1994). Biotite granodiorite is typically light gray in color, medium- to coarse-grained rocks, locally porphyritic with abundant potassium feldspar phenocrysts of up to 2.5 cm long and foliation is rare. Biotite granodiorite is generally composed of plagioclase, quartz, potassium feldspar, and 2 – 8 % biotite (Johnson et al., 1988).

2.2.4 Soils

The soils within the DCW result from the weathering of the Idaho Batholith. In 1997, the United States Department Agriculture (USDA) - Natural Resource Conservation Service (NRCS) completed a Soil Survey of the Boise Front to be used in land planning programs in the Boise Front. There are three generalized soil map groups within the DCW; the 300 map group, 500 map group and 700 map group consisting of soil map units delineated by taxonomic classifications of the dominant soils or miscellaneous areas. All of the map units in the DCW are made up of two or more soil series or miscellaneous areas called complexes. Complexes consist of soil series or miscellaneous areas in an intricate pattern or very small areas therefore cannot be shown separately on the soil survey maps (Table 2.1and Figure 2.2). The soil complexes in the DCW are made up of twenty-four soil series composed of three general soil taxonomies: Argixerolls, Haploxerolls, and Haplocambids (USDA, 1997). Please refer to Appendix A for a brief description of the soil series found in the DCW.

Table 2.1. NRCS Soil Map Groups and Soil Map Units in the Upper Dry Creek Watershed.

Soil Map Group	Area - km^2	Soil Map Units
300	0.5	358 – Qualiridge-Fortbois Complex
		360 – Picketpin-Van Dusen Complex
		361 – Quailridge-Hullsgulch-Crane Gulch Complex
		371 – Quailridge-Fortbois-Rock Outcrop Complex
500	14.0	506 – Brownlee-Robbscreek-Whisk Complex
		508 – Dobson-Roney-Rock Outcrop Complex
		511 – Olaton-Roney-Schiller Complex
		525 – Robbscreek-Dobson-Brownlee Complex
		526 – Cartwright-Brownlee-Robbscreek Complex
		527 – Dobson-Roney Complex
		528 – Roney-Dobson-Olaton Complex
		529 – Roney-Whisk-Olaton Complex
		533 – Olaton-Roney Complex
		534 – Shanks-Gwin-Olaton Complex
		535 – Whisk-Roney-Rock Outcrop Complex
		536 – Borid-Shanks-Schiller Complex
		537 – Schiller-Shanks Complex
		539 – Olaton-Roney-Schiller Complex, dry
700	12.5	702 – Deerrun-Whisk-Drybuck Complex
		703 – Whisk-Rock Outcrop-Drybuck Complex
		710 – Northfork-Shirts-Zimmer Complex
		713 – Crumley-Charters-Shirts Complex
		715 – Zimmer-Eagleson Complex
		717 – Northfork-Shirts Complex
		718 – Crumley-Northfork-Shirts Complex
		719 – Crumley-Northfork-Shanks Complex
		720 – Drybuck-Deerrun-Whisk Complex
		721 – Shirts-Zimmer-Northfork Complex
		722 – Zimmer-Eagleson-Rock Outcrop Complex

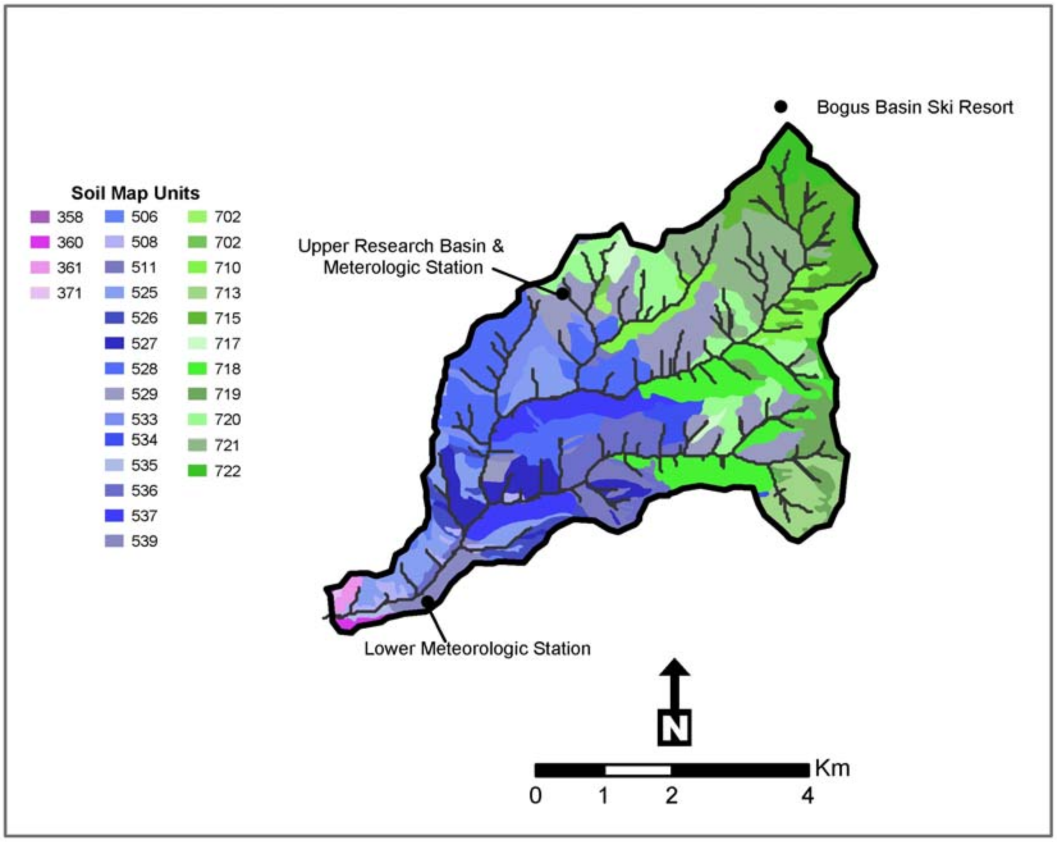

Figure 2.2. Dry Creek Watershed Soil Types as mapped by the NRCS in the Soil Survey of the Boise Front Project Idaho.

A sieve analysis was completed on soils from both research sites to determine the particle size distribution (Table 2.2). The soils were classified based the particle size distribution using the United States Department of Agriculture (USDA) textural classification of soil (Figure 2.3). The soils for the upper research site classified as sandy loam and the soils at the lower research site classified as loam.

Table 2.2. Grain Size Distribution for soils at the Upper Dry Creek Research Basin and the Lower Dry Creek Research Site.

Upper Research Site				
Soil Depth	**% Sand**	**% Silt**	**% Clay**	**Porosity**
0 – 8 cm	75.8	17.2	7.0	0.38
8 – 26 cm	71.5	20.3	8.2	0.39
26 – 54 cm	74.9	16.8	8.3	0.40
54 – 70 cm	76.1	16.9	7.0	0.38
70 +	Granite			
Lower Research Site				
Soil Depth	**% Sand**	**% Silt**	**% Clay**	**Porosity**
0 – 14 cm	49.0	40.0	12.0	0.45
14 – 50 cm	50.0	35.0	15.0	0.43
50 – 88 cm	50.0	34.0	16.0	0.43
88 – 115 cm	46.0	35.0	19.0	0.46
115 – 130 cm	51.0	32.0	17.0	0.45
130 +	Granite			

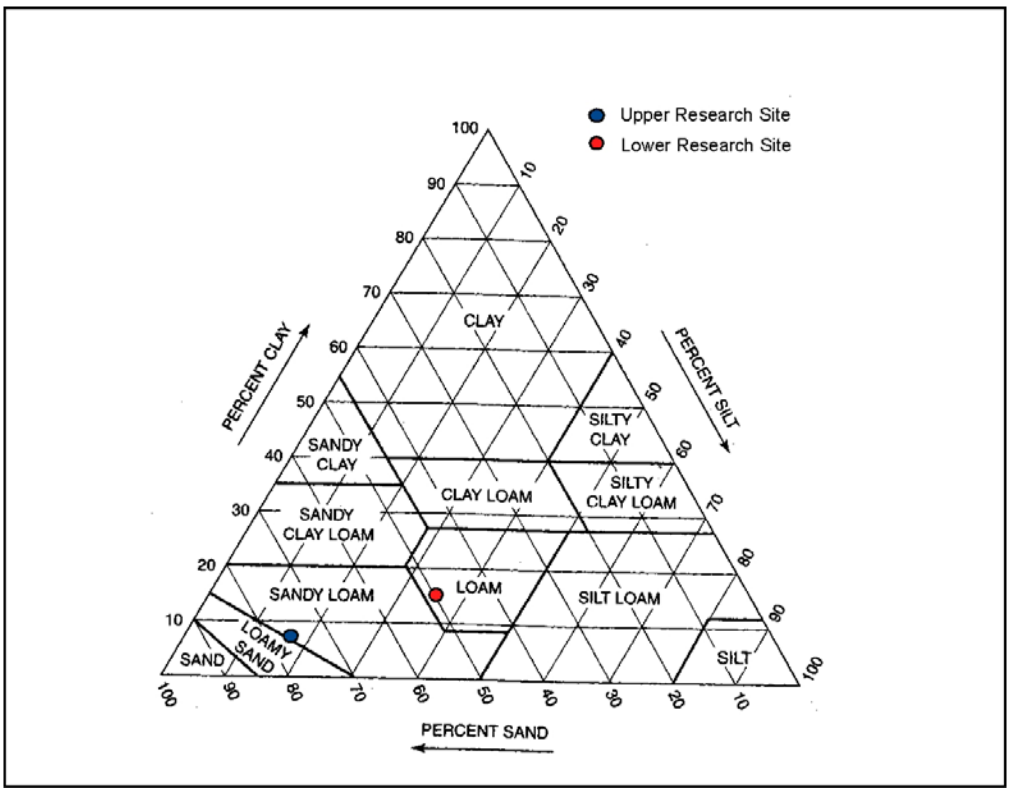

Figure 2.3. USDA Soil Textural Classification Triangle for the grain size distribution for the Upper Research Site and Lower Research Site in the DCW.

2.2.5 Vegetation

Vegetation in the DCW is strongly associated with elevation, geology, microclimate, soil type, slope aspect, and landforms. The dominant flora and dominant tree species classify the vegetation habitat. In the low elevations, grass/brush communities dominate the watershed. Grass/brush communities with areas of dry ponderosa pine and Douglas - Fir habitat, dominate intermediate elevations. The microclimate and slope aspects greatly influence the distribution of communities in these elevations. Upper elevations are predominantly Douglas-Fir habitat with ponderosa pine as the dominant component (USDA, 1974).

2.2.6 Land Ownership/Uses

Within the DCW, land use includes forestry, rangeland, and recreational activities. Forestry activities are concentrated in the upper 2846 acres (11.52 km^2), approximately 42.1% of the basin owned by the Boise National Forest. The remaining 57.9% of the basin hosts agricultural and recreational activities on lands owned by the Bureau of Land Management (BLM) (11.06 acres or 0.05 km^2), the State of Idaho (162.09 acres or 0.70 km^2), and private parties (3729.42 acres or 15.10 km^2). Agricultural activities are limited to cattle and sheep ranching. Recreation activities are vast including hiking, mountain biking, horseback riding, photography, nature study, camping, hunting, and off-road vehicle use including motorcycle, ATV, and snowmobiles (Figure 2.4)(USDA, 1997).

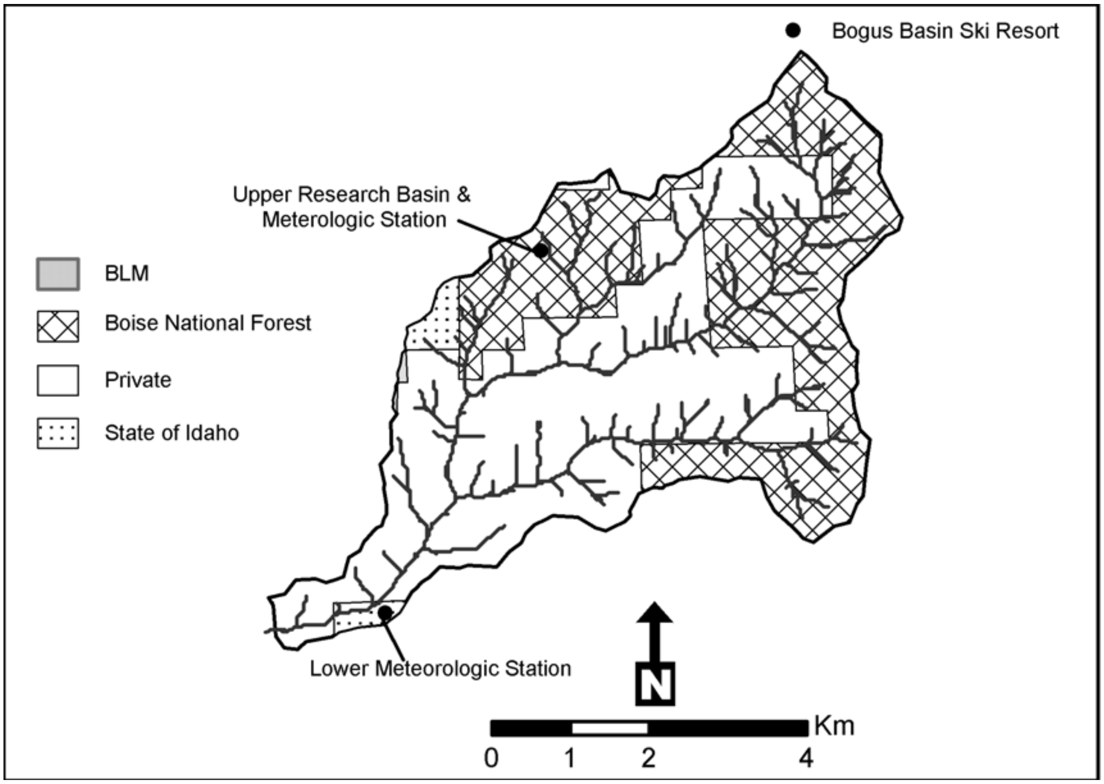

Figure 2.4. Upper Dry Creek Watershed Land Ownership.

2.3 Upper Dry Creek Experimental Watershed

The Dry Creek Experimental Watershed (UDCEW) is a small ephemeral headwater basin encompassing approximately 0.02 km^2 within the DCW. UDCEW is characterized by frequent snowmelt events in late winter and early spring, and may experience rain-on-snow events throughout the winter months. The ephemeral stream located in the basin typically begins flowing in early winter and continues until mid- to late-spring. There are occasional summer and fall thunderstorms, but the soil is typically dry and no streamflow occurs after snowmelt.

2.3.1 UDCEW Field Instruments

Beginning in 1998, field measurement devices were installed in conjunction with the United States Department of Agriculture (USDA), Agricultural Research Service (ARS). A meteorological station was installed to observe weather conditions including air temperature, wind speed, wind direction, barometric pressure, relative humidity, solar radiation, precipitation, as well as soil temperature, and snow depth. Total precipitation is measured by weighing bucket gauges mounted on posts approximately 1.5 meters from the ground at fifteen-minute intervals (Figure 2.5). Snow depth is measure by a Judd sonic depth sensor as well as weekly snow surveys in the winter months. Volumetric soil moisture and soil pore-water pressure were measured by Campbell Scientific water content reflectometers, time domain reflectometry (TDR) probes and tensiometers installed along a depth profile. Thermocouples record soil temperatures at the depth. Overland flow is routed to two 500-gallon collection tanks where depth is recorded hourly. Pressure transducers and electrical conductivity probes at the three locations measure streamflow, electrical conductivity and stream temperature. Output from all sensors is logged on Campbell Scientific CR10x dataloggers. Several field measurement devices were installed to collect water samples: an autosampler was used to sample stream water. Suction lysimeters were installed on a 10-meter grid to collect soilwater. Snowmelt pans and rain buckets were installed in order to collect snowmelt and rain, respectively (Figure 2.6).

Figure 2.5. Dry Creek Experimental Watershed Meteorological Station.

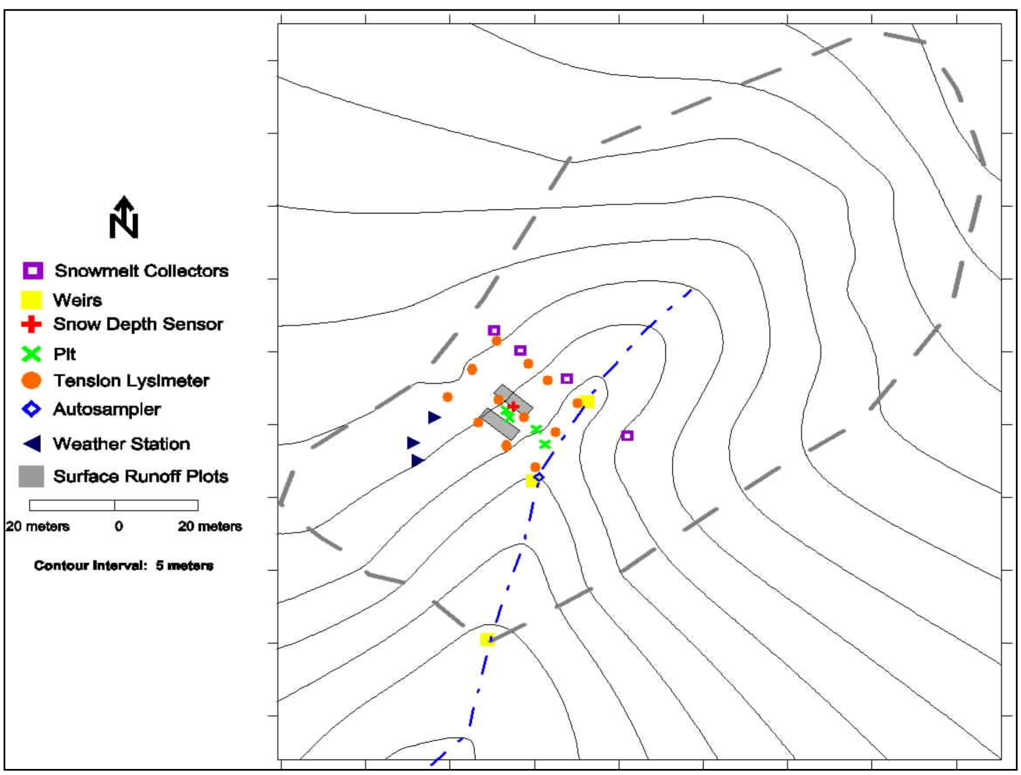

Figure 2.6. UDCEW instrumentation locations.

2.3.2 UDCEW Hydrometric Data

The water year used for the UDCEW was chosen to be July to July instead of the traditional October to October used by regulatory agencies in order to better incorporate both the wet and dry seasons in this semi-arid region. The results presented here are limited to the July 2000 – July 2001 water year.

2.3.2.1 Temperature

Air temperature measurements were recorded every fifteen minutes in the UDCEW. The water year temperatures range from –11.8º C to 35.3º C with an average temperature of 8.5º C (Figure 2.7). The minimum temperature occurred in the month of January and maximum temperature occurred in July. The monthly temperature averages for the water year is summarized in Table 2.3. The highest average temperature occurs in the month of August and the lowest average temperature occurs in the month of January.

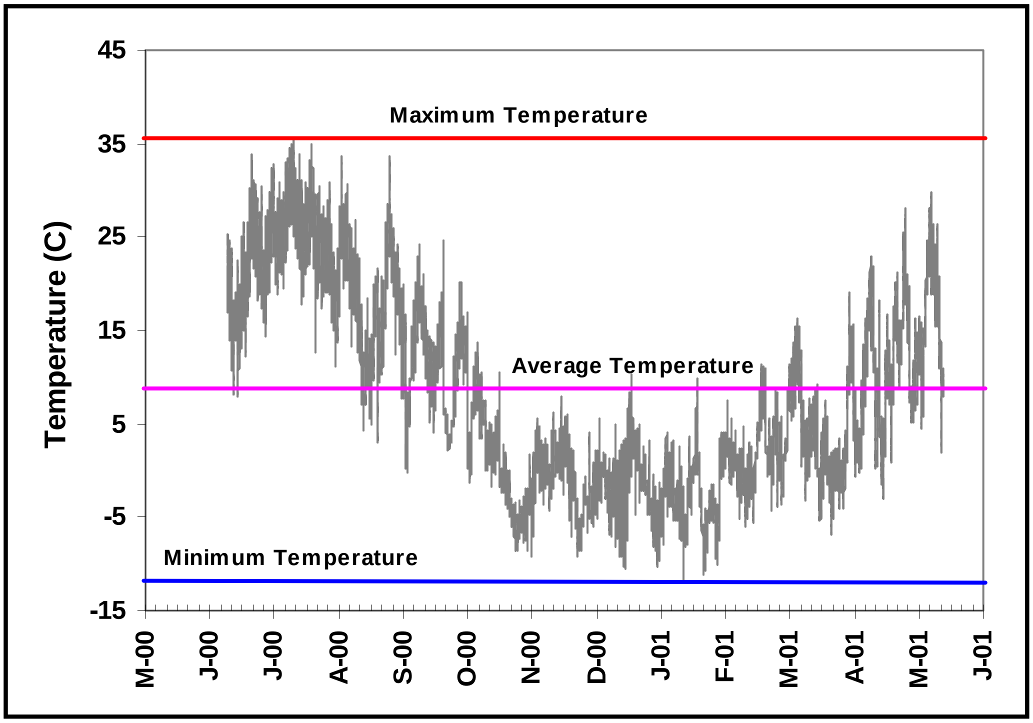

Figure 2.7. UDCEW Temperature record from May 2000 to May 2001. The red, pink, and blue lines denote maximum temperature, average temperature, and minimum temperature, respectively.

Table 2.3. UDCEW monthly temperature averages.

Month	Average Temperature (º C)
July 2000	23.0
August 2000	23.2
September 2000	14.9
October 2000	8.5
November 2000	-1.7
December 2000	-1.9
January 2000	-2.2
February 2000	-1.7
March 2001	4.1
April 2001	5.0
May 2001	13.8
June 2001	16.2

2.3.2.2 Precipitation

The majority (65%) of the precipitation in the UDCEW falls in the cold season. Precipitation measurements were taken every fifteen minutes using weighing bucket gauges mount 1.5 meters from the ground surface on posts. The total precipitation for the 2000/2001 water year was 56.6 cm with 28.7 cm (or 51%) falling as snow and 27.9 cm (or 49%) falling as rain. Figure 2.8 summarizes the precipitation by month and precipitation type.

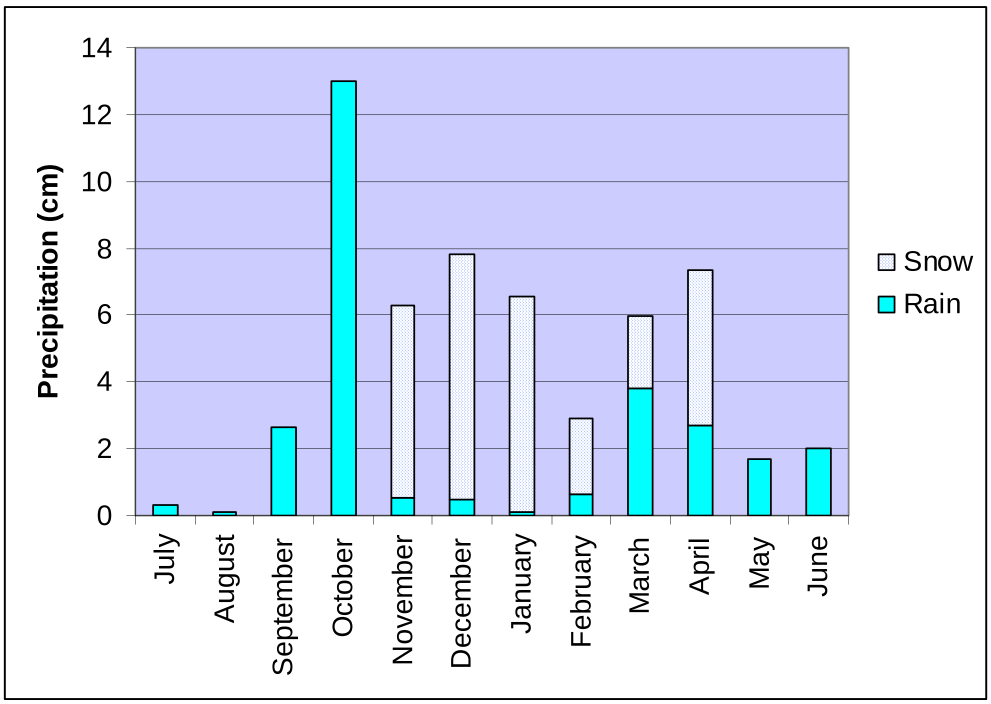

Figure 2.8. UDCEW precipitation occurring between July 2000 and July 2001 summarized by month and precipitation type.

1.1.1.1 Water Discharge

The UDCEW is a small ephemeral headwater basin. Streamflow in the 2000/2001 water year commenced in November 2000 and ceased in May 2001. Water discharge measured in UDCEW ranged from 0.002 L/min to 51.3 L/min. The water discharge data for the period of January 17, 2001 to February 12, 2001 are missing due to a pressure transducer malfunction. Peak water discharges on the hydrograph were attributable to rain events and snowmelt events. The hydrograph – hyetograph for the 2000/2001 cold- season illustrates the UDCEW stream's response to precipitation (Figure 2.9).

Diurnal melts and numerous mid-winter small snowmelt events characterized the 2000/2001 cold season (Figure 2.10). On March 3, 2001, the first major snowmelt event (SM1) commenced and by March 24, 2001 most of the basin was snow-free. The peak discharge in SM1 was 51.3 L/min occurring on March 9, 2001 (Figure 2.11). A rain event occurred on a snow-free basin March 25, 2001. In April 2001, a second snowpack accumulated in the basin. A second snowmelt event (SM2) commenced on April 7, 2001 with the peak discharge of 24.96 L/min on April 14, 2001 (Figure 2.12). Water discharge continued until early May and ceased when the basin was devoid of snow.

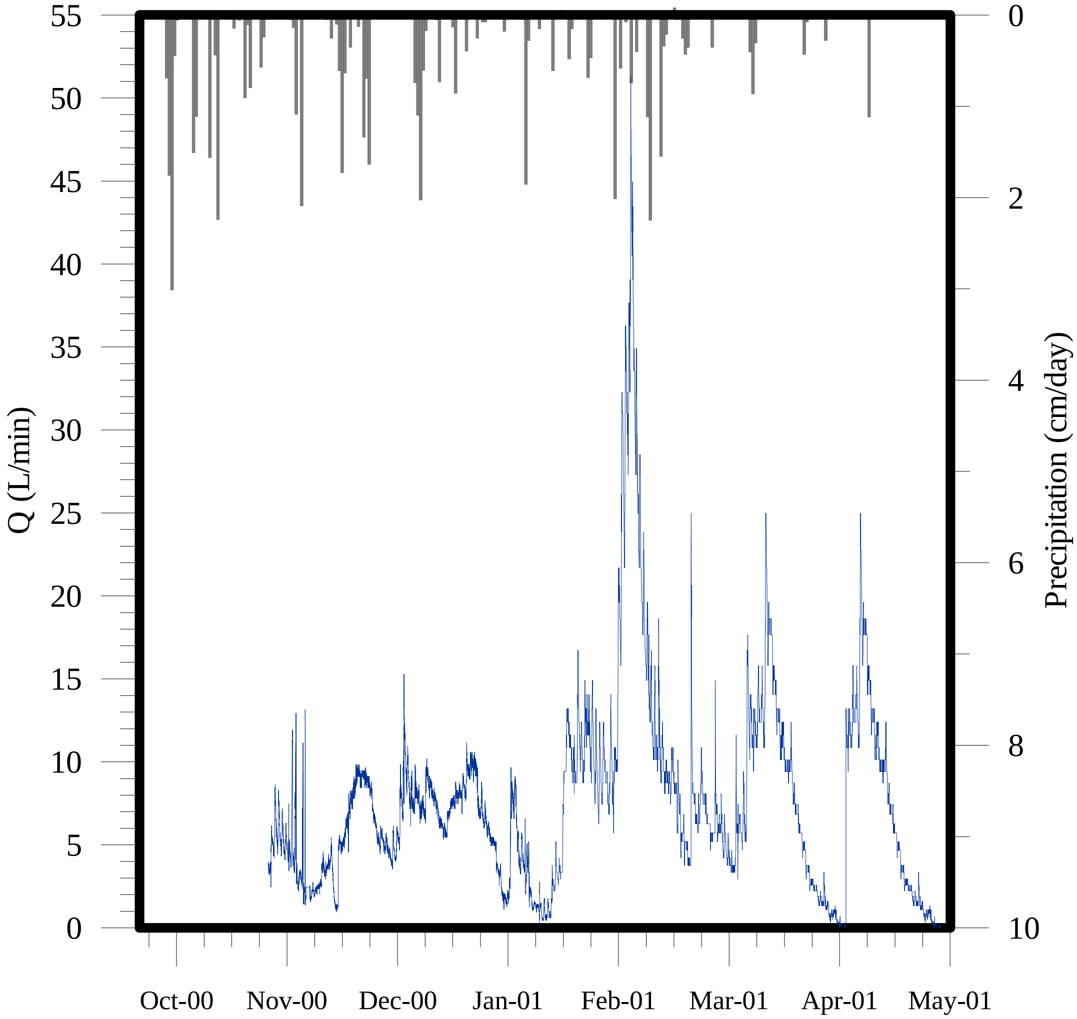

Figure 2.9. UDCEW 2000-2001 cold season hydrograph – hyetograph.

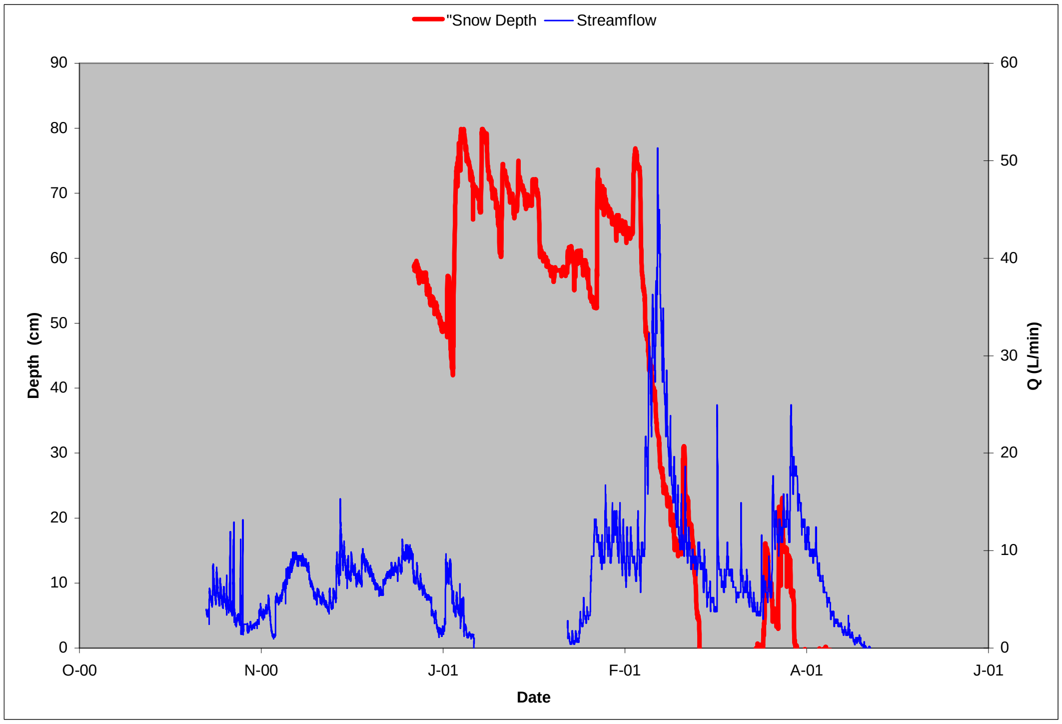

Figure 2.10. UDCEW Judd Sensor Snow depth and Streamflow for the 2000/2001 Cold Season.

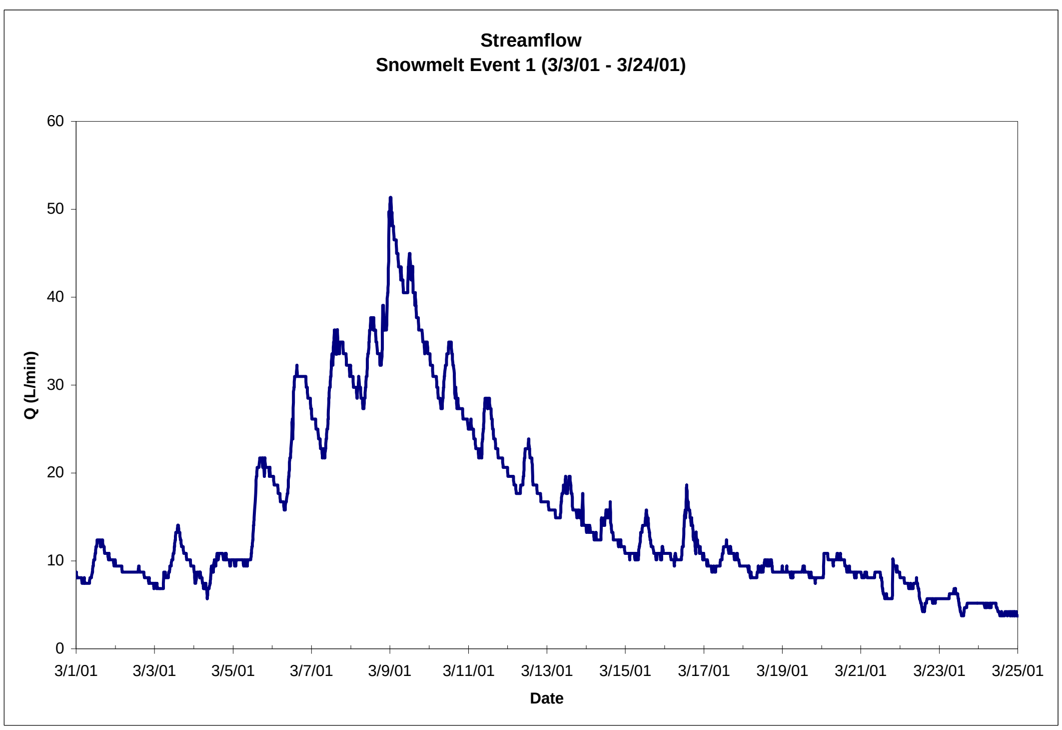

Figure 2.11. UDCEW Snowmelt Event 1 Hydrograph.

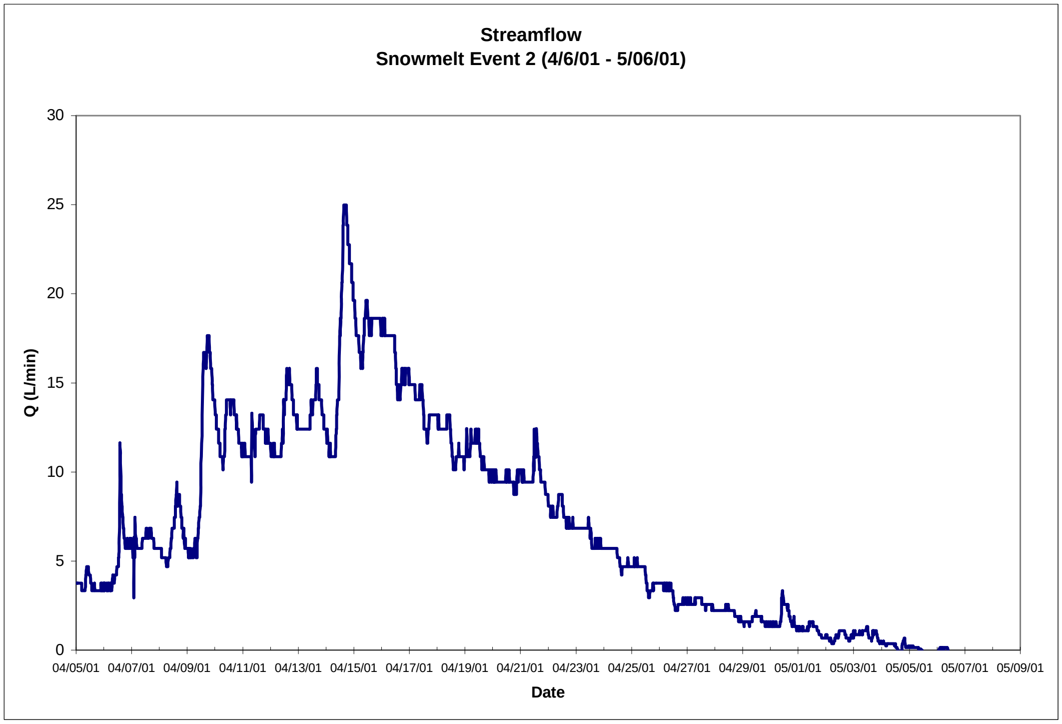

Figure 2.12. UDCEW Snowmelt Event 2 Hydrogaph.

1.1.1.2 <u>Soil Moisture</u>

The mid-slope soil pits monitored soil moisture between the depths of 5 cm and 100 cm (Figure 2.13), illustrates the seasonal variation of soil moisture in UDCEW. In the summer months the soil moisture content at the surface to 5 cm depth consistently between 0 $cm^3/cm^3$and 0.05 cm^3/cm^3. In the rest of the soil column, the soil moisture content is relatively stable throughout the summer months between 0.05 $cm^3/cm^3$and 0.1 cm^3/cm^3. Occasional summer thundershowers wet the soil surface and a small amount precipitation infiltrates to depth, however most precipitation is lost to evapotranspiration. In early fall, the rain events become more frequent and the antecedent soil moisture content increases. As the soil moisture content increases in the soil column the potential for deep infiltration of precipitation increases and the evapotranspiration rate decreases.

As a result of the fall rain events, the soil moisture content in the soil column to a depth of 30 cm steadily increases. The soil moisture content at the 45 cm depth lags behind the upper soil column and the increase corresponds to a rapid decrease in the upper soil moisture content. The moisture contents in the upper soil column continue to rise until the precipitation changes to snow in the late fall and then stabilize. The soil moisture content at the base of the soil column steadily increases through the winter. In March 2001, the soil moisture contents throughout the entire soil column respond to precipitation and snowmelt in similar manners.

The water discharge measured in UDCEW responds to increases in soil moisture content in the soil column (Figure 2.13). Streamflow in the basin commenced soon after the rise in soil moisture content resulting from the fall rain events and the basin was snow covered. Snowmelt events, SM1 and SM2, hydrograph peaks correspond to a rapid rise in soil moisture content.

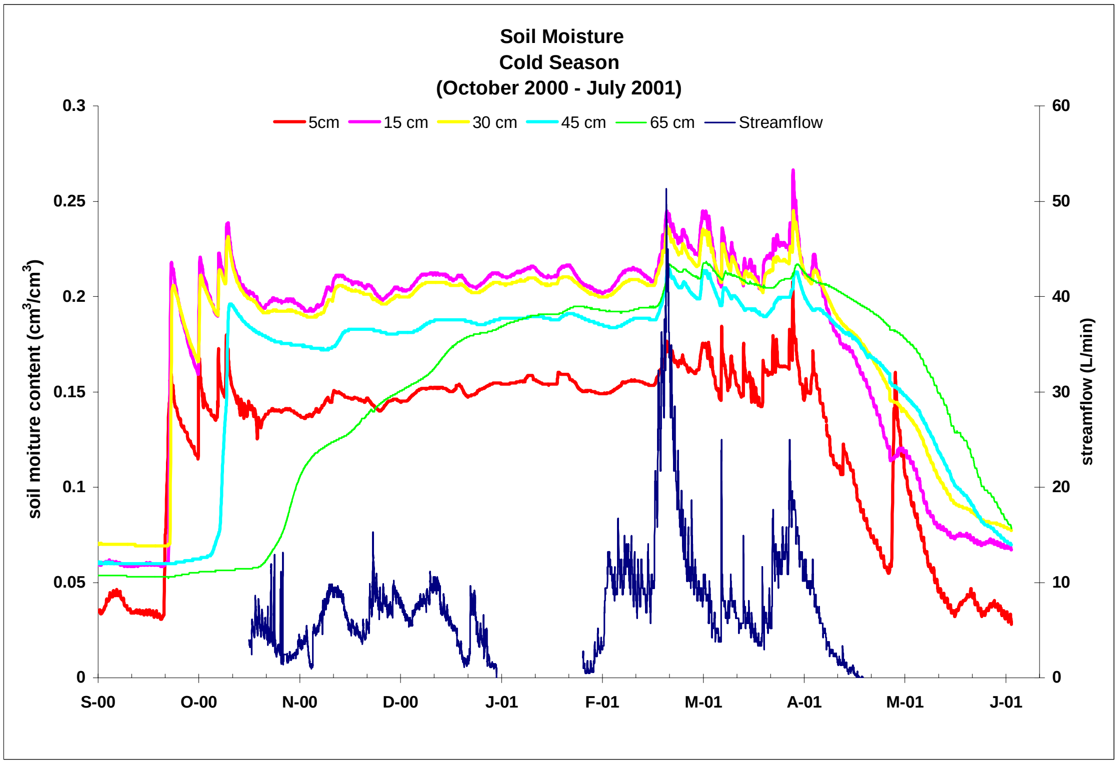

Figure 2.13. UDCEW soil moisture content measured at mid-slope pit October 2000 to May 2001.

2.3.3 <u>UDCEW Water Balance</u>

McNamara (unpublished) completed a water balance for UDCEW using Simultaneous Heat and Water (SHAW) model (Ferchinger, Hanson, and Wright, 1996). The SHAW model computes a daily water balance using the following equation:

$$P - INT - ET - \delta S_{canopy} - \delta S_{snow} - \delta_{residue} - \delta S_{soil} - Ponding - Runoff - DeepPerc + error = 0 \quad (2.1)$$

where P is precipitation, INT is precipitation intercepted on the top of the canopy, ET is the total evapotranspiration, δS_{canopy} , δS_{snow} $\delta S_{residue}$, and δS_{soil} are the change in storage related to the canopy, snow, residue, and soil, respectively, Ponding is the water lost to ponding, Runoff represents the surface runoff, and DeepPerc is the water lost to vertical deep percolation within the soil profile. The model completes a daily water balance considering each of the water balance components independently. The error represents the value need to solve equation for zero. See Flerchinger et al., (1996) for a more detailed discussion of the SHAW model.

It is hypothesized that there is a lateral subsurface flow component contributing to streamflow in UDCEW. The deep percolation component in the SHAW model water balance accounts for the vertical movement of water through the soil profile computed by darcian flux. McNamara, unpublished, expanded the deep percolation component of the Shaw Model to account for lateral subsurface flow in the UDCEW by inferring that once the vertical deep percolation component reaches the impermeable bedrock boundary the water flows laterally. The DeepPerc component in the Shaw model was substituted by the bedrock flow (BF) component (Equation 2.2). The BF is represented by Equation 2.3.

$$DP = BF \tag{2.2}$$

$$BF = GW_{out} + L_{out} \tag{2.3}$$

Equation 2.3 is substituting into Equation 2.1 and allowing for the lateral flow subsurface flow (L_{in}) and groundwater (GW_{in}), the water balance becomes:

$$P - INT - ET - \delta S_{canopy} - \delta S_{snow} - \delta_{residue} - \delta S_{soil} - Ponding - Runoff - GWout + Lout + error = 0 \tag{2.4}$$

The water balance for water year 2000/2001 is presented in Table 2.4. The SHAW model computed the BF component of the water balance for this water year at 18.8 cm. McNamara (unpublished) used the chloride mass balance for UDCEW to estimate the components that comprise BF; L_{out} and GW_{out}. The chloride mass balance indicates that 30% of the snowmelt entering the soil does not make it to the stream. This water is assumed to be stored as soil water and then evaporated or taken up by plants in the spring and summer. Approximately 5.0 cm of the snowmelt can be assumed to be stored as soil water. The amount of water constituting the L_{out} is 13.8 cm. The stream yielded 14.3 cm of water in the 2000/2001 water year. The stream water yield is approximately 3.5% greater than the calculated L_{out}.

Table 2.4. UDCEW Water balance for water year 2000.

<table>
<tr><th colspan="2">Water Budget Component</th><th>Value (cm)</th></tr>
<tr><td colspan="2">Precipitation</td><td>56.78</td></tr>
<tr><td colspan="2">ET</td><td>41.25</td></tr>
<tr><td colspan="2">Storage Canopy</td><td>0.00</td></tr>
<tr><td colspan="2">Storage Snow</td><td>0.00</td></tr>
<tr><td colspan="2">Storage Residue</td><td>0.00</td></tr>
<tr><td rowspan="2">Bedrock Flow</td><td>GW_{out}</td><td>5.0</td></tr>
<tr><td>L_{out}</td><td>13.8</td></tr>
<tr><td colspan="2">Streamflow</td><td>14.3</td></tr>
<tr><td colspan="2">Error</td><td>-3.28</td></tr>
</table>

3. METHODS

Characterization of the Upper Dry Creek Watershed's hydrology with emphasis on the hydrometric and geochemical properties involved fieldwork, laboratory, and numerical investigations. Fieldwork included measuring water discharge, changing data modules on meterorologic station and stream gauging sites, and collection of snow, snowmelt, soilwater and streamwater samples. Laboratory analysis included chemical analysis of water samples at the Utah State University Analytical Laboratory. Numerical investigations included analysis of hydrometric and geochemical data, hydrograph separation, End-Member Mixing Analysis (EMMA), and concentration-discharge (c-Q) relationships.

Hydrometric and geochemical data was used to test the following hypotheses:

- There is no regional groundwater input into the UDCEW system during the cold-season flow period. The UDCEW hydrograph separation and EMMA was used to explain the streamwater chemistry as a mixture of snowmelt and soilwater sources. The UDCEW water balance provides additional evidence for no regional groundwater contribution.
- All discharge within the UDCEW originates from the cold-season precipitation (rain and snowmelt events) and soil water components. The UDCEW hydrograph separation provides support that both event and pre-event sources contribute to streamflow during the cold-season in UDCEW.

EMMA was then used to further define the pre-event and event water components into the end-members contributing to UDCEW streamflow.

3.1 Geochemical Data

Snow, snowmelt, soilwater, and streamwater were collected in order to characterize the major inorganic chemistry of the samples. Periodically snowcores were taken throughout the cold season and melted to sample the chemical composition of the snowpack. Snowmelt pans were used to collect snowmelt at the base of the snowpack. Samples were collected from a storage vessel that was set underground. Soilwater was sampled from tension lysimeters installed on a ten-meter grid at two depths (30- and 60-cm average depths). Soilwater sampling was attempted every ten days. Streamwater was sampled by an Isco Autosampler and periodic grab samples. During snowmelt events the autosampler took samples every 6 hours. Samples were retrieved using a 60 mL latex free syringe. Before sampling streamwater, all sample collection equipment and bottles were rinsed three times with water from the channel. Before sampling soilwater and snowmelt, the sampling equipment and bottles were rinsed with deionized water. All water samples were passed through a 25-mm filter at the time the sample was taken. All water samples were refrigerated prior to analysis. Samples collected for cation analysis were acidified with a 2N HCL solution in order to keep the cations from precipitating on the bottle before analysis. The major inorganic chemistry analysis was completed at the USU Analytical Laboratory in Logan, UT. Cation analysis was completed by ICP elemental analysis and the Cl^{-1} was completed by Cl^{-1} colormetric analysis. Electrical

Conductivity and pH measurements were taken with a Denver Instruments AP50 meter at the time of collection for snow, snowmelt, soilwater, and grab streamwater samples. Additional water sampling was completed on springs found in the upper portions of the UDCW and the Main Dry Creek during the dry season (spring/summer) to quantify the regional ground water geochemical signature. Appendix B contains the complete geochemical data set.

A statistical analysis was completed on the geochemical data to determine outliers in the observed data set. An outlier is defined as any observation that lies unusually far from the main body of data. The formal definition of an outlier is any observation that is 1.5 fourth spread (f_s) from the closest fourth. The lower fourth and upper fourth are the median of the smallest half and largest half, respectively, of the data. A measure of the spread that is resistant to the outliers is the fourth spread (f_s) given by f_s = upper fourth – lower fourth (Devore, 2000). The median value for the data set is determined and then the upper and lower outlier is computed adding $1.5f_s$ to the median and subtracting 1.5fs from the median, respectively.

The hydrometric and geochemical data was used to analyze the concentration discharge (C-Q) relationships during the 2000 cold-season. Construction of C-Q plots requires stream discharge (Q) data and stream chemistry at the catchment outlet where the concentration is plotted against the $\log_{10}$ Q data.

3.1.1 Hydrograph Separation

The two-component hydrograph separation was completed to evaluate the amount of water that contributed to the snowmelt event hydrograph from pre-event water and event water. Pre-event water in this study included soilwater components and event water incorporated both rain and snowmelt.

For this study the two-component mixing model was considered due to the assumption of no contribution from a regional deep groundwater system. The two-component hydrograph separation was completed using the streamwater electrical conductivity. The pre-event water component for this study is defined as the soil water component and the event water component is defined as the snowmelt.

Pinder and Jones (1969) introduced a simple mixing model involving a two-component mass balance to differentiate between event and pre-event water contributing to streamflow. This method involves identifying a conservative tracer in each component (event and pre-event water), a known stream flow rate, known concentrations of tracers, and then applying the following two-component mass balance equations:

$$Q_s(t) = Q_e(t) + Q_{pe}(t) \tag{3.1}$$

$$Q_s(t)C_s(t) = Q_e(t)C_e(t) + Q_{pe}(t)C_{pe}(t) \tag{3.2}$$

where Q is discharge, C is the tracer concentration in the stream, t is a time instant, and the subscripts s, e, and pe indicate stream, event, and pre-event water respectively. Several assumptions must be made in order to use the two-component model: 1) the tracer composition of the event water must be significantly different from the pre-event water, 2) the tracer composition must remain stable for the duration of the event, and 3) the contributions from other potential sources is negligible.

3.1.2 EMMA

The starting point of using EMMA is to examine the mixing patterns using pairwise plots in order to determine which solutes are appropriate to use in the analysis. These diagrams are simple x-y plots of all chemical species to be considered for three proposed end-members and stream water. All stream water samples are plotted due to the variability in chemical composition with flow. Only the medians of the proposed end-members are plotted because the chemical composition of the waters are generally less variable. Given that the end-members are characterized on the median chemical concentrations for all solutes, the end-members chemical concentrations must be significantly different. The proportion of each stream water sample, with respect to time, from each end-member can be determined using two chemical species. However a third constraint is needed to meet the requirement that the sum of the three end-member is equal to one. If all end-members have been identified and mix conservatively to form stream water, then the stream water samples should lie within the triangle formed by a plot of the three end-members (Christopherson et al., 1990). Conservative mixing is defined as a mixing process in which the solutes do not participate in any chemical reactions (Christopherson and Hooper, 1992). If two end-members mix in a non-conservative way the mixing diagram will not indicate the relative contribution from each end-member. The mixing diagrams can not be used to authenticate conservative mixing but they can be used to determine if the end-members have been characterized correctly shown by stream water samples plotting outside the triangle area enclosed by the end-members (Christopherson et al., 1990).

The next step in EMMA is to perform a principal component analysis (PCA) on the data to determine the U Space. U space is defined as a lower-dimensional space where the majority of the observed data lie within a specified accuracy. The observed data must first be standardized to prevent solutes with greater variation from exerting more influence on the model than those with lesser variation. The correlation matrix is found for the standardized data. The correlation matrix, which scales the data by their variance, gives each solute equal weight in the analysis. PCA is then preformed on the correlation matrix. The U space is defined by the eigenvectors of the correlation matrix. The eigenvectors form new variables which represent the coordinates in the U space. By the definition of orthogonality, each of these new variables is uncorrelated to one another. The variance of each variable is associated with its eigenvalue, where the largest eigenvalue represents the largest variation. A model is selected that accounts for the greatest amount of variability with two principal components, implying a three end-member model when the correlation matrix is used. The median concentrations for the end-members were standardized to the stream water and projected into the U space defined by the stream water PCA by multiplying the standardized values by the matrix of eigenvectors. The extent by which the end-members bound the stream water observations is examined in U space. The EMMA model can then be used to calculate the proportion of stream water derived from each end-member. The proportions of end-member can then be used to predict stream water concentrations in order to test against the observed data. A goodness-of-fit of solute concentrations predicted by EMMA compared to observed stream solute concentrations are completed by a least-squared linear regression (Christopherson and Hooper, 1992).

For this study the EMMA model was completed on the two-snowmelt events that occurred during the 2000/2001 cold season. An initial analysis of which solutes are appropriate for use in EMMA was made. One necessary condition is there must be differences in solute concentrations between end-members. Solutes considered for use in EMMA included Calcium (Ca^{+2}), Magnesium (Mg^{+2}), Sodium (Na^{+1}), Sulfate (SO_4^{-2}), Silicon (Si^{+4}) assumed to be dissolved silica, and Chloride (Cl^{-1}). Sulfate was dismissed for use in EMMA because it is generally used to examine acid-base reactions in congress with alkalinity but alkalinity concentrations were not measured in UDCEW for this study. The Chloride concentration varies little in the soil profile, the concentration pattern is consistent with atmospheric input sources in UDCEW and is considered non-reactive in the soil profile. The remaining solutes are products of mineral weathering of the granitic bedrock and ion exchange. All of these solutes are assumed to mix conservatively under the conditions in UDCEW. Dissolved silica has been shown not to mix conservatively in Birkenes and Plynlimon, however at Panola (which has similar geology and soils as UDCEW) it was found that silica was more mobile. At Panola, silica concentrations were shown to increase with depth, in contrast to maximum silica concentrations occurring mid-soil profile typical of spodosols (Hooper et al., 1990). The following assumptions were made about the UDCEW in order to complete EMMA model:

- All solutes mix conservatively;
- Silica concentration increases with soil residence time in the soil profile; and

- Snowmelt is an end-member contributing to streamflow.

The EMMA model for each snowmelt event was developed according to the procedure outlined by Christopherson and Hooper (1992):

1. A data set was obtained for the streamwater observations collected during the 2000/2001 cold-season consisting of the solute concentrations for four solutes (Ca^{+2}, Mg^{+2}, Na^{+1}, and Si^{+4}). A statistical analysis was completed to identify the outliers, which were subsequently removed from the data set. Data sets for both snowmelt event 1 (SM1) and snowmelt event 2 (SM2) were identified from the entire cold-season data set.
2. Each data set was then standardized into a correlation matrix such that the solutes with greater variation would not exert more influence on the model than those with lesser variation.
3. A principal component analysis (PCA) was performed on the SM1 and SM2 correlation matrices using all four solutes. The PCA identified the two principal components that account for 93% of the variance for SM1 and 87% of the variance for SM2, indicating a three end-member model.
4. End-members were selected by determining the waters that bound the streamwater for all solutes considered in the pairwise plots.
5. The concentrations of the median end-member values were standardized and projected into U space defined by the streamwater PCA by multiplying the standardized values by the matrix eigenvectors.
6. The extent to which the end-members bounded the streamwater observations for each snowmelt event was examined in U space.

7. The goodness-of-fit of solute concentrations predicted by the EMMA model for each event were then compared to the concentrations measured for each event through least squares linear regression. The validity of end-members choices are tested by the goodness-of-fit between observed and predicted streamwater concentration. If the predictions do not match the observations for one or more of the solutes, the end-member composition is suspect (Hooper et al., 1990)
8. A three-component hydrograph separation was completed using the EMMA results to determine the portion of the hydrograph that each end-member contributed.

4. RESULTS AND DISCUSSION

4.1 Results

4.1.1 Geochemical Data

Outliers in a data set can affect the value of numerical summaries. Streamwater, soilwater, groundwater and snowmelt data were analyzed for outliers in the following solutes; calcium (Ca^{+2}), magnesium (Mg^{+2}), sodium (Na^{+1}), sulfate (SO_4^{-2}), silicon (Si^{+4}) assumed to be dissolved silica, and chloride (Cl^{-1}) (Table 4.1).

Table 4.1. UDCEW geochemical data set outlier analysis results for Ca^{+2}, Mg^{+2}, Na^{+1}, Si^{+4}, $SO4^{-2}$, Cl^{-1}.

	Ca	Mg	Na	Si	SO4	Cl
Reporting Limit	0.2	0.2	0.2	0.05	0.2	0.25
Stream water						
Sample Size	134	133	134	134	64	139
Mean	2.16	0.37	4.97	7.51	0.25	0.69
Median	2.13	0.37	4.93	7.43	0.25	0.68
Maximum	3.30	0.55	8.63	8.83	0.35	1.78
Minimum	1.49	0.25	3.39	6.15	0.20	0.28
Standard Deviation	0.35	0.06	0.99	0.57	0.03	0.23
Lower Outlier	1.35	0.2199	1.843	6.1925	0.12	0.205
Upper Outlier	2.95	0.5135	7.859	8.7325	0.36	0.965
# of Outliers	5	3	1	3	0	7
Soil water						
Sample Size	23	23	23	23	23	18
Mean	7.69	1.36	7.26	5.52	0.83	2.29
Median	6.52	1.26	6.27	5.79	0.84	1.60
Maximum	21.80	3.06	16.10	6.83	1.95	8.62
Minimum	1.79	0.30	1.73	2.53	0.27	0.31
Standard Deviation	4.49	0.68	3.99	1.09	0.41	2.34
Lower Outlier	-1.16	-0.07	-1.44	2.75	-0.27	-1.91
Upper Outlier	16.06	2.73	15.40	8.49	1.86	5.13
# of Outliers	1	1	1	1	0	2
Snowmelt						
Sample Size	18	Mg concentrations undetectable in Snowmelt	18	15	10	16
Mean	0.504627778		2.56951111	0.15972	0.36994	1.050625
Median	0.42135		2.88	0.1273	0.3	0.635
Maximum	1.09		3.97	0.38	0.82	4.88
Minimum	0.22		0.7825	0.05	0.25	0.08
Standard Deviation	0.237915024		1.05442161	0.09363042	0.1791742	1.3043234
Lower Outlier	-0.0515	NA	-0.5675	-0.117375	0.06325	-0.5325
Upper Outlier	1.0229	NA	5.5245	0.422425	0.58605	1.8475
# of Outliers	0	NA	0	0	1	2

A boxplot illustrates the distribution of data including the center (or median), variation (or spread), the extent and nature of any departure from symmetry or skewness, and outliers of the data set (Devore, 2000) (Figure 4.1). All identified outliers were removed from the data set used for analysis.

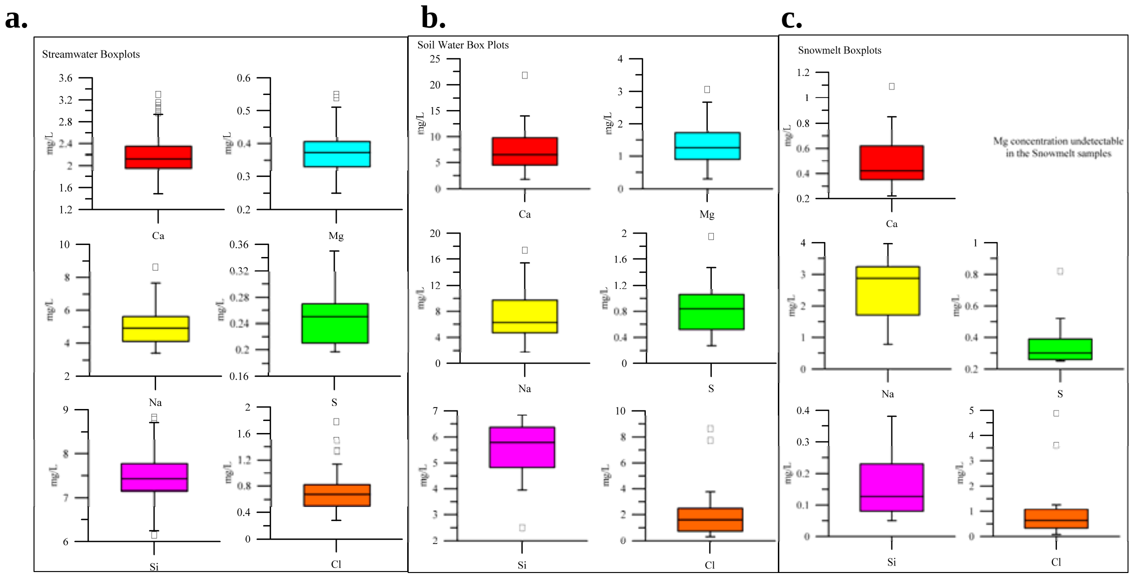

Figure 4.1. UDCEW chemistry data set boxplots for Ca^{+2}, Mg^{+2}, Na^{+1}, Si^{+4}, $SO4^{-2}$, Cl^{-1}: a) Streamwater, b) Soilwater, and c) Snowmelt.

Streamwater chemistry was analyzed with respect to Ca^{+2}, Mg^{+2}, Na^{+1}, Si^{+4}, $SO4^{-2}$, Cl^{-1} (Figure 4.2a and b) and electrical conductivity (Figure 4.3) in relation to water discharge throughout the cold season. For the chemical species analyzed, there were no strong trends associated with increasing stream discharge. Electrical conductivity has a decreasing trend with increasing flow, with the majority of the electric conductivity points clustered at low flow values and has low r^2 values, 0.20 with the log function (Figure 4.4). Ca^{+2}, Mg^{+2}, and Si^{+4} show a slight decreasing concentration trend with increasing discharge, with very low r^2 values (linear function); 0.06 for Ca^{+2}, 0.01 for Mg^{+2}, and 0.26 for Si^{+4}. In contrast, Na^{+1}, $SO4^{-2}$, and Cl^{-1} concentrations illustrate a slight increasing trend with increasing discharge, with very low r^2 values (linear function); 0.02, 0.18, and 0.09, respectively (Figure 4.5).

a.

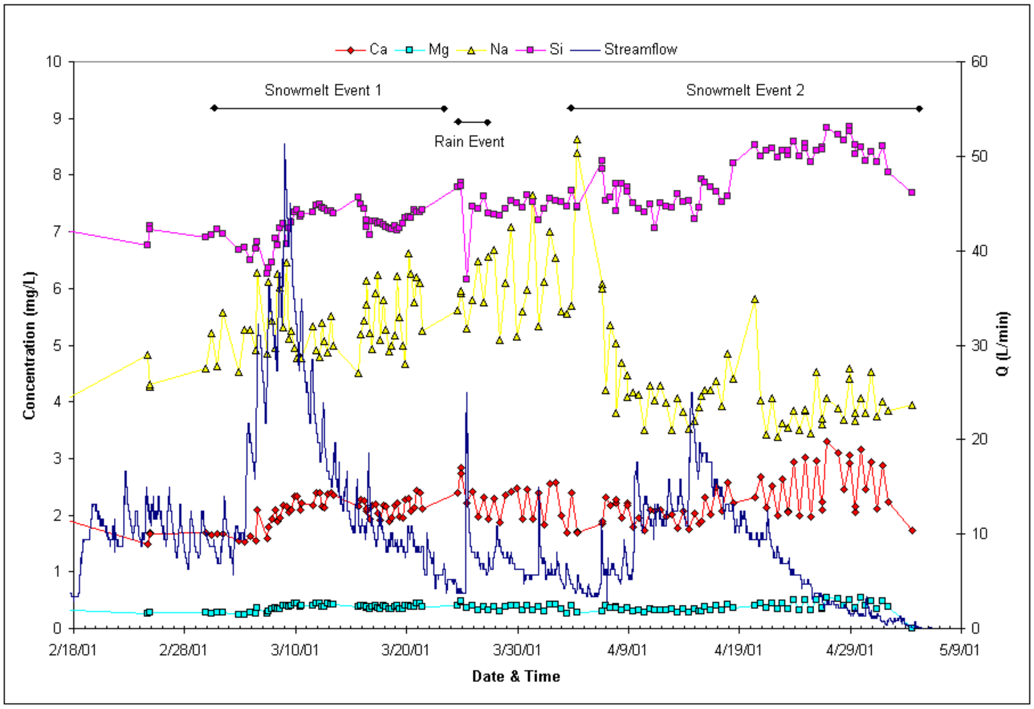

b.

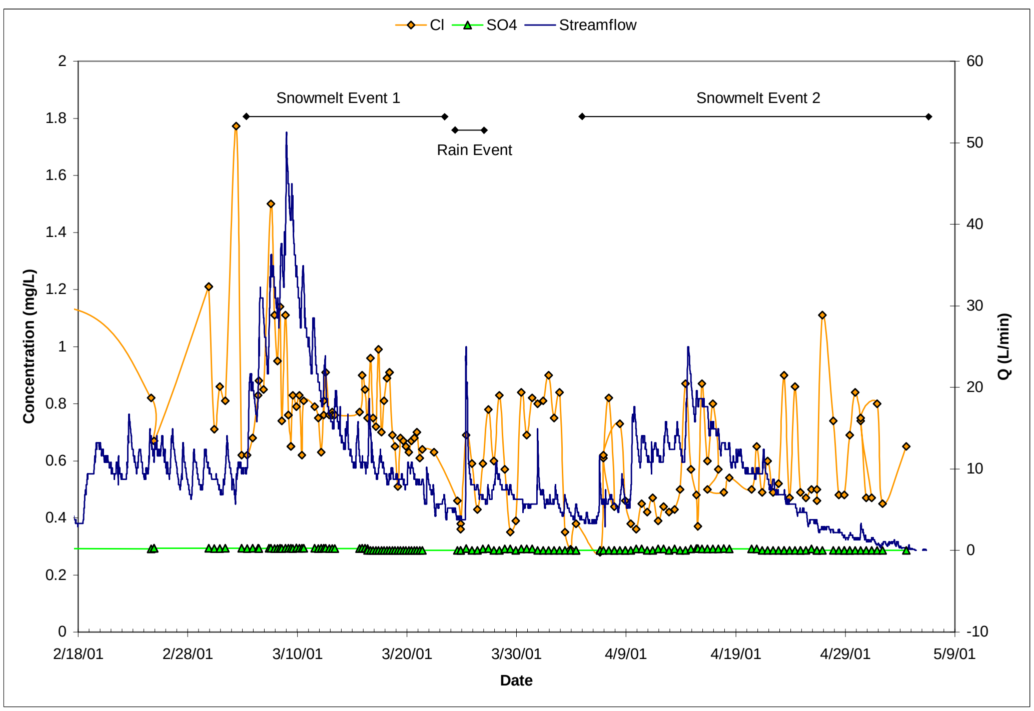

Figure 4.2. UDCEW 2000- 2001 Cold-Season Streamwater Chemistry: a. Cation Streamwater Chemistry, b. Anion Streamwater chemistry.

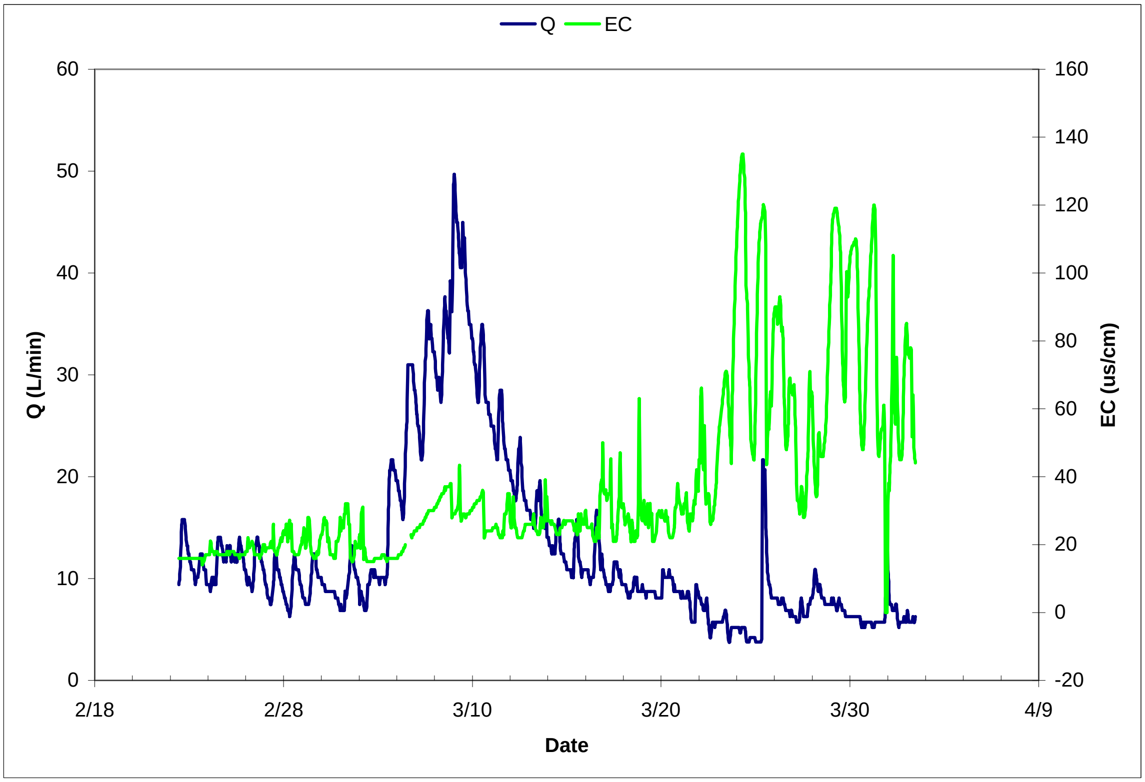

Figure 4.3. Stream water electrical conductivity (EC) and water discharge (Q) from February to April 2001.

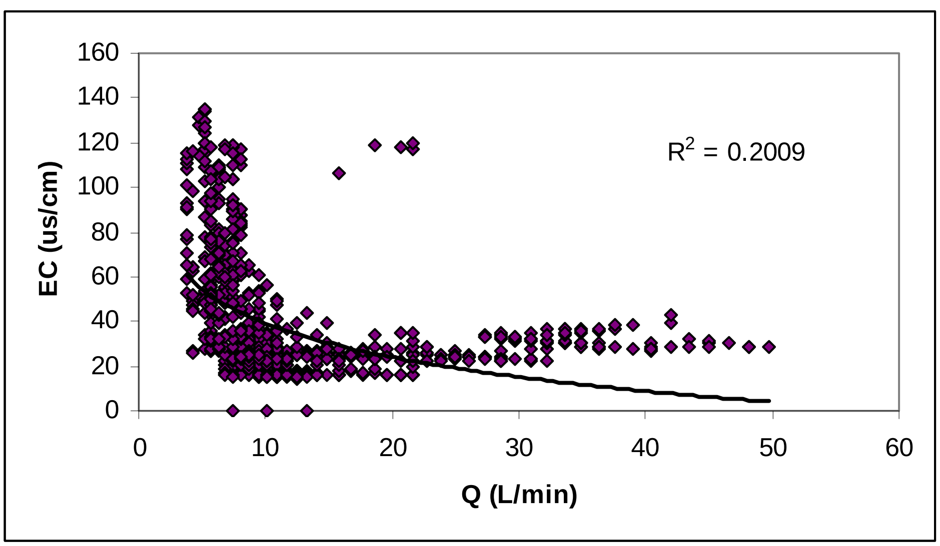

Figure 4.4. Electrical conductivity of streamwater against water discharge with logarithmic trend line.

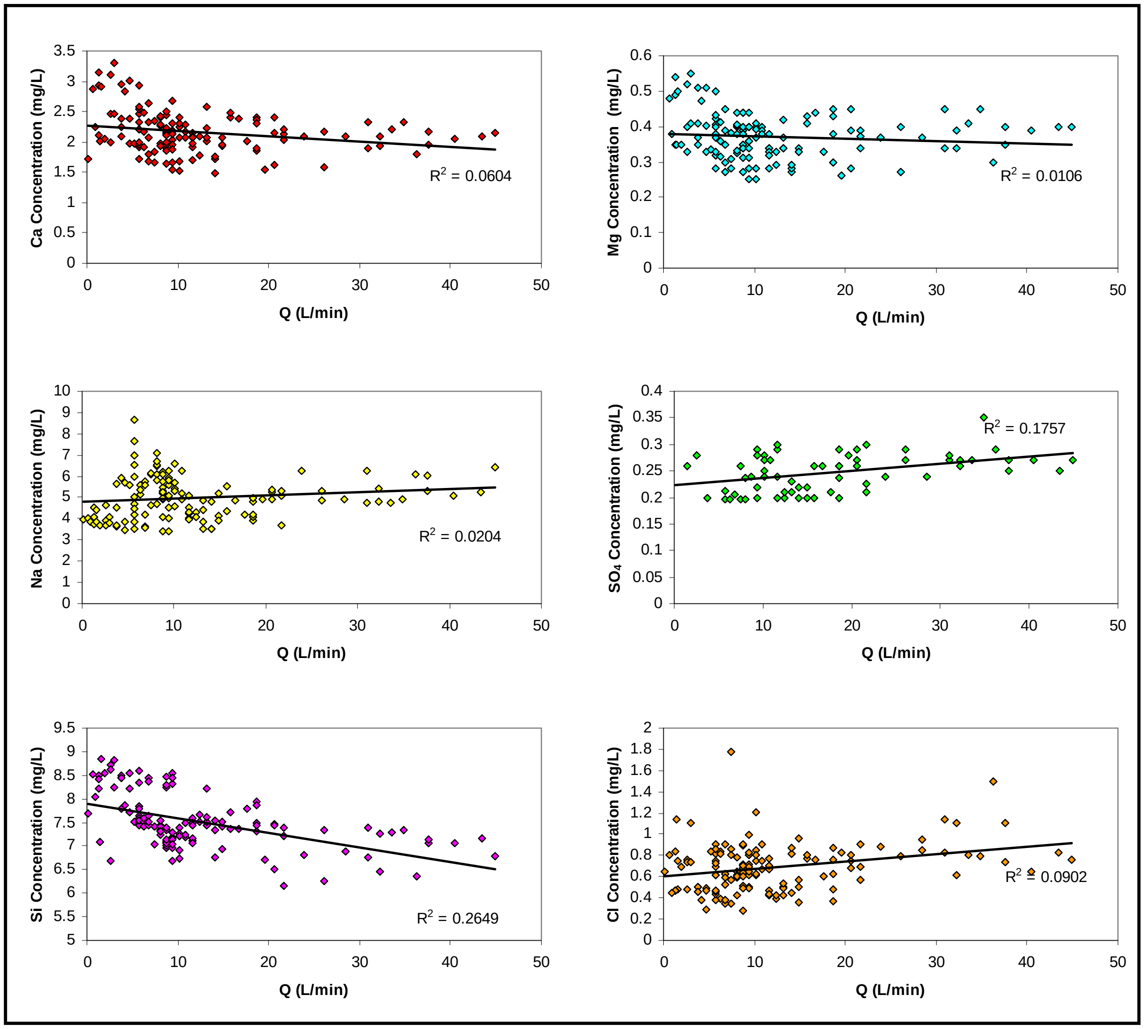

Figure 4.5. Concentrations of solutes against water discharge with a linear trend line.

Silica concentrations were plotted against log discharge for the two-snowmelt events in the 2000/2001 cold season. Both snowmelt events show that the rising limb of the hydrograph is associated with lower silica concentrations than the falling limb for the like discharges. The SM1 C-Q plot for silica shows a dominant counter-clockwise hysteresis rotation with a minor clockwise rotation (Figure 4.6). The SM2 C-Q plot for silica also shows a dominant counter-clockwise hysteresis rotation with two minor clockwise rotations (Figure 4.7). Dominant counter-clockwise rotation of the hysteresis loops indicates activation of a flow source with greater silica concentration as the melt events progressed. A counter-clockwise loop indicates that a freshwater source, such as precipitation, contributes to flow early in the storm and those a more concentrated source, such as soilwater, contribute later in the storm event.

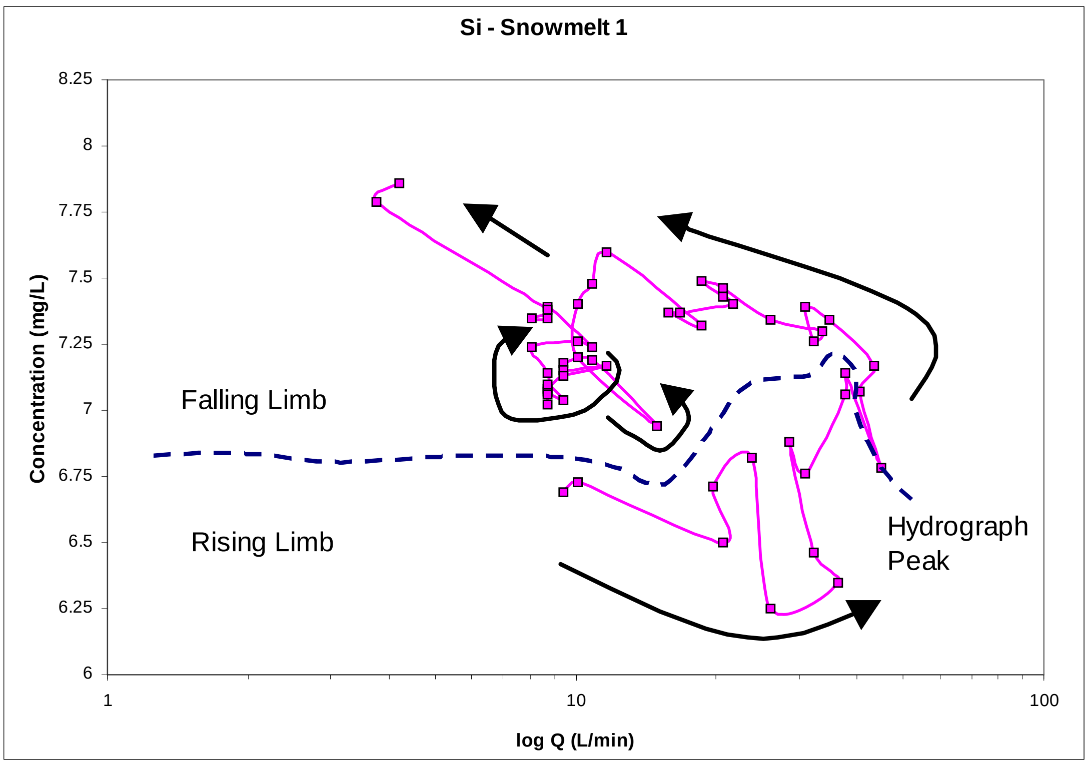

Figure 4.6. Si concentration versus log discharge for Snowmelt Event 1.

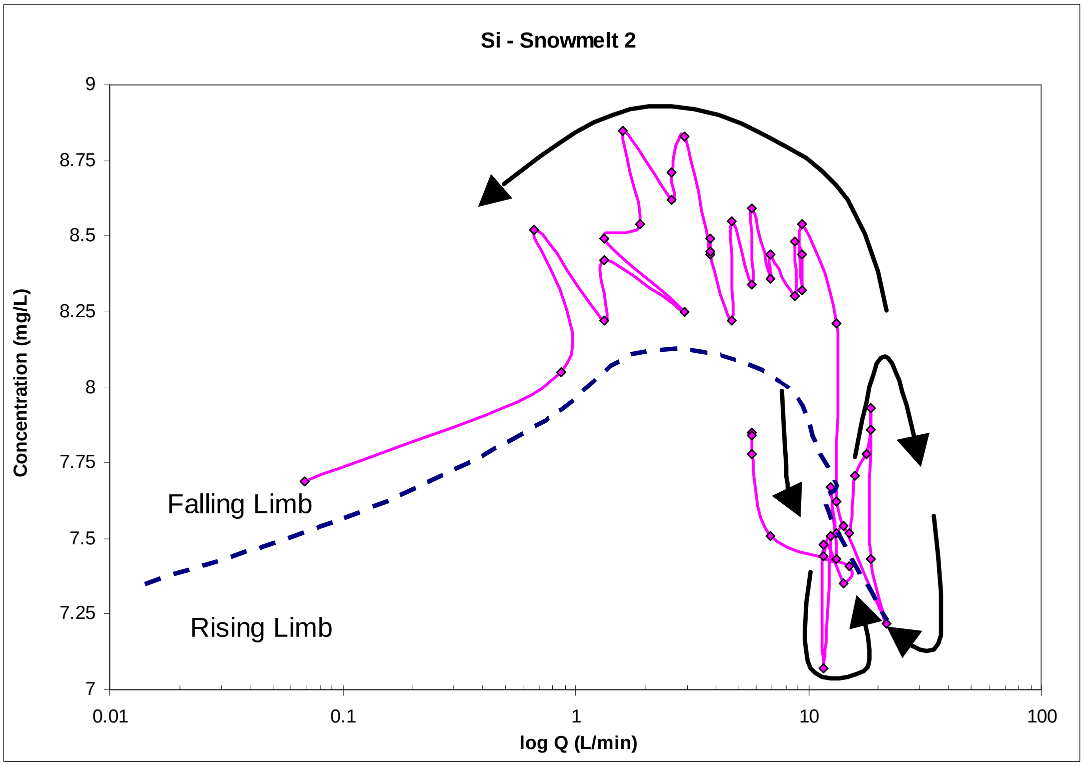

Figure 4.7. Si concentration versus log discharge for Snowmelt Event 2.

4.1.2 Hydrograph Separation

A two-component hydrograph separation was completed for SM1 with electrical conductivity (EC) as the tracer. The hydrograph separation was not completed on SM2 due to a malfunction with the electrical conductivity sensor at the end of March 2001. The SM1 EC hydrograph was separated into 59% event water (snowmelt) and 41% pre-event water (soilwater) (Figure 4.8).

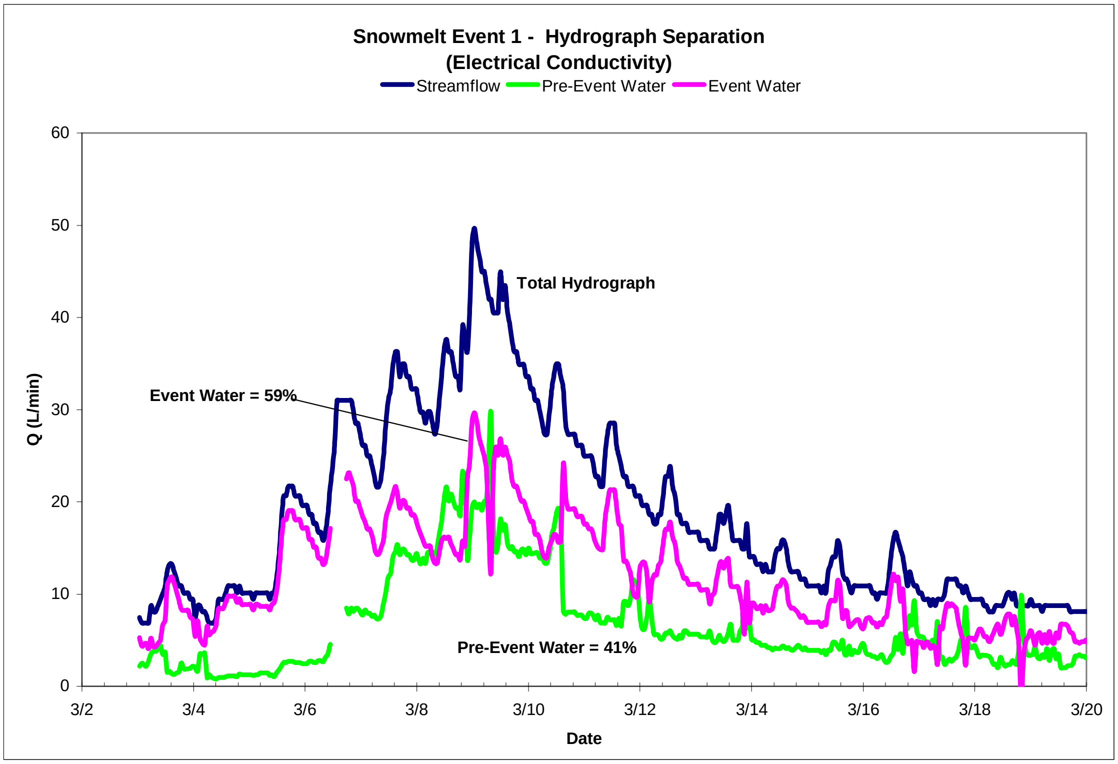

Figure 4.8. Snowmelt event 1 electrical conductivity hydrograph separation.

4.1.3 End-Member Mixing Analysis (EMMA)

4.1.3.1 Snowmelt Event 1

Six two-dimensional plots were constructed by plotting each of the four solutes chosen for EMMA against one another (Figure 4.9). The possible end-members, deep soilwater, shallow soilwater, groundwater, and snowmelt that were sampled in UDCEW did not bound the streamwater samples for SM1 (Figure 4.9). For SM1, it is evident that a silica source was not sampled. Additional soilwaters, other than those sampled are needed to explain the streamwater chemistry. A hypothesized end-member to represent the soil-bedrock interface (weathered in place granitic bedrock) water for each snowmelt event was developed. The hypothesized end-member assumes that the solutes Ca^{+2},

Mg^{+2}, and Na^{+1} are saturated in the soilwater and the silica concentration continues to increase with depth. This assumption was made since the soilwater and snowmelt sampled end-member concentrations for Ca^{+2}, Mg^{+2}, and Na^{+1} are very similar to the observed streamwater concentrations for those solutes. The groundwater spring samples and Dry Creek baseflow samples silica concentrations were used as a guide for the silica concentrations in the hypothesized end-member. The hypothesized end-member was chosen to "bound" the stream water samples in conjunction with the two other end-members (soilwater and snowmelt).

Additional evidence for the hypothesized end-member is provided by comparison of the SHAW water balance lateral flow component and streamwater silica concentration.

Figure 4.10 illustrates that when there is a rise in the deep percolation component of the modeled water balance (assumed to be lateral flow) the silica concentration in the stream increases concurrently.

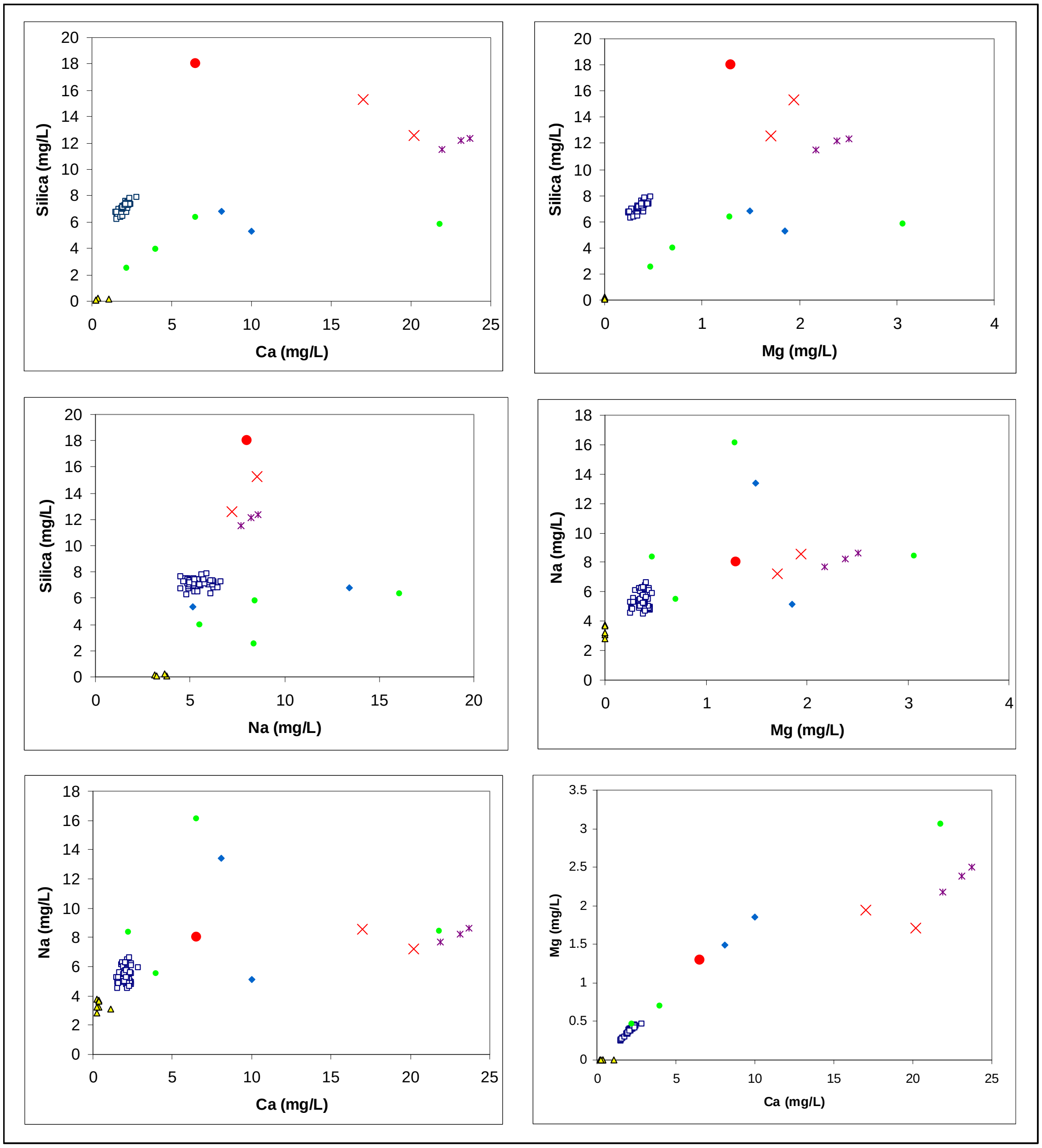

Figure 4.9. UDCEW snowmelt 1 pairwise plots.
Blue Square – Streamwater samples, blue diamond – soilwater shallow, green circle – soilwater deep, red x – springs, * - Main Dry Creek baseflow, yellow triangle, and red circle – hypothesized end-member.

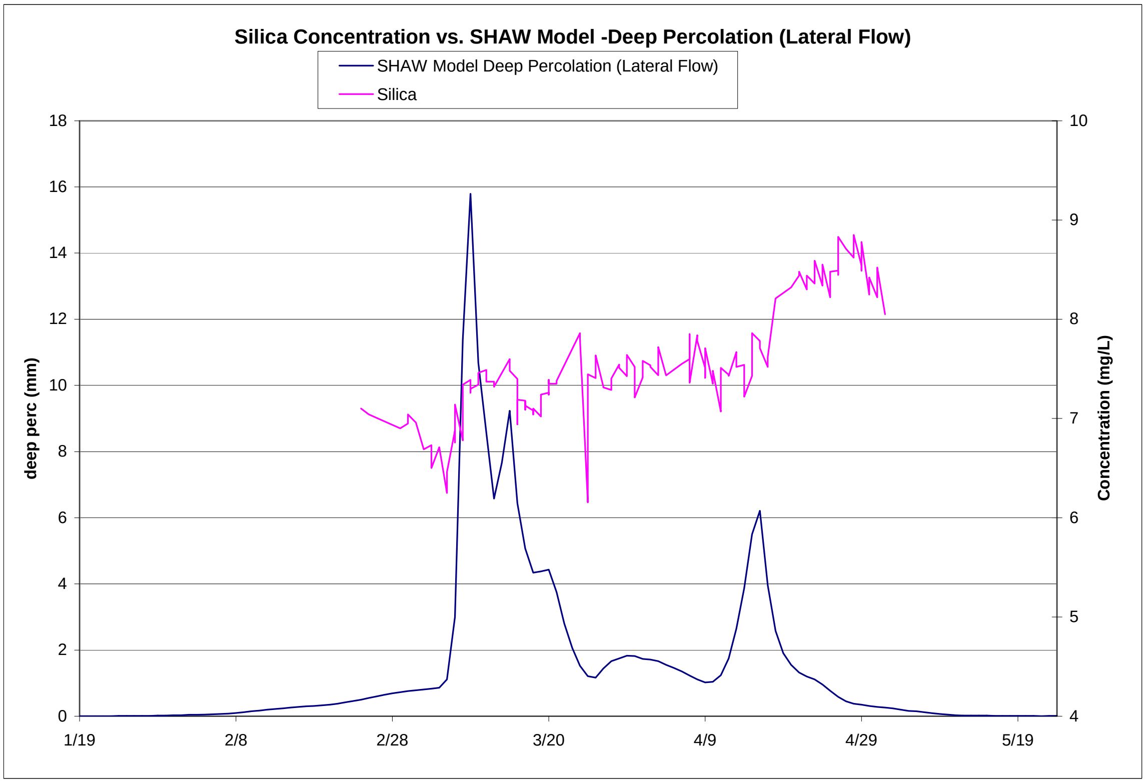

Figure 4.10. UDCEW SHAW model deep percolation component compared to streamwater silica concentration.

The hypothesized end-member was developed in order to test the hypothesis that an un-sampled soil-bedrock interface water source is activated during snowmelt events and contributes to streamflow. The hypothesized end-member, snowmelt and all soilwater bound streamwater samples in all pairwise plots for SM1 (Figure 4.9).

The PCA that was used in SM1 EMMA incorporated four solutes (Ca^{+2}, Mg^{+2}, Na^{+1}, Si^{+4}). The first two principal components accounted for 93% of the variability in the SM 1 data set (Appendix C). EMMA was completed a total of three times with different end-members for SM1. EMMA was completed twice with the sampled end-members that did not bound the solute concentrations of the streamwater samples illustrated in Figure 4.9. First, EMMA was completed with soilwater, groundwater and snowmelt representing the end-members in EMMA. Second, soilwater deep (60 cm depth), soilwater shallow (30 cm depth), and snowmelt were used in EMMA to represent the end-members. SM1 EMMA was completed a third time with the soilwater, snowmelt and the hypothesized soil-bedrock interface end-members. The streamwater data was plotted in U space, as defined by the correlation matrix. The compositions of the end-members are defined by the median solute values, must be extreme points and outside the observed data in order to explain the mixture (Christopherson and Hooper, 1992).

4.1.3.1.1 SM1 EMMA End-Members: Soilwater, Groundwater and Snowmelt

The mixing plot for SM1 using the sampled end-members, soilwater, groundwater and snowmelt illustrate that the three end-member solutions do not adequately describe the streamwater samples, none of the observed samples are contained in the U-space mixing triangle (Figure 4.11).

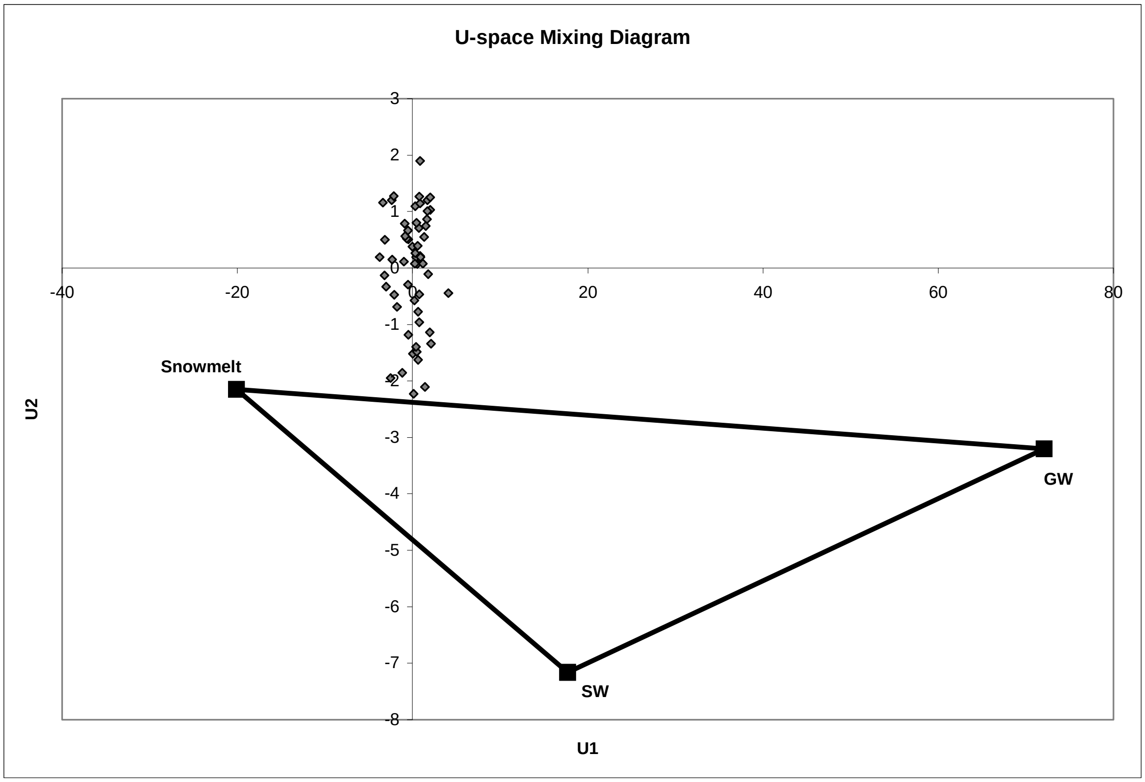

Figure 4.11. SM1 EMMA mixing plot representing soilwater, groundwater, and snowmelt end-members.

The goodness-of-fit between the observed and predicted streamwater concentrations provides a validity test of the end-member choice. If the predictions do not match the observations for one or more of the solutes, the end-member choice is suspect (Hooper et al., 1990). A comparison of the predicted concentrations with the observed streamwater concentrations for this EMMA is presented in Figure 4.12. Each solute provides an independent test of end-members because there's no balance constraint imposed by EMMA (Hooper et al., 1990). The percent of variance is explained by the r^2, which ranges from 4% for sodium and 96% for calcium. The magnesium is well predicted (r2 = 0.94) supporting the assumption of conservative mixing, silica has a lower r^2 value (r^2 =0.77) than calcium and magnesium, suggesting an end-member has not been properly constrained or silica does not behave conservatively in UCDEW. The silica median values for the end-members used in this EMMA range from 0.39 mg/L to 12.36 mg/L. These concentration values under-predict the silica concentration in EMMA as compared to the observed streamwater silica concentrations. Sodium shows a substantial lack of fit with a r^2 value of 0.04. The pattern of EMMA predictions for the sodium suggests that the concentrations of sodium is too high in one of the end-members accounting for the over-prediction of sodium by EMMA or the other the ratio of sodium to other ions is incorrect in at least one of the end-members.

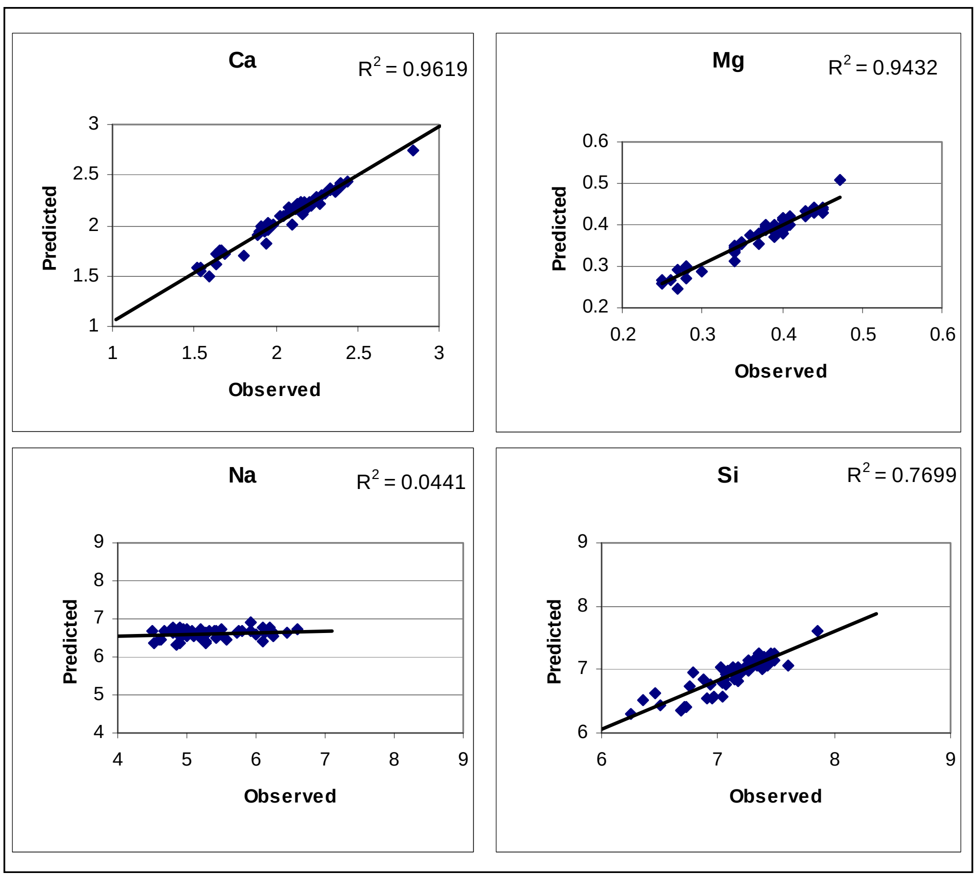

Figure 4.12. SM1 predicted versus observed concentrations from EMMA completed using soilwater, groundwater, and snowmelt end-members.

Residuals are another method to compare the EMMA predicted versus observed solute concentrations. Residuals are defined as the predicted solute concentrations minus the observed solute concentrations. Over-predictions of solute concentrations are represented by positive residual values and under-predictions are represented by negative residual values. The residuals of the calcium, magnesium, and sodium show very little variation between solutes, and each is under-predicted in EMMA completed with soilwater, groundwater, and snowmelt end-members. Sodium is over-predicted by EMMA (Figure 4.13)

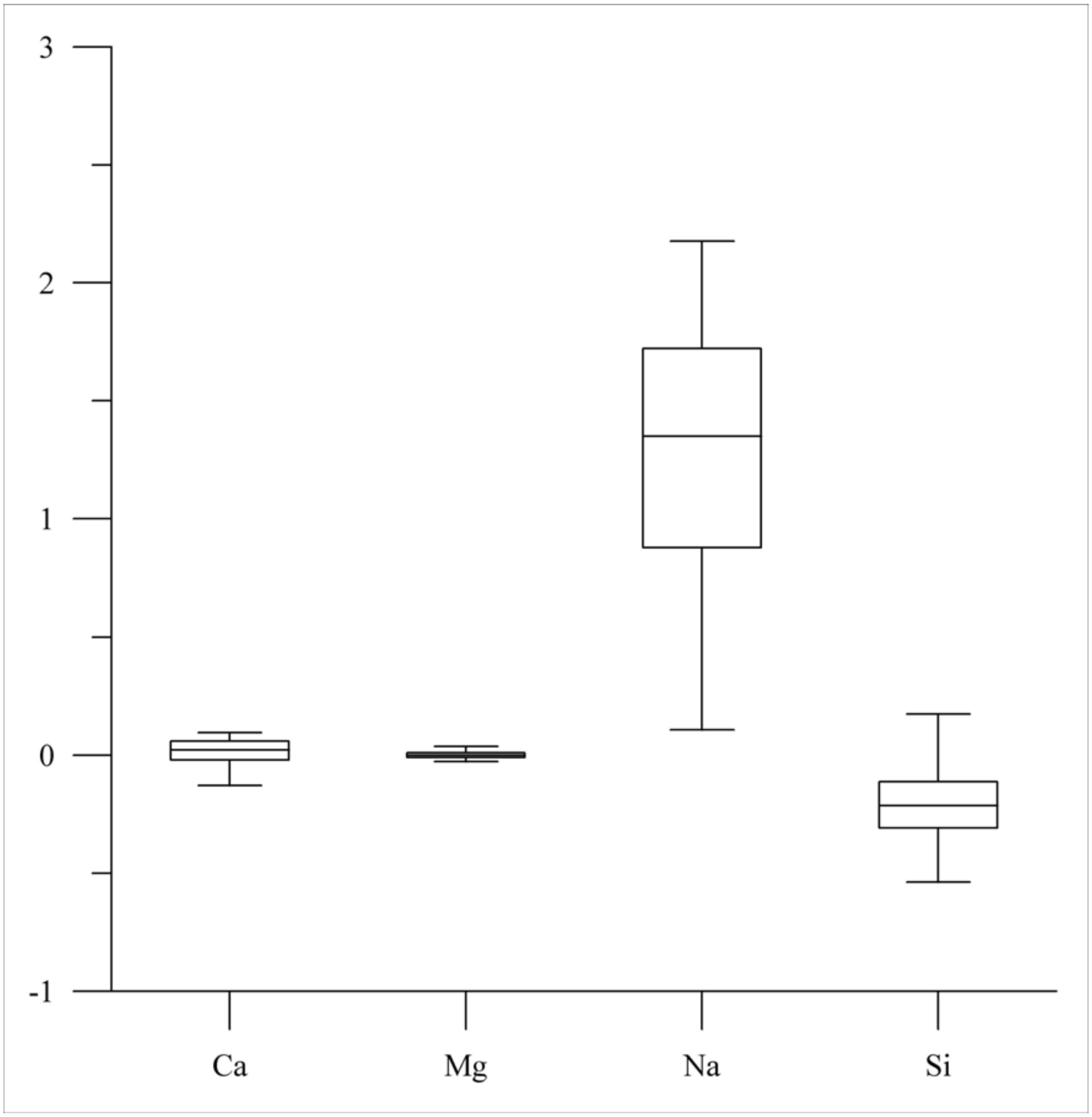

Figure 4.13. Boxplots of the residuals for SM1 EMMA representing soilwater, groundwater, and snowmelt end-members.

4.1.3.1.2 SM1 EMMA End-Members: Soilwater deep, Soilwater shallow, and Snowmelt

The mixing plot for SM1 using the sampled end-members, soilwater deep, soilwater shallow and snowmelt, shows that the three solutions do not adequately describe the streamwater samples, since none of the observed streamwater samples are contained in the U-space mixing triangle (Figure 4.14).

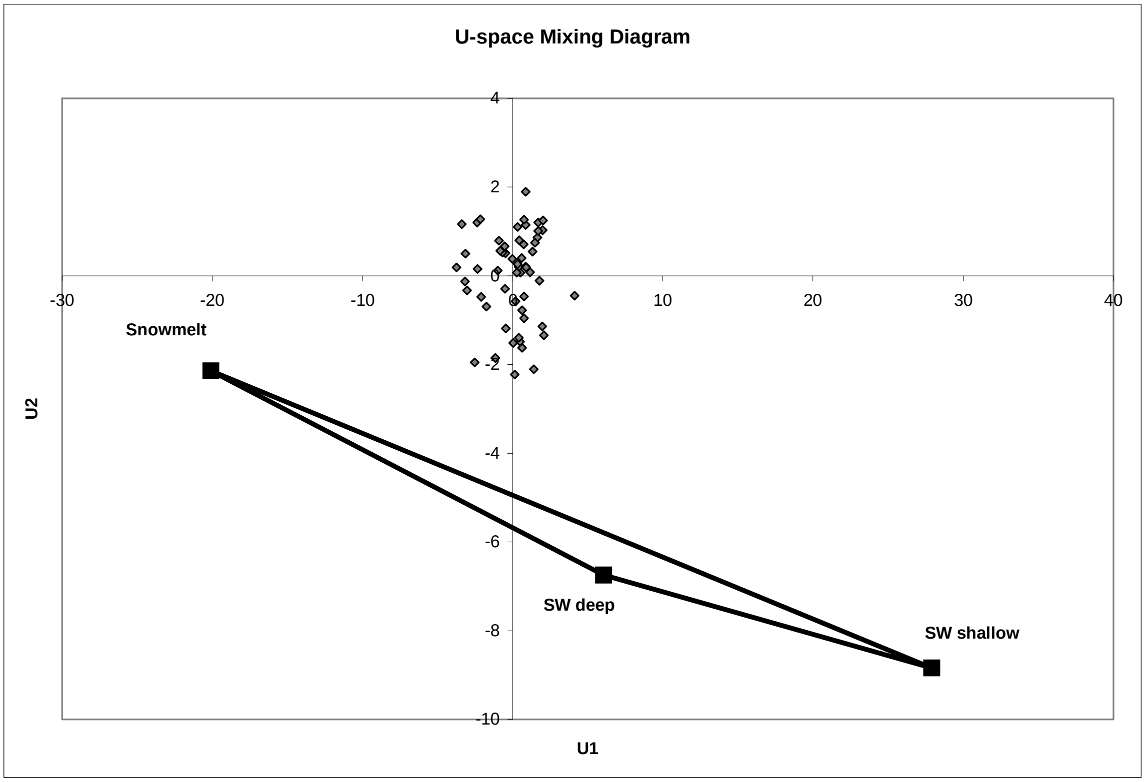

Figure 4.14. SM1 EMMA mixing plot representing soilwater deep, soilwater shallow, and snowmelt end-members.

The goodness-of-fit for the predicted versus observed streamwater concentrations indicated that both sodium and silica were not well predicted by EMMA (Figure 4.15). The percent of variance is explained by the r^2, which ranges from 8% for sodium and 96% for calcium. The magnesium is well predicted (r^2 = 0.94) supporting assumption of conservative mixing. Silica has a lower r^2 value (r^2 = 0.72) than calcium and magnesium suggesting that an end-member has not been properly constrained or silica does not behave conservatively in UDCEW. The highest median silica value of an end-member was 6.075 mg/L, which is too low to account for the streamwater observations ranging from 6.25 to 7.86 mg/L. Sodium shows a substantial lack of fit r^2 value of 0.08. The pattern of the EMMA predictions for the sodium suggests that either the concentrations for sodium are too high in one end-member accounting for the over-prediction of sodium or the ratio of sodium to other ions is incorrect in at least one of the end-members. The median sodium concentration from the deep soilwater and shallow soilwater end-members, 8.39 mg/L and 9.28 mg/L, respectively, are too high to account for stream observations, which range from 4.5 mg/L and 6.61 mg/L. The high sodium concentrations in both the deep and shallow soilwater samples maybe the result of evapotranspiration during the spring and summer months. During the dry times, the sodium precipitate remains in the soil profile and is mobilized in the fall rain events. Hooper et al. (1990) found that the using the median concentration values does not account for such temporal variations.

The residuals of the calcium, magnesium, and silica show very little variation between the solutes and each is under-predicted in SM1 EMMA completed with soilwater deep, soilwater shallow, and snowmelt. Sodium is over-predicted by EMMA (Figure 4.16).

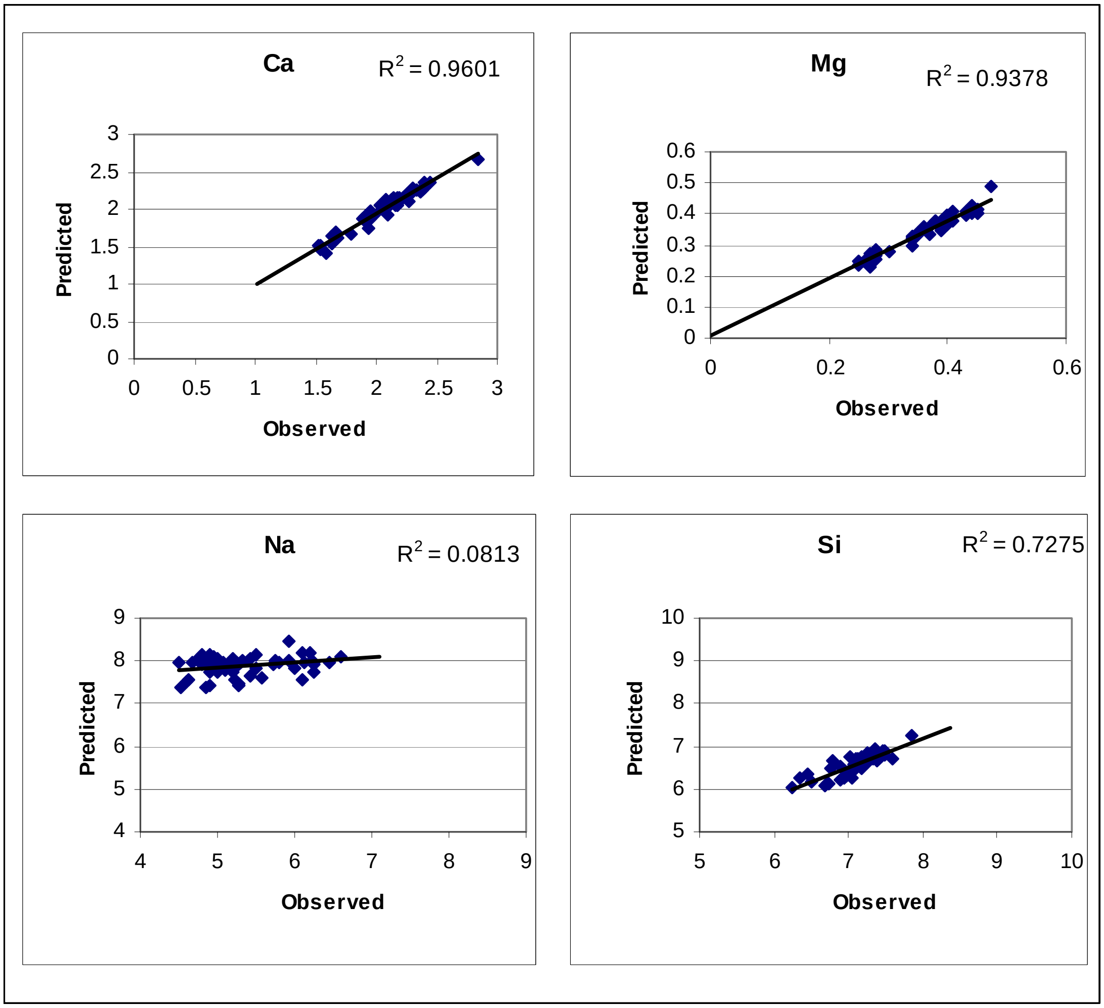

Figure 4.15. SM1 predicted and observed concentrations for EMMA completed with soilwater deep, soilwater shallow, and snowmelt end-members.

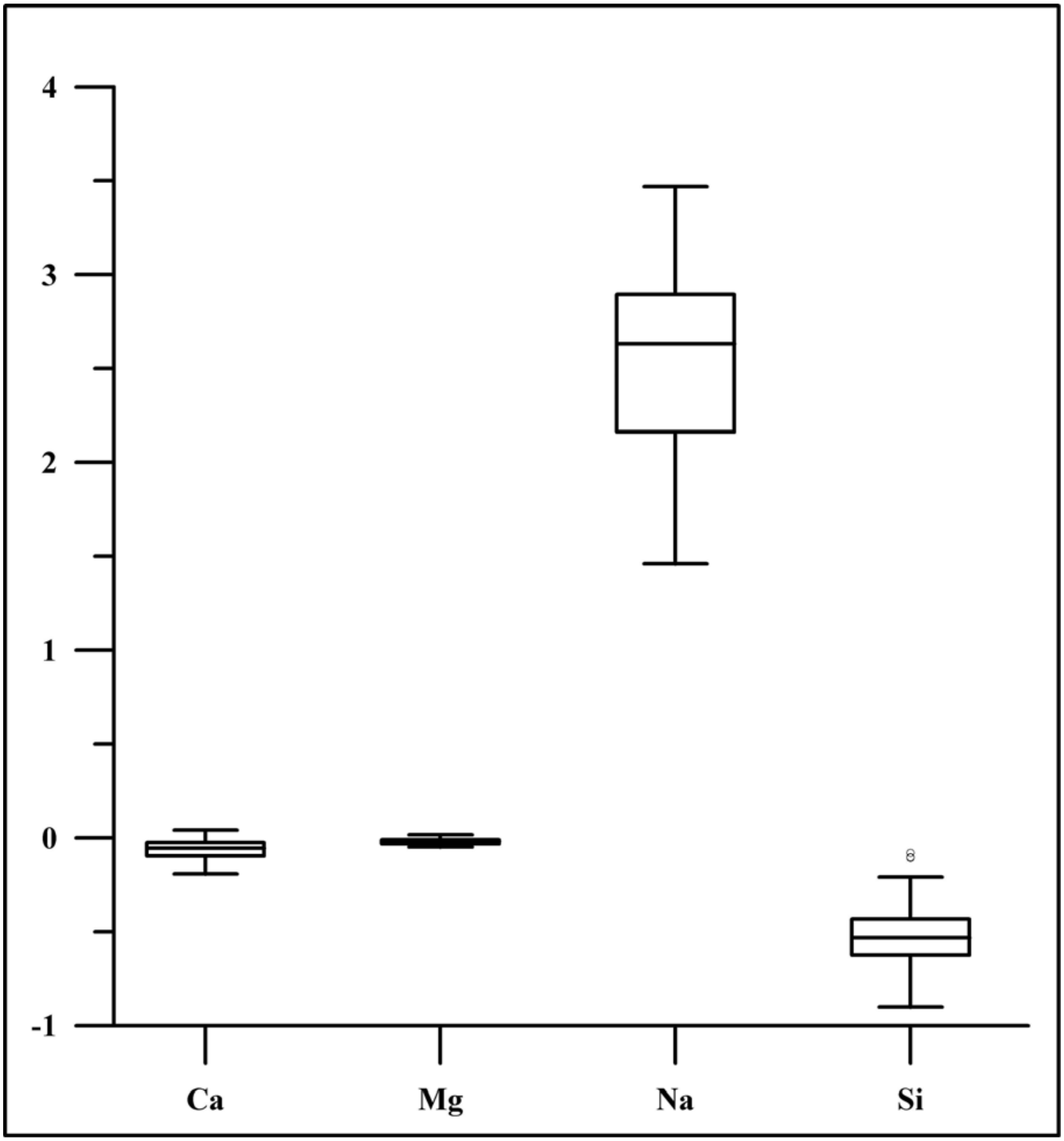

Figure 4.16. Box plots of residuals for SM1 EMMA completed with soilwater deep, soilwater shallow, and snowmelt end-members.

4.1.3.1.3 <u>SM1 EMMA End-Members: Soilwater, Soil-Bedrock Interface, Snowmelt</u>

Examination of the pairwise plots and the mixing diagrams projected into U space indicated that the end-member for silica concentration was not identified. The hypothesized soil-bedrock interface end-member was developed to bound the streamwater samples and an attempt to improve the fit of the model. The observed streamwater sampled projected into U-space are better contained in the mixing triangle in this model (Figure 4.17). The goodness-of-fit for the observed streamwater concentrations versus the EMMA predicted concentration was improved for all solutes (Figure 4.18). The percent of variance is explained by the r^2, which ranges from 82.8% for sodium and 96% for calcium, indicating better end-member identification. The residuals of the calcium and magnesium show very little variation between the solutes and each is slightly under-predicted in SM1 EMMA hypothesized. Both silica and sodium range from under-predicted to over-predicted in EMMA hypothesized (Figure 4.19).

The EMMA hypothesized results were used to complete a three-component hydrograph separation for SM1 (Figure 4.20). The snowmelt end-member dominated the event hydrograph contributing 65% of the discharge, the soilwater end-member contributed 7% of discharge, and the soil bedrock hypothesized end-member contributed 28% of discharge.

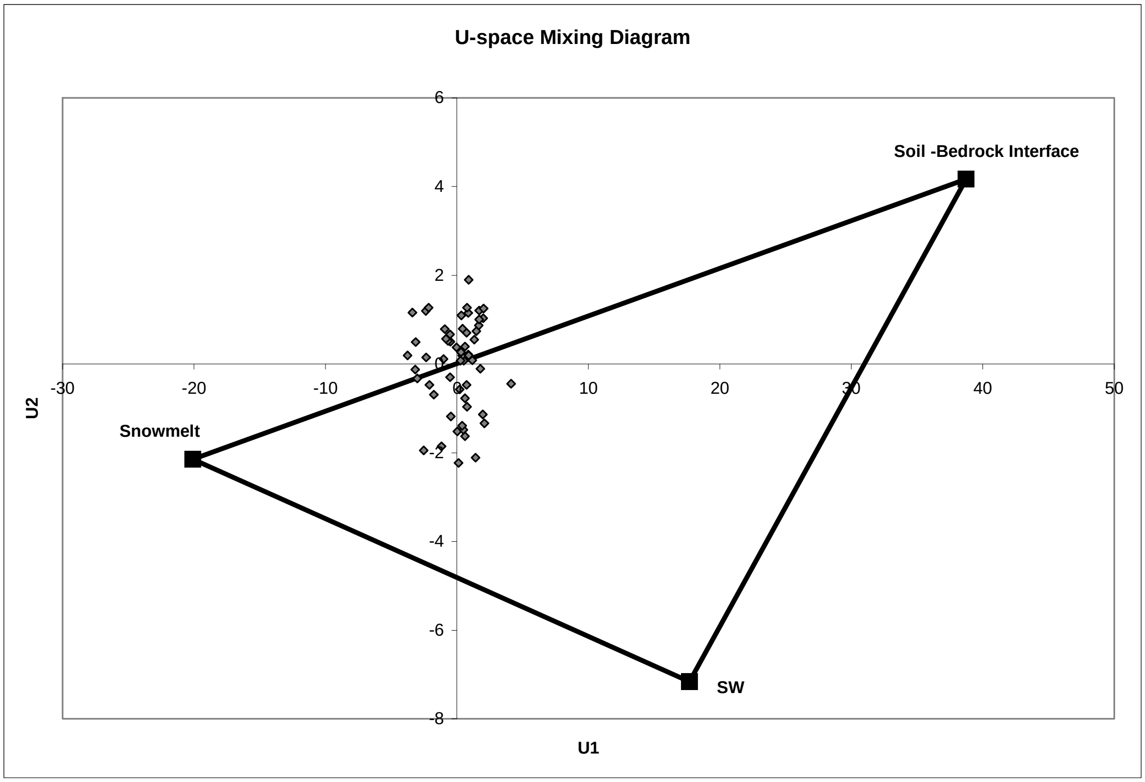

Figure 4.17. SM1 EMMA mixing plot representing hypothesized soil-bedrock interface, soilwater, and snowmelt end-members.

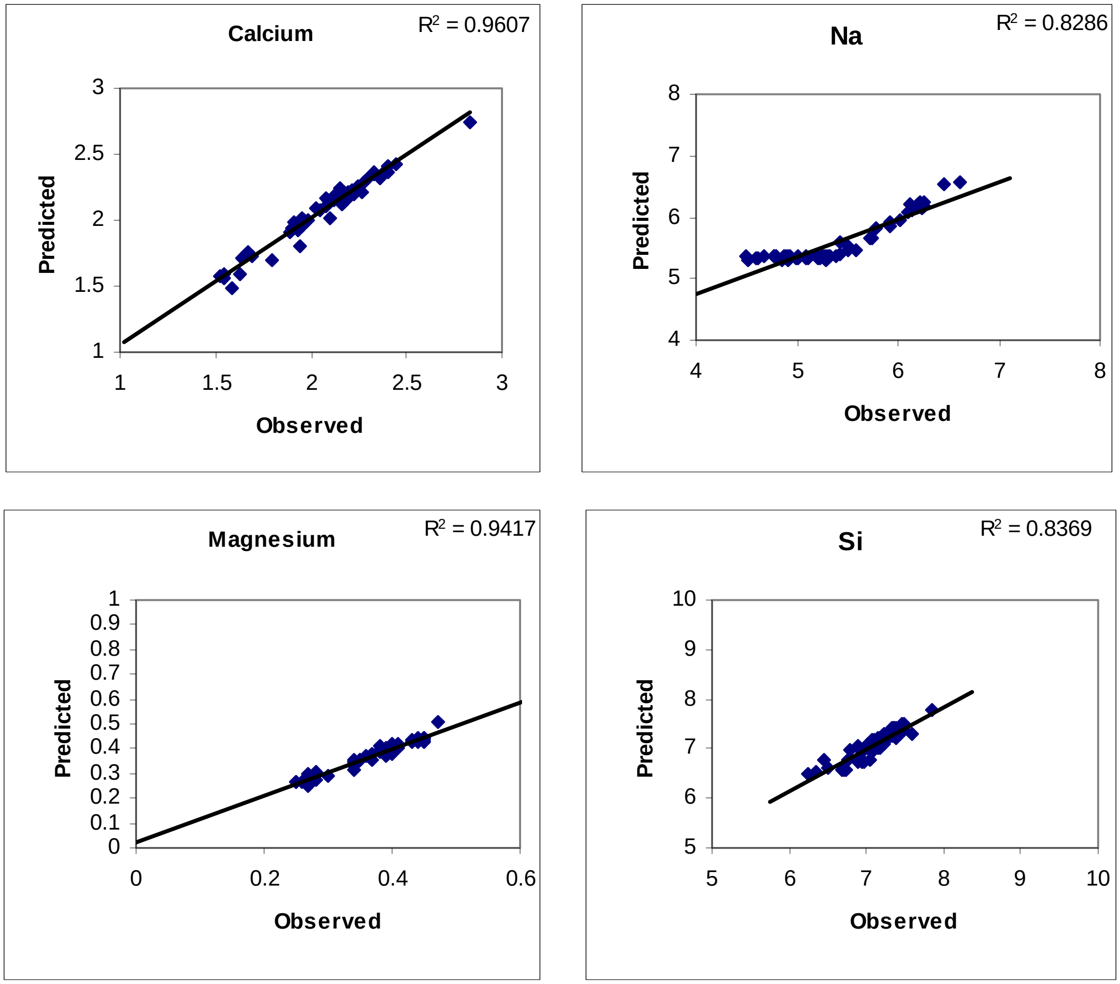

Figure 4.18. SM 1 predicted versus observed concentrations for EMMA completed with soil-bedrock interface, soilwater, and snowmelt end-members.

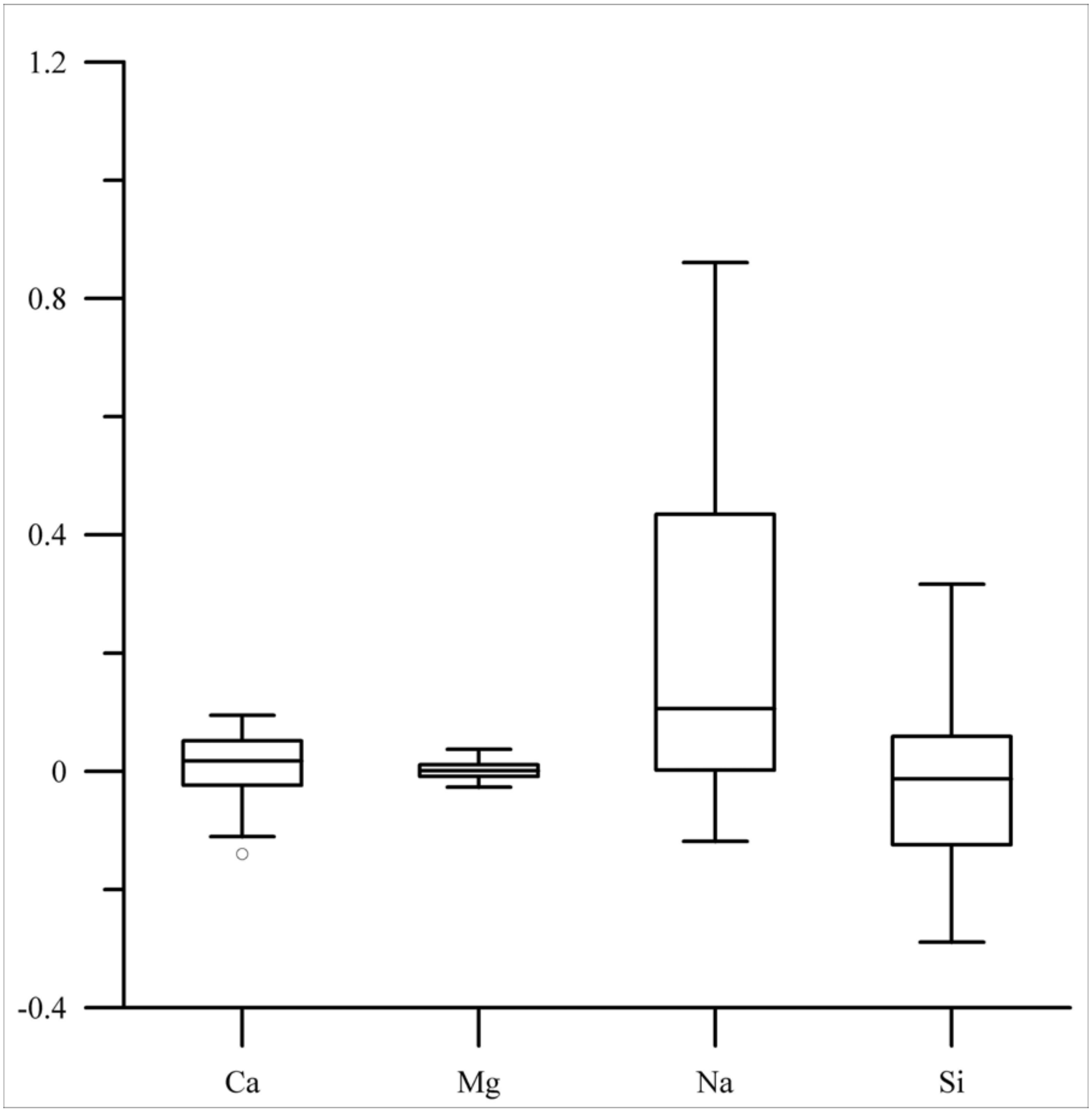

Figure 4.19. Box plots of residuals for SM1 EMMA representing soil-bedrock interface, soilwater, and snowmelt end-members.

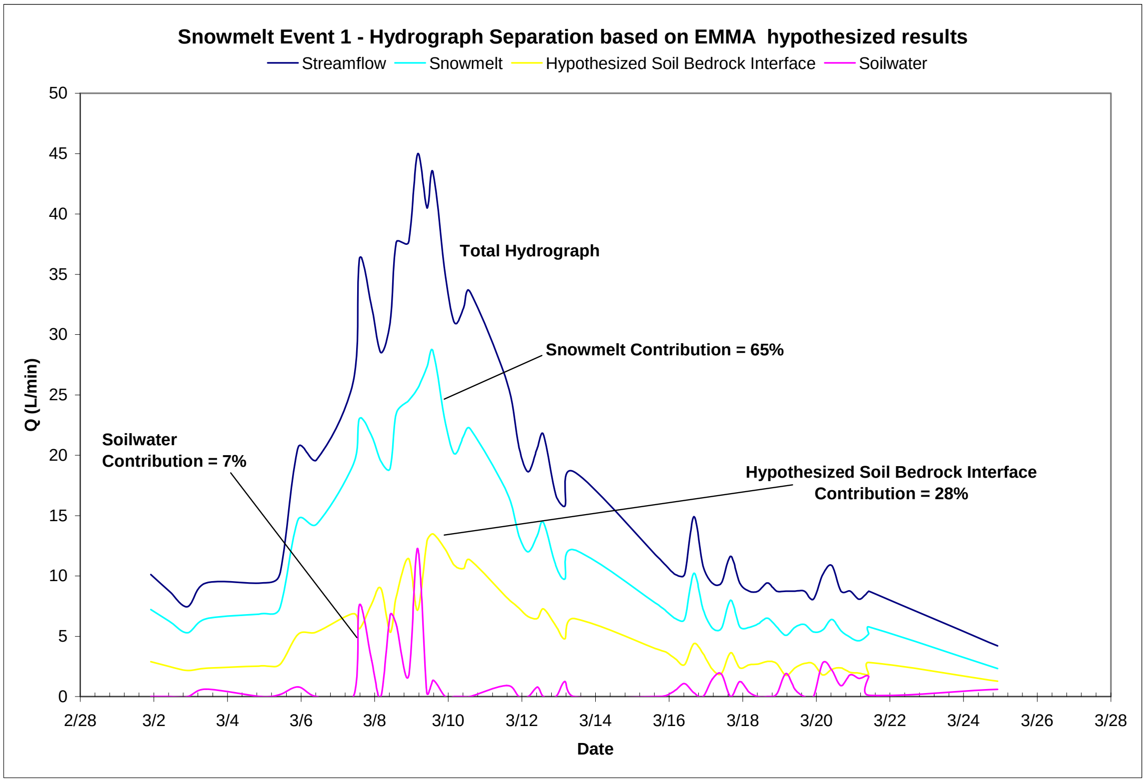

Figure 4.20. Hydrograph separation for SM1 based on EMMA completed with the soil-bedrock interface, soilwater, and snowmelt end-members.

4.1.3.2 Snowmelt Event 2

Six two-dimensional plots were constructed by plotting each of the four solutes chosen for EMMA against one another (Figure 4.21). The possible end-members, soilwater deep, soilwater shallow, and snowmelt that were sampled in UDCEW did not bound the streamwater samples for SM2. In SM2 it is evident that a silica source was not sampled. The hypothesized soil-bedrock end-member was also used in EMMA for SM2 as an attempt to better enclose the streamwater observations in the mixing triangle.

The PCA that was used in SM 2 EMMA also incorporated four solutes (Ca, Mg, Na, Si) in which the first two principal components accounted for 87% of the variability in the SM2 data set (Appendix D).

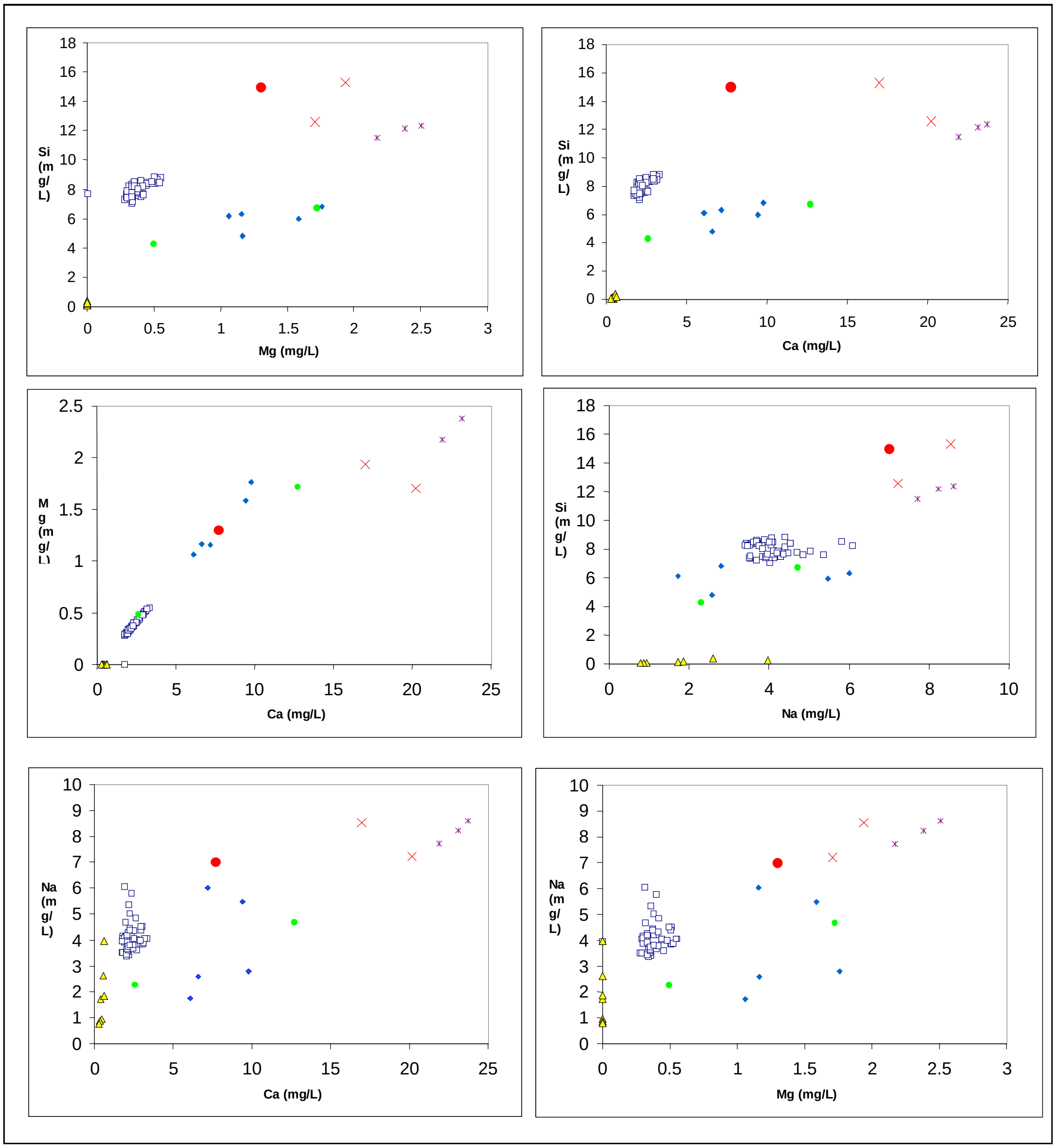

Figure 4.21. UDCEW snowmelt 2 pairwise plots.
Blue Square – Streamwater samples, blue diamond – soilwater shallow, green circle – soilwater deep, red x – springs, * - Main Dry Creek baseflow, yellow triangle, and red circle – hypothesized end-member.

4.1.3.2.1 SM2 EMMA End-Members: Soilwater, Groundwater, and Snowmelt

The mixing plot for SM2 using soilwater, groundwater, and snowmelt illustrates that the three solutions does not adequately describe the streamwater samples, only a small number of the samples are contained in the mixing triangle (Figure 4.22).

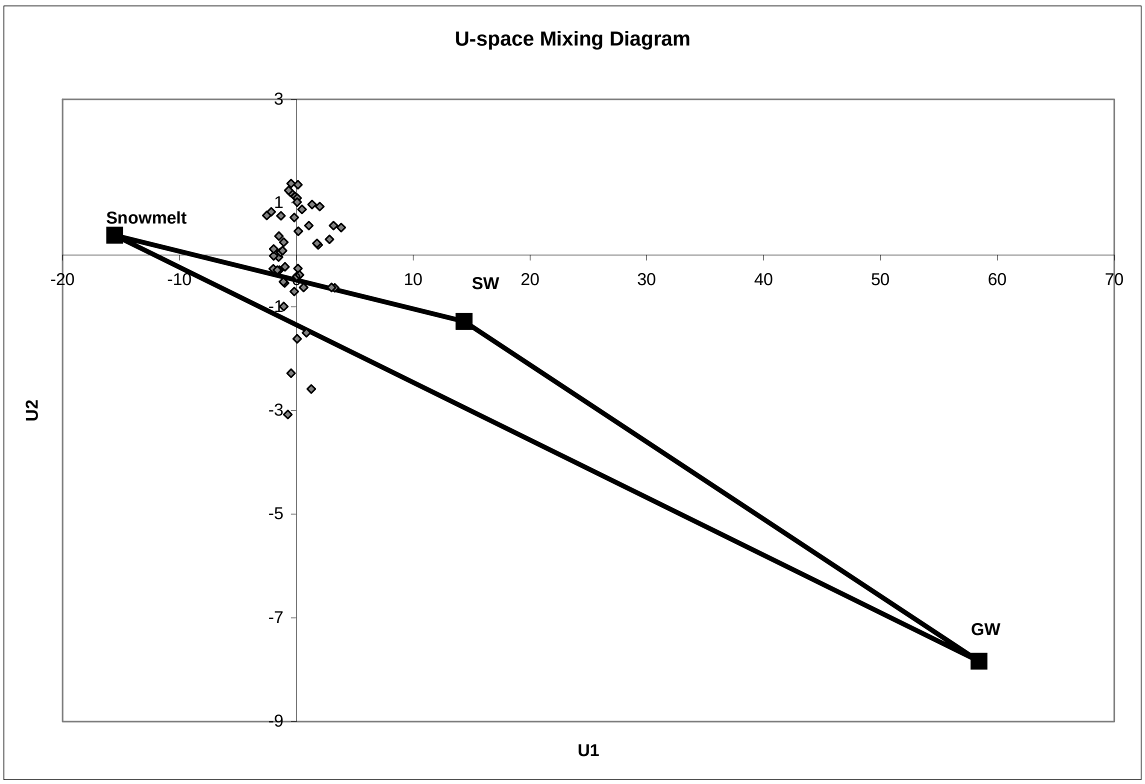

Figure 4.22. SM2 EMMA mixing plot representing soilwater, groundwater, and snowmelt end-members.

The goodness-of-fit for the EMMA predicted concentrations versus the observed streamwater concentrations indicates that the end-members were not properly constrained (Figure 4.23). The percent of variance is explained by the r^2, which ranges from 5% for calcium to 45% for silica. All solutes have low r^2 values suggesting that an end-member has not been properly constrained.

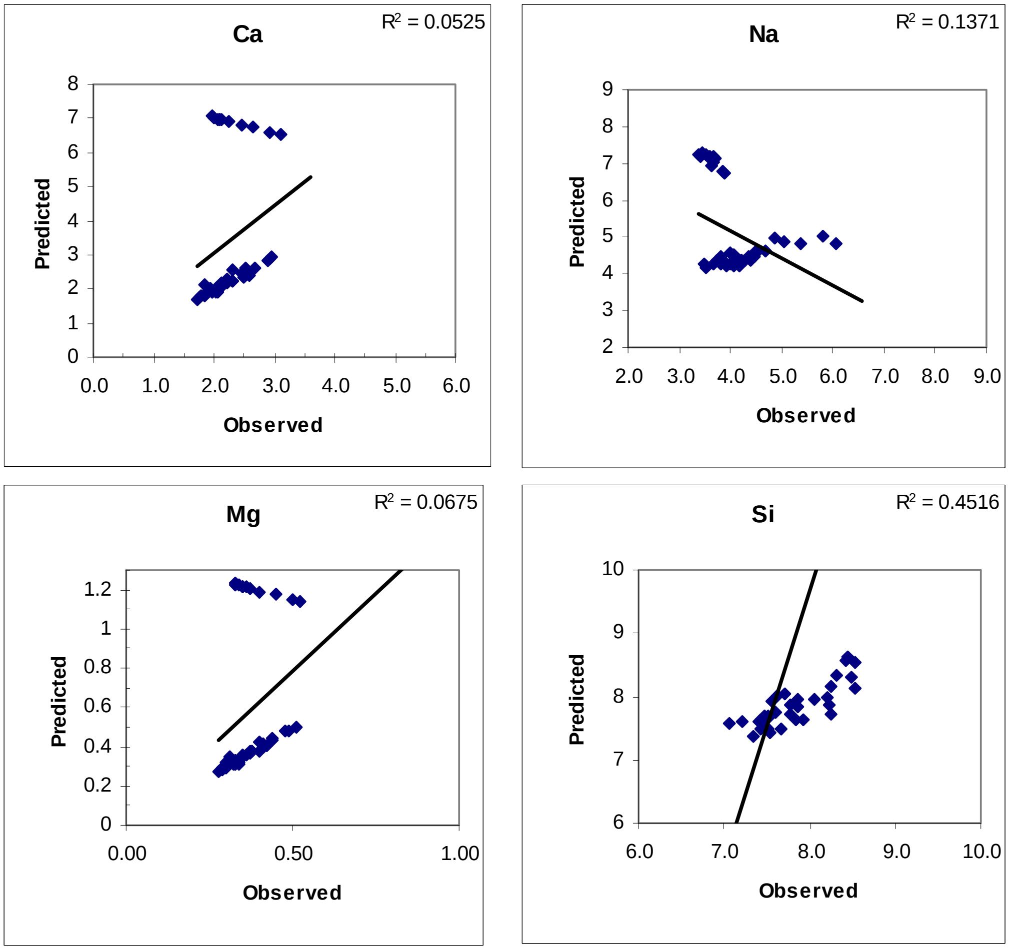

Figure 4.23. SM2 predicted versus observed concentrations for EMMA completed with groundwater, soilwater, and snowmelt end-members.

The residuals for SM2 for this EMMA show very little variation between the solutes as related to the median. The range of values is larger for all solutes with sodium and silica showing over- and under predictions of concentration and calcium and magnesium over predictions (Figure 4.24).

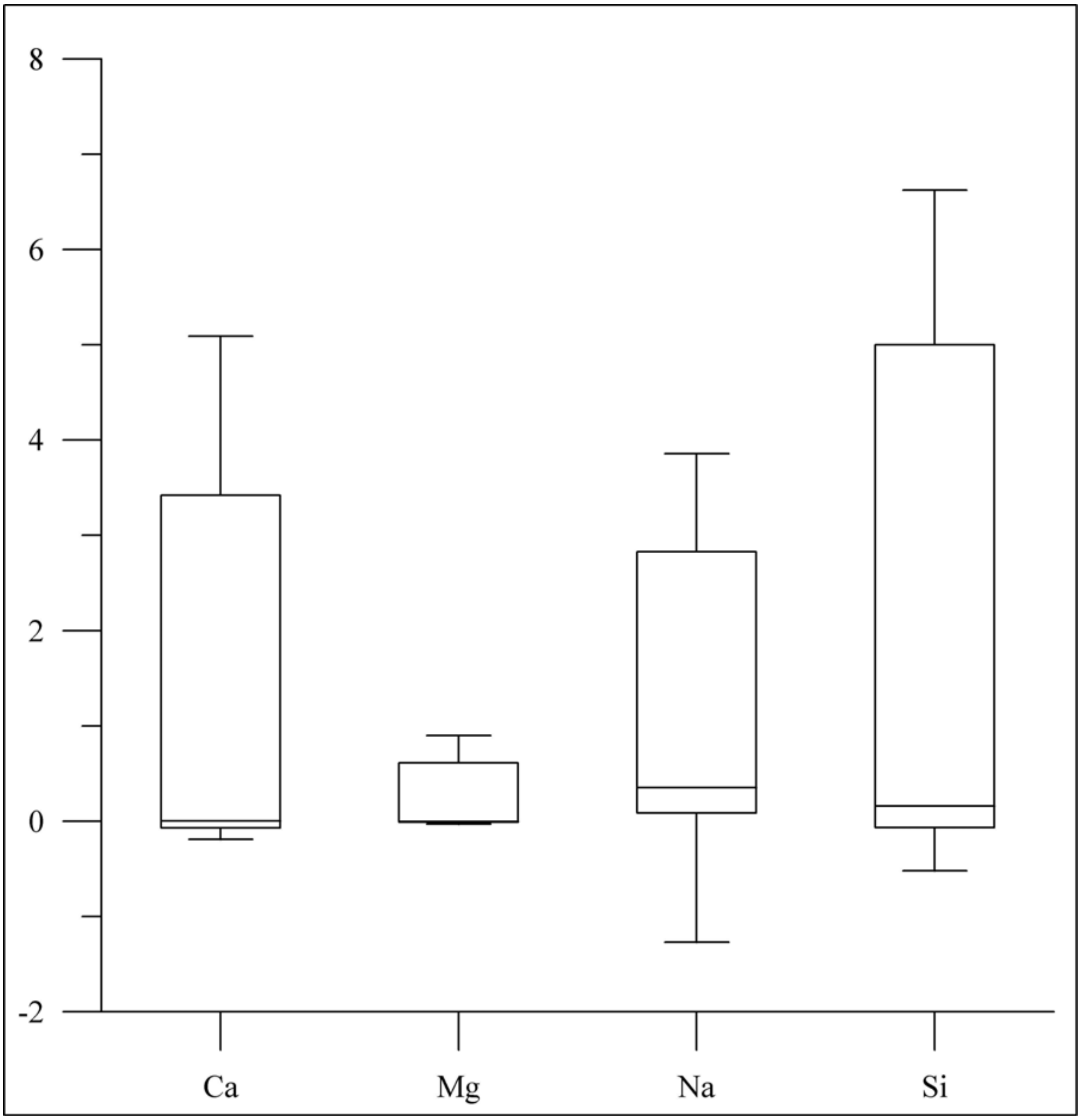

Figure 4.24. SM2 residuals for EMMA completed with groundwater, soilwater, and snowmelt end-members.

4.1.3.2.2 SM2 EMMA End-Members: Soilwater deep, Soilwater shallow, and Snowmelt

The mixing plot for SM2 using soilwater deep, soilwater shallow, and snowmelt illustrates that a small portion of the observed streamwater samples fall within the mixing triangle (Figure 4.25).

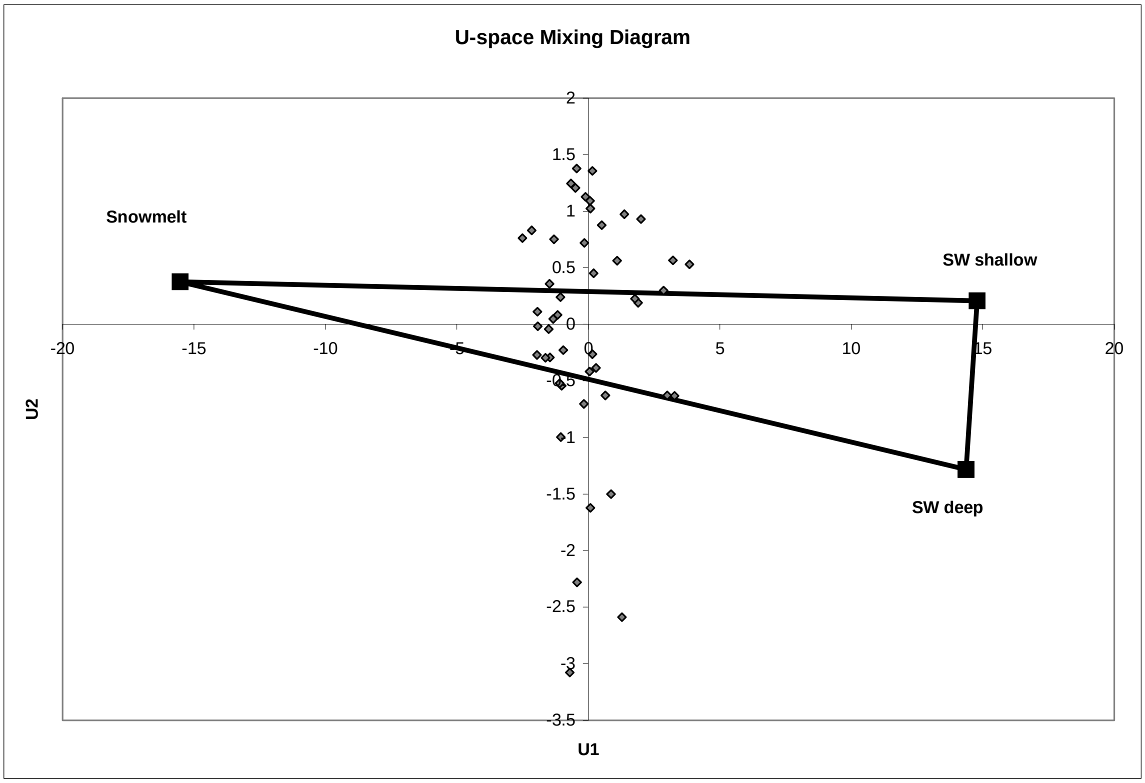

Figure 4.25. SM2 EMMA mixing plot representing soilwater deep, soilwater shallow, and snowmelt end-members.

The comparison of the predicted concentrations with the observed streamwater concentrations illustrates the goodness-of-fit for this EMMA (Figure 4.26). The percent of variance is explained by the r^2, which ranges from 63% for sodium and silica and 94% for magnesium. The calcium and magnesium are well predicted (r^2 = 0.91 and r^2 = 0.94, respectively) supporting the assumption of conservative mixing. Silica and sodium have a lower r^2 values (r^2 = 0.63) than calcium and magnesium suggesting that an end-member has not been properly constrained or the solutes do not behave conservatively in UDCEW. The highest median silica value of an end-member was 6.15 mg/L, which are too low to account for the streamwater observations ranging from 7.07 to 8.71 mg/L. The median sodium concentration was from the soilwater deep and shallow end-members, 3.5

mg/L and 2.8 mg/L, respectively, which are too low to account for stream observations, which range from 3.4 mg/L and 6.0 mg/L.

The residuals for this EMMA show very little variation between the solutes as related to the median. The range of values is larger for sodium and silica showing more over- and under predictions of concentration than calcium and magnesium (Figure 4.27).

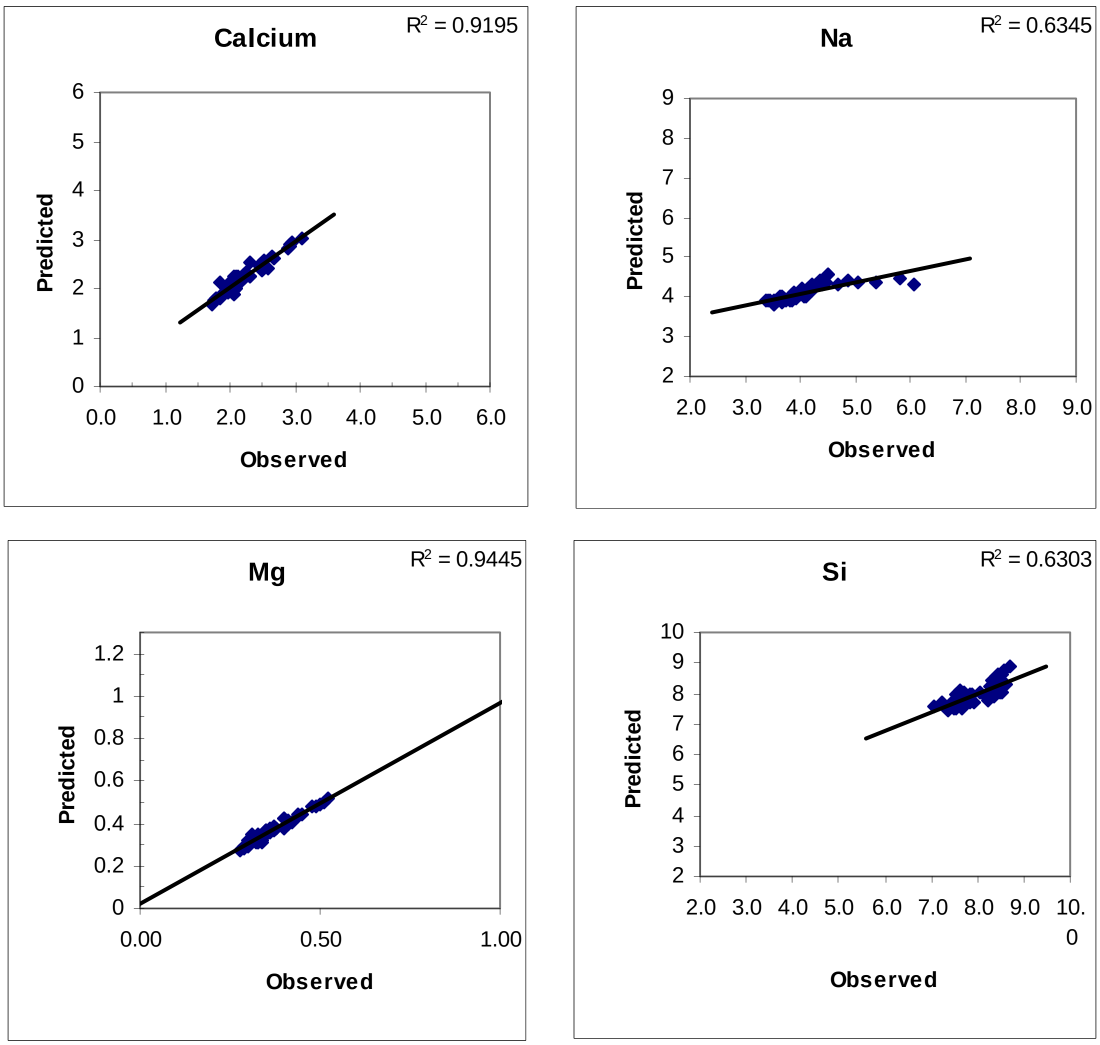

Figure 4.26. SM2 predicted versus observed concentrations for the solutes in the EMMA completed with soilwater deep, soilwater shallow, and snowmelt end-members.

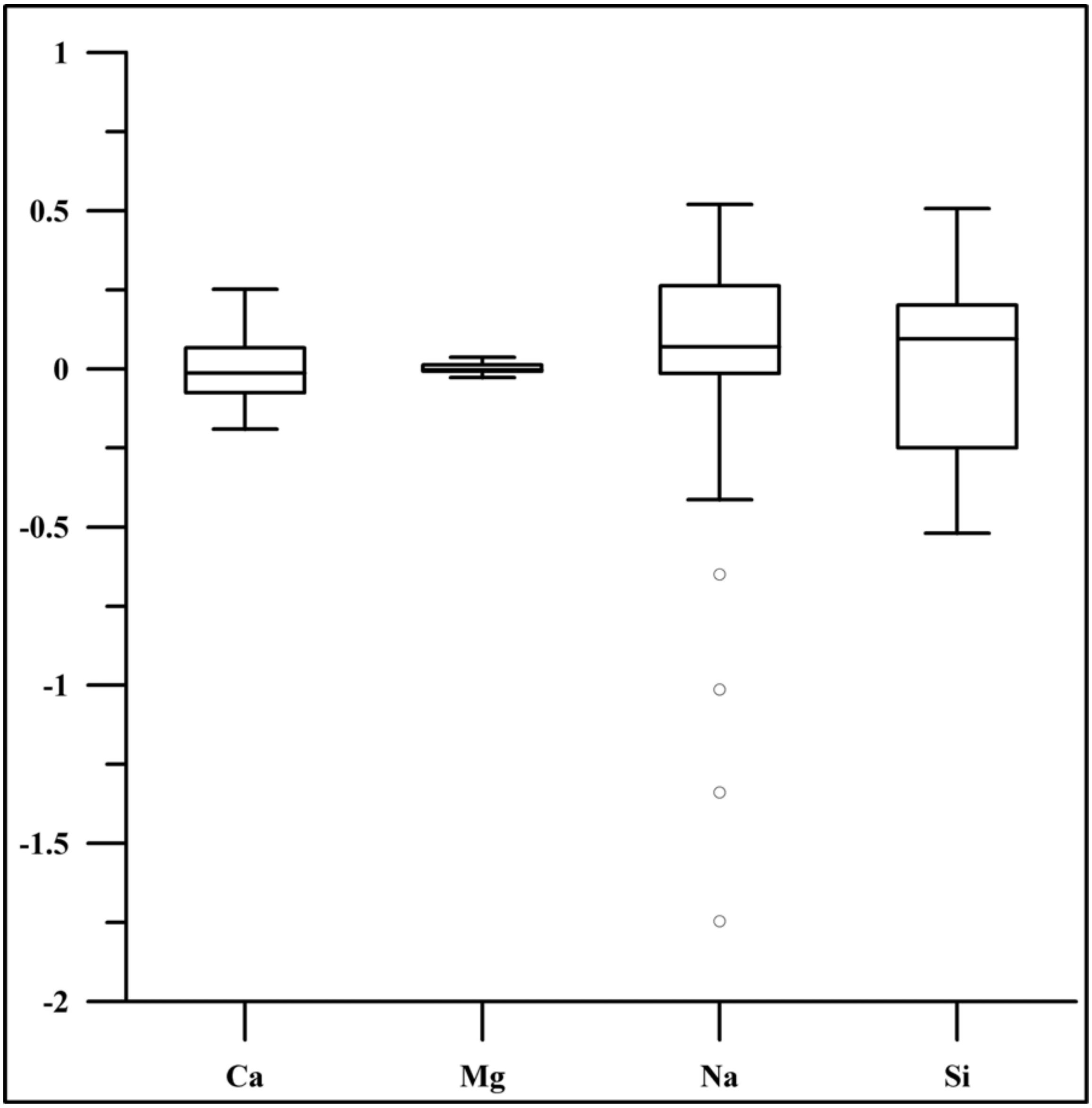

Figure 4.27. Box plots of residuals for SM2 EMMA completed with soilwater deep, soilwater shallow, and snowmelt end-members.

4.1.3.2.3 SM2 EMMA End-Members: Soilwater, Soil-Bedrock Interface, and Snowmelt

The observed streamwater sampled projected into U-space are better contained in the mixing triangle in the EMMA model using the soil-bedrock hypothesized, soilwater and snowmelt end-members Figure 4.28). The goodness-of-fit for the observed streamwater concentrations versus the EMMA predicted concentration was improved for all solutes (Figure 4.29). The percent of variance is explained by the r^2, which ranges from 64.1% for sodium and 94.5% for calcium. The silica and sodium in this model still have only marginal r^2 values (r^2 = 0.69 and r^2 = 0.64, respectively), indicating that the end-members have not been properly constrained. Sampling of the hypothesized soil-bedrock interface water would better identify median end-member values than the estimations used for this study. The residuals for SM2 (hypothesized) show very little variation between the solutes as related to the median. The range of values is larger for calcium, sodium, and silica showing more over- and under- predictions of concentration than magnesium (Figure 4.30).

The EMMA hypothesized results were used to complete a hydrograph separation for SM2 (Figure 4.31). The snowmelt end-member dominated the event hydrograph contributing 57% of the discharge, the soilwater end-member contributed 33% of discharge, and the soil bedrock hypothesized end-member contributed 9% of discharge.

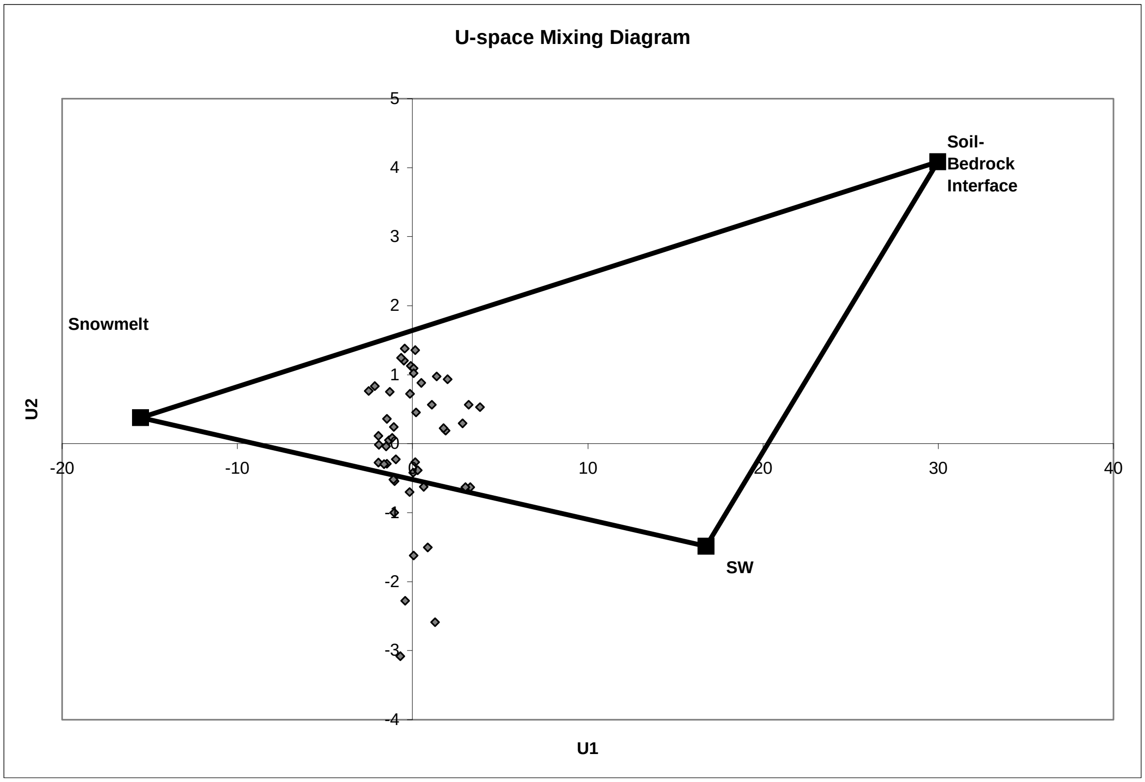

Figure 4.28. SM2 EMMA mixing plot representing soil-bedrock hypothesized, soilwater, and snowmelt end-members.

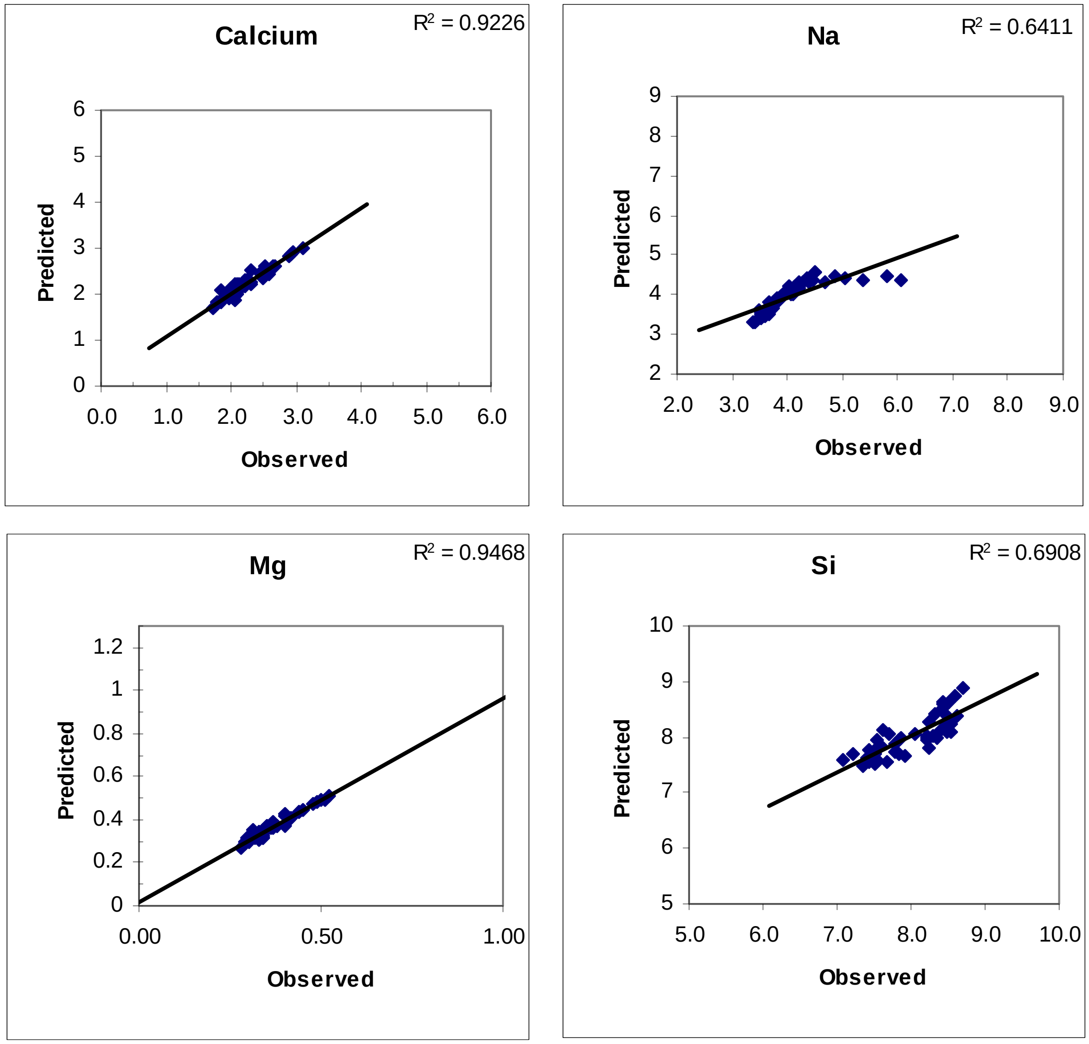

Figure 4.29. SM 2 predicted versus observed concentrations for EMMA completed for soil-bedrock interface, soilwater, and snowmelt end-members.

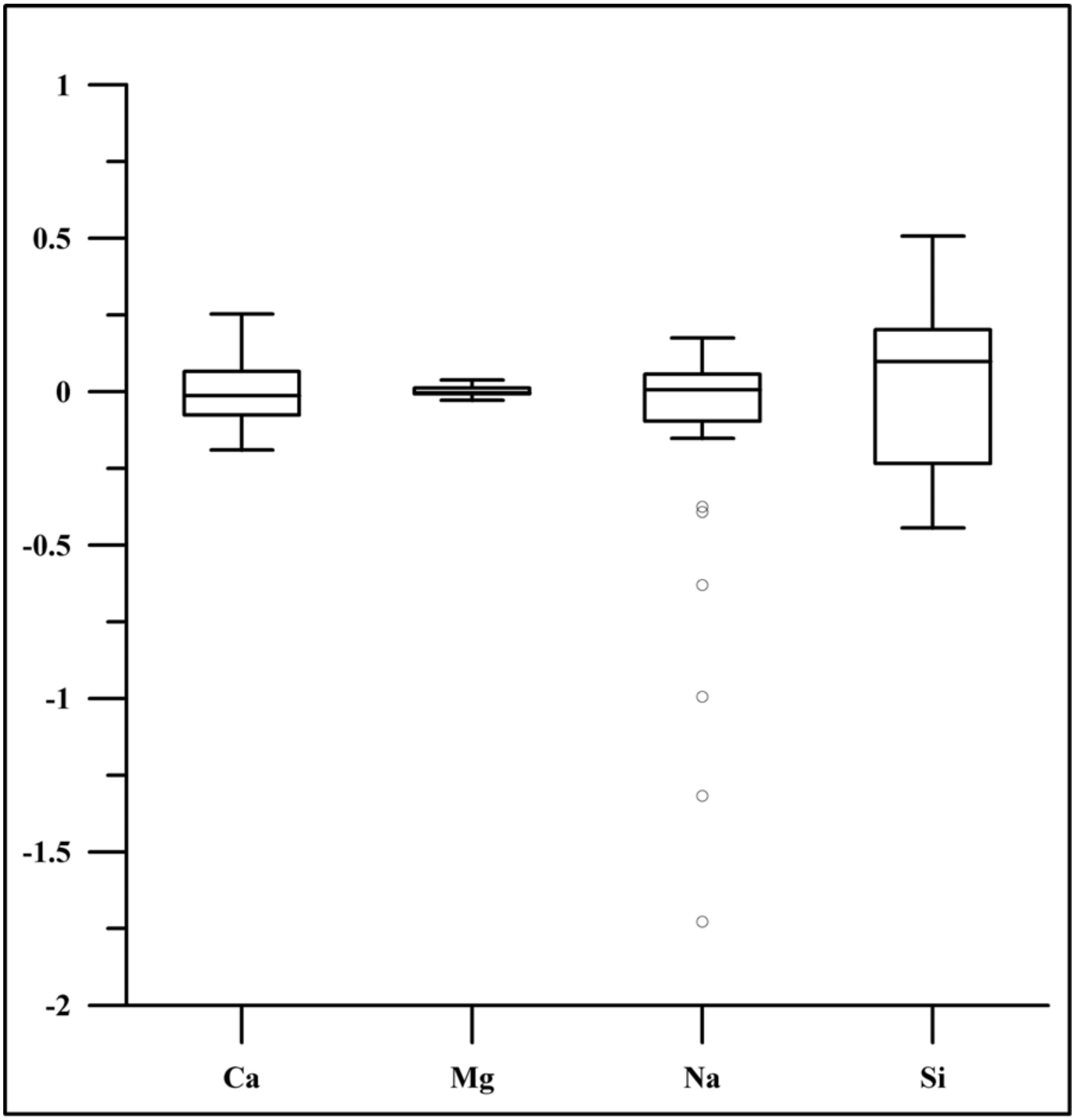

Figure 4.30. Box plots of residuals for SM2 EMMA completed with soil-bedrock interface, soilwater, and snowmelt end-members.

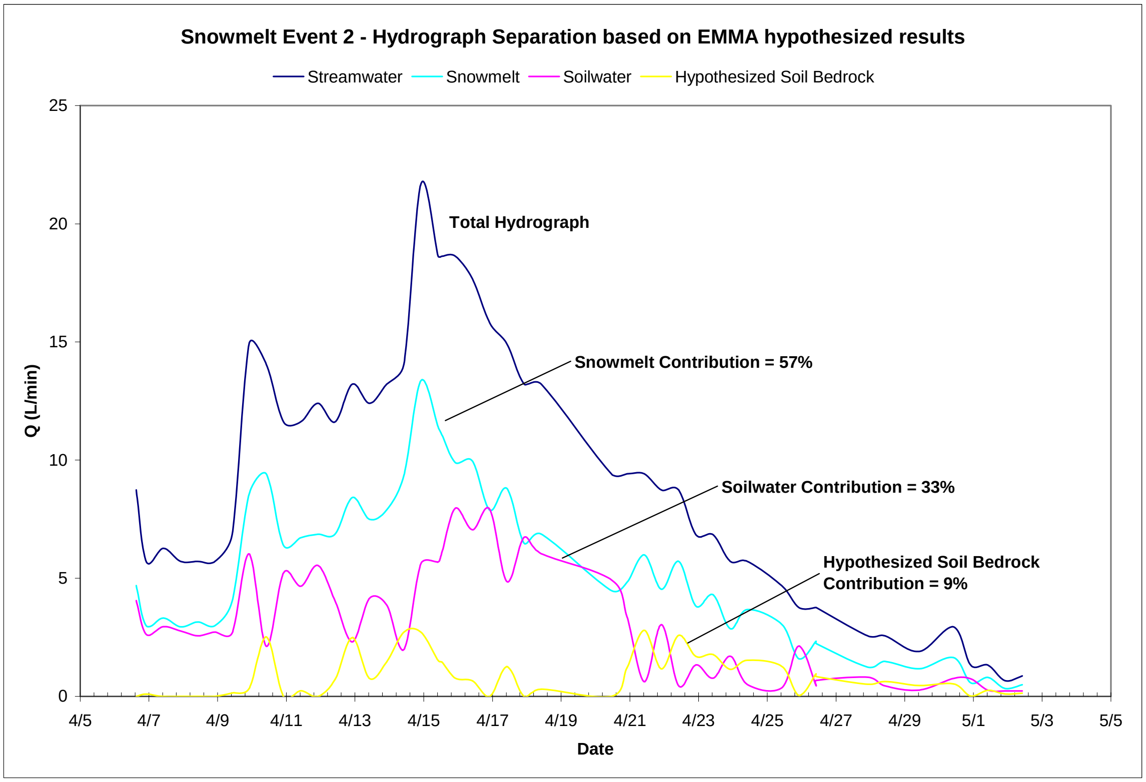

Figure 4.31. Hydrograph separation for SM2 based on EMMA representing soil-bedrock interface, soilwater, and snowmelt end-members.

4.2 Discussion

Streamflow in the UDCEW commenced in early November 2000 following the accumulation of the snowpack. The chemical signature of the stream was variable through out the cold-season and appears to be controlled by the flow sources contributing to the streamflow. Flow sources in the UDCEW are dependent the soil moisture conditions. The water discharge measured in UDCEW responds to increases in soil moisture content in the soil column. The hydrograph peaks for SM1 and SM2 correspond to a rapid rise in the soil moisture content. The extent to which each flow source component contributed to streamflow varied as a function of the timing, magnitude, and basin soil moisture conditions.

The following discussion evaluates the following cold-season processes occurring in UDCEW: 1) evidence of regional groundwater contribution to streamflow, and 2) the evidence for all water discharge originating from cold-season precipitation.

4.2.1 Evidence of regional groundwater contribution to streamflow

In regard to streamflow contributions from the regional groundwater system, the hydrometric and geochemical evidence poses a broad paradox. Physical observations and soil moisture sensors indicate that there is not a saturated zone in the mid-slope soil column at anytime in the UDCEW. The SHAW water balance for UDCEW provided additional evidence that there is no regional groundwater input into UDCEW (McNamara, unpublished). However, a comparison of the streamwater and other sampled waters, snowmelt, shallow soilwater, and deep soilwater, silica concentrations, indicates that there is another source contributing to the silica concentration in the stream throughout the cold-season. Two springs and the Main Dry Creek in the UDCW, outside of the UDCEW boundary, were sampled during the summer months to characterize the regional groundwater chemistry. The silica concentrations found in both the spring and Dry Creek base flow could account for silica concentration in UDCEW streamflow. But the lack of participation of the regional groundwater system is evident by the lack of UDCEW streamwater chemistry to display higher Ca^{+2} and Mg^{+2} concentrations and higher stream electrical conductivity values that would be expected if there was a regional groundwater contribution. Additionally, in the pairwise plots constructed for the

EMMA analysis, the groundwater samples in concert with other possible end-members failed to bound the UDCEW streamwater for all solutes considered, indicating that the regional groundwater is not an end-member contributing to streamflow. EMMA completed using groundwater, soilwater, and snowmelt for both SM1 and SM2 failed to accurately predict the streamwater concentrations as compared to the observed streamwater concentrations.

In summary, hydrometric evidence suggested that there is no regional groundwater contribution to streamflow in UDCEW. Geochemical evidence indicated that there is an un-sampled flow source contributing to streamflow. The hypothesized soil-bedrock interface end-member was offered in this study as a flow source area to explain the silica concentration observed in the streamwater chemistry. Other possible explanations to reconcile the flow source area contributing silica to the stream include:

- A localized saturated zone forms in the basin as the cold-season progresses as evidenced by an observed clay layer at the base of the slope;
- The soilwater studied is not representative of the basin. There maybe a soilwater source contributing to flow in other basin areas not included in this study which better bound streamwater chemistry; and
- A local reservoir system forms through the cold-season in the fractured granitic bedrock activating bedrock fracture flow to stream channel during precipitation events as evidenced by the willows in the UDCEW immediately down stream from the sample site.

4.2.2 The evidence for all water discharge originating from cold-season precipitation within UDCEW

Hydrometric evidence supporting this include the precipitation timing, streamflow duration, and the water balance. Approximately 65% of the precipitation in UDCEW falls in the cold season. The occasional summer rain event generally wets the soil surface with very little infiltrates to depth. The water balance demonstrated that most precipitation falling in the warm season is lost to evapotranspiration in UDCEW (McNamara, unpublished). Streamflow only occurs in UDCEW from late fall to early winter and ceases soon after snowmelt. The SHAW water balance for UDCEW showed that no regional groundwater input was required to account for the water discharge produced by UDCEW (McNamara, unpublished).

Snowmelt, soilwater shallow (30 cm), soilwater deep (60 cm) and regional groundwater were sampled with the expectation of identifying the end-members contributing to streamflow. Hydrometric and geochemical evidence has shown that there is no regional groundwater contribution to UDCEW streamflow. The pairwise plots constructed for both SM1 and SM2 EMMA showed that an additional end-member was needed to explain the streamwater chemistry. The hypothesized soil-bedrock interface end-member was offered in this study as an alternative flow source area within UDCEW to account for the silica concentration observed in the streamwater chemistry.

All water considered in the two-component hydrograph separation preformed for SM1 originated from cold season precipitation. Pre-event water consists of water in the system as soilwater before a precipitation or melt event. Event water is defined as water input into the system as rain or snowmelt. The hydrograph separations completed for

SM1 with electrical conductivity showed that event water composed 59% of the total hydrograph. A three-component hydrograph separation was completed using the results from SM1 EMMA representing the end-members; soilwater, soil-bedrock interface, and snowmelt in order to further divide the pre-event and event waters into the end-member components. The EMMA hydrograph separation showed that the hydrograph was composed of 28% soil-bedrock interface water, 7% soilwater, and 65% snowmelt. These results indicate that EMMA can be used to further evaluate two-component hydrograph separation components flow sources (Figure 4.32). The similarity between the hydrograph separation pre-event component and the EMMA pre-event components (soil water and soil-bedrock interface end-members) contributing to the hydrograph provides additional evidence for the hypothesized soil-bedrock end-member.

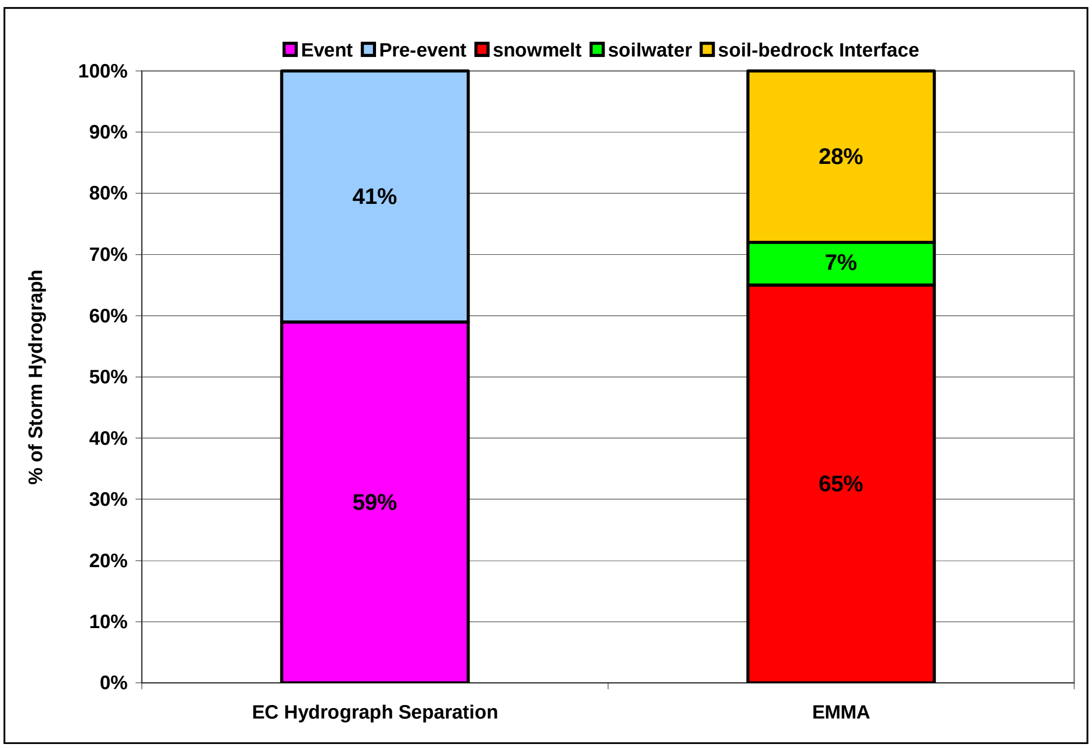

Figure 4.32. Comparison of electrical conductivity hydrograph separation and EMMA results for SM1.

The silica C-Q plots for SM1 and SM2 have dominant counter-clockwise hysteresis loops. This demonstrates that during both snowmelt events the silica concentration on the rising limb is lower than on the falling limb for like discharges. The dominant counter-clockwise rotation observed in the hysteresis loops indicates activation of a flow source with greater silica concentration as the melt events progressed. The UDCEW water balance validates this with the modeled deep percolation (or lateral flow) component addition at the same time as a rise in streamwater silica concentration (McNamara, unpublished). The hydrograph separations generated from the EMMA results for both SM1 (Figure 4.20) and SM2 (Figure 4.31) also validates the activation of flow sources with higher silica concentration as the melt event progresses. Both hydrograph separations show that sources with higher silica concentrations (soilwater and soil-bedrock interface) contribute greater proportion to the hydrograph later in the events.

5. CONCLUSIONS

Hydrometric and geochemical evidence has shown that there are no regional groundwater inputs into the UDCEW system during the cold season. All water in the basin can be accounted for by precipitation (rain and snowmelt) occurring during the cold season.

Cold season streamflow flow sources in UDCEW are controlled by the soil moisture conditions within the basin. There is a positive response in observed discharge, streamwater electrical conductivity, and silica concentration as the soil moisture content in the basin increases throughout the cold season. The silica C-Q plots for SM1 and SM2 show a dominate counter-clockwise rotation, illustrating that there are lower silica concentrations on the rising limb than on the falling limb of the hydrograph for similar discharges. The counter-clockwise hysteresis loops indicates that there is activation of a flow source with greater silica concentration as snowmelt progresses and soil moisture increases. This is validated by UDCEW water balance lateral flow component and the SM1 and SM2 hydrograph separations based on the EMMA results. The increase in observed streamwater silica concentration as the melt events progress can be linked to the increase inputs by soilwater and the hypothesized soil-bedrock interface (or lateral flow) sources.

EMMA indicates that three end-members contribute to streamflow; snowmelt, and two-soilwater end-members. The EMMA analysis illustrates that an additional soilwater other than those sampled is needed to explain the observed streamwater chemistry. A hypothesized soil-bedrock interface end-member is offered as an alternative flow source for study in an attempt to account for the streamwater chemistry. The UDCEW water balance provided additional evidence supporting lateral flow along the soil-bedrock interface. Both EMMA and the two-component hydrograph separation show that the majority of streamflow during SM1 and SM2 is derived from direct input of snowmelt with smaller contributions of soilwater sources. The results of the two-component electrical conductivity hydrograph separation and the three-component hydrograph separation based on the EMMA result for SM1 correlate well.

When results of this study are compared to those in other semi-arid watersheds there are both similarities and differences. Newman et al. (1998) found in a study of a semi-arid ponderosa pine hillslope that there are temporal controls of lateral subsurface flow chemistry, flow volume, and old/new water proportions. Approximately 90% of the lateral subsurface flow generated on this hillslope occur at or near saturation. In the UDCEW study the lateral subsurface flow occurs under unsaturated conditions coupled with significant variation in flow chemistry during snowmelt events. The semi-arid Reynolds Creek Experimental Watershed (RCEW), located in the Owyhee Mountains across the Snake River plain from DCW, has many parallels to DCW in elevation, freeze-thaw cycles and climate but there are considerable differences in geology, soil types and the groundwater systems. Research in RCEW, illustrated the spatial organization of flow paths, the dynamic nature of near stream saturated areas in response to drift snowmelt, and the controls on stream groundwater linkages at the catchment scale. The development of a variable source area within the altered basalt was identified as the primary mechanism in RCW (Unnikrishna et al., unpublished).

This study was the first comprehensive study of the flow sources controlling streamflow in the UDCEW. These results indicate that snowmelt is the major contributor to cold season streamflow. However, the geochemical evidence demonstrates that the soilwater flow sources control the streamwater chemical signature. Additional processes remain to be studied at the hillslope scale to fully explain and understand the significance of these results. Further research into the relationship between the granite weathering products, in particular the clays present in the mineral soil and dissolved silica behavior as water moves both vertically and laterally through soil profile in order to identify the flow sources and runoff generation mechanisms.

REFERENCES

Blackburn, W.H., 1975. Factors influencing infiltration and sediment production of semiarid rangelands in Nevada. Water Resources Research, 11(6): 929-937.

Bishop, K.H., H. Grip, A. O'Neill, 1990. The origins of acid runoff in a hillslope during storm events. Journal of Hydrology, 116: 35-61.

Bonnell , M., 1993. Progress in the understanding of runoff generation dynamics in forests. Journal of Hydrology, 150: 217-275.

Brammer, D.D. and J.J. McDonnell, 1996. An evolving perceptual model of hillslope flow at the Maimai catchment, In: Anderson, M.G. and S.M. Brooks (editors), Advances in Hillslope Hydrology. Wiley, New York, pp. 35-60.

Branson, F.A., G.F. Gifford, K.G. Renard, and R.F. Hadley, 1981. Rangeland Hydrology, Range Science Series, No. 1, Second Edition, edited by E.H. Reid, Kendall/Hunt Publishing Co., pp. 340.

Brown, V.A., J.J. McDonnell, D.A. Burns and C. Kendall, 1999. The role of event water, a rapid shallow flow component, and catchment size in summer stormflow. Journal of Hydrology, 217: 171-190.

Burns, D.A., J.J. McDonnell, R.P. Hooper, N.E. Peters, J.E. Freer, C. Kendall and K. Beven, 2001. Quantifying contributions to storm runoff through end-member mixing analysis and hydrologic measurements at Panola Mountain Research Watershed (Georgia, USA). Hydrological Processes, 15: 1903-1924.

Buttle, J.M. and K. Sami, 1992. Testing the groundwater ridging hypothesis of streamflow generation during snowmelt. Journal of Hydrology, 135: 53-72.

Chanat, J.G., K.C. Rice, and G.M. Hornberger, 2002. Consistency of patterns in concentration-discharge plots. Water Resource Research, 38(8): 1-10.

Christopherson, N. and R.P.Hooper, 1992. Multivariate Analysis of Stream Water Chemical Data: The use of Principal Components Analysis for End-Member Mixing Problem. Water Resources Research, 28(1): 99-107.

Christopherson, N., Neal, C., R.P. Hooper, R.D. Vogt, S., and Andersen, S., 1990. Modelling Streamwater Chemistry as a Mixture of Soilwater End-Members - A Step toward Second-Generation Acidification Models. Journal of Hydrology, 116: 307-320.

Christopherson, N., H.M. Seip, and R.F. Wright, 1982. A model for streamwater chemistry at Birknes, Norway. Water Resources Research, 18: 977-996.

Devore, J.L., 2000. Probability and Statistics for Engineers and the Sciences. Duxbury Thomson Learning, United States.

Dewalle, D.R., B.R. Swistock and W.E. Sharpe, 1988. Three-Componenet Tracer Model for Stormflow on a Small Appalachian Forest Catchment. Journal of Hydrology, 104: 301-310.

Dincer, T., B.R. Payne, and T. Florkowski, 1970. Snowmelt, Runoff from Measurements of Tritium and Oxygen - 18. Water Resources Research, 6(1): 110-124.

Elsenbeer, H., A. West, M. Bonnell, 1994. Hydrologic pathways and stormflow hydrochemistry at South Creek, northeast Queensland. Journal of Hydrology, 162, 1-21.

Evans, C. and T.D. Davies, 1998. Causes of concentration/discharge hysteresis and its potential as a tool for analysis of episode hydrochemistry. Water Resources Research, 34(1): 129-137.

Flerchinger, G.N., C.L. Hanson, and J.R. Wright, 1996. Modeling evapotranspiration and surface energy budget across a watershed. Water Resources Research, 32(8): 2539-2548.

Flerchinger, G.N., K.R. Cooley, and D.R. Ralston, 1992. Groundwater response to snowmelt in a mountainous watershed, Journal of Hydrology, 133:293-311.

Hinton, M.J., S.L. Schiff, and M.C. English, 1994. Examining the contributions of glacial till water to storm runoff using two- and three-component hydrograph separations. Water Resources Research, 30(4): 983-993.

Hooper, R.P. and N. Christophersen, 1992. Predicting Episodic Stream Acidification in the Southeastern United Stated: Combining a Long-Term Acidification Model and End-Member Mixing Concept. Water Resources Research, 28(7): 1983-1990.

Hooper, R.P., N. Christopherson, and R.E. Peters, 1990. Modelling Streamwater Chemistry as a Mixture of Soilwater End-Members - An Application to the Panola Mountain Catchment, Georgia, U.S.A. Journal of Hydrology, 116: 321-343.

Hooper, R.P. and C.A. Shoemaker, 1986. A Comparison of Chemical and Isotopic Hydrograph Separation. Water Resources Research, 22(10): 1444-1454.

Hornberger, G.M., T.M. Scanlon, and J.P. Raffensperger, 2001. Modelling transport of dissolved silica in a forested headwater catchment: the effect of hydrological and chemical time scales on hysteresis in the concentration-discharge relationship. Hydrologic Processes, 15: 2029-2038.

Johnson, C.W. and R.P. McArthur, 1973. Winter storm and flood analysis, Northwest Interior. Proceedings of the Hydraulic Div. Spec. Conf., ASCE, Bozeman, MT.

Johnson, K.M., R.S. Lewis, E.H. Bennett, and T.H. Kiilsgaard, 1988. Cretaceous and Tertiary intrusive rocks of south-central Idaho. In: Link, P.K. and W.R. Hackett (editors), Guidebook to the Geology of Central and Southern Idaho. Idaho Geologic Survey, Bulletin 27, pp. 55-86.

Johnson, F.A. and J.W. East, 1982. Cyclical relationships between river discharge and chemical composition during flood events. Journal of Hydrology, 57: 93-106.

Joreskog, K.G., J.E. Klovan, and R.A. Reyment, 1976. Geologic Factor Analysis. Elsevier, New York.

Kendall, K.A., J.B. Shanley and J.J. McDonnell, 1999. A hydrometric and geochemical approach to test transmissivity feedback hypothesis during snowmelt. Journal of Hydrology, 219: 188-205.

Lane, L.J., M.H. Diskin, and K.G. Renard, 1971. Input-output relationships for an ephermal stream channel system. Journal of Hydrology, 13:22-40.

Lewis, R.S., T.H. Kiilsgaard, E.H. Bennett, W.E. Hall, 1987. Lithologic and chemical characteristics of the central and southeastern part of the southern lobe of the Idaho Batholith. In: Vallier, T.L. and H.C. Brooks (editors), Geology of the Blue Mountains region of Oregon, Idaho, and Washington –the Idaho Batholith and its border zone: U.S. Geologic Survey, Professional Paper 1436, pp. 171-196.

McCord, J.T. and D.B. Stephens, 1987. Lateral moisture flow beneath a sandy hillslope without an apparent impeding layer. Hydrologic Processes, 1: 225-238.

McDonnell, J.J., I.F. Owens, and M.K. Stewart, 1991. A case study of shallow flow paths in a steep zero-order basin. Water Resources Research, 27: 679-685.

McDonnell, J.J., 1990. A Rationale for Old Water Discharge Through Macropores in a Steep, Humid Catchment. Water Resources Research, 26(11): 2821-2832.

McNamara, J.P., unpublished. Evidence on the timing of hillslope-stream connectivity from water budget calculations. Draft Paper for peer review journal.

McNamara, J.P., Kane, D.L., Hinzman, L.D., 1997. Hydrograph separations in an Artic watershed using mixing models and graphical techniques. Water Resources Research, 33(7): 1707-1719.

Miller, D.R. and J.I. Drever, 1977. Water Chemistry of a stream following a storm, Absaroka Mountains, Wyoming. Geologic Society of America Bulletin, 88: 286-290.

Mulholland, P.J., 1993. Hydrometric and stream chemistry evidence of three storm flowpaths in Walker Branch Watershed. Journal of Hydrology, 151: 291-316.

Mulholland, P.J., G.V. Wilson, and P.M. Jardine, 1990. Hydrogeochemical Response of a Forested Watershed to Storms: Effects of Perferential Flow Along Shallow and Deep Flow Pathways, Water Resources Research, 26(12): 3021-3036.

Neal, C., C.J. Smith, J. Walls, and C.S. Dunn, 1986. Major, minor, and trace element mobility in acid upland forested catchment of the Upper River Severn, mid-Wales, Journal Geol. Soc., London, 143: 635-648.

Newman, B.D., A.R. Campbell, and B.P. Wilcox, 1998. Lateral subsurface flowpaths in a semi-arid ponderosa pine hillslope. Water Resources Research, 34(12): 3485-3496.

Osborn, H.B. and L. Lane, 1969. Precipitation-runoff relations for very small semiaird rangeland watersheds. Water Resources Research, 5(2): 419-425.

Othberg K.L. and V.S. Gillerman, 1994. Field Trip Guide to the Geology of the Boise Valley. Idaho Geologic Survey, Special Report.

Oxley, N.C., 1974. Suspended sediment delivery rates and solute concentrations of stream discharge in two Welsh catchments. Fluvial Processes in Instrumented Watersheds. Inst. Of Br. Geogr., London.

Peters, D.L., J.M. Buttle, C.H. Taylor, and B.D. LaZerte, 1995. Runoff production in a forested shallow soil, Canadian Shield basin. Water Resources Research, 31: 1291-1304.

Pilgrim, D.H., D.D. Huff, and T.D. Steele, 1979. Use of specific conductance and contact time relations for separating flow components in storm runoff. Water Resources Research, 15: 329-339.

Pinder, G.F. and J.F Jones, 1969. Determination of the Ground-Water Component of Peak discharge from the Chemistry of Total Runoff. Water Resources Research, 5(2): 438-445.

Puigdefabregas, J., G. del Barrio, M. M. Boer, L. Gutierrez, and A. Sole, 1998. Differential responses of hillslope and channel elements to rainfall events in a semi-arid area. Geomorphology, 23: 337-351.

Ross, D.S., R.J. Bartlett, F.R. Magdoff, and G.J. Walsh, 1994. Flow path studies in forested watersheds in headwater tributaries of Brush Brook, Vermont. Water Resources Research, 30, 2611-2618.

Scanlon, T.M., J.P. Raffensperger, and G.M. Hornberger, 2001. Modelling transport of dissolved silica in a forested headwater catchment: Implications for defining the hydrochemical response of observed flowpaths. Water Resources Research, 37(4): 1071-1082.

Scanlon, T.M., J.P. Raffensperger, and G.M. Hornberger, 2000. Shallow subsurface storm flow in a forested headwater catchment: Observations and modeling using a modified TOPMODEL. Water Resources Research, 36(9): 2575-2586.

Schumm, S.A. and G.C. Lusby, 1963. Seasonal variation of infiltration capacity and runoff on hillslopes in western Colorado. Journal of Geophysical Research, 68(12): 3655-3666.

Seyfried, M.S. and B.P. Wilcox, 1995. Scale and nature of spatial variability: Field examples having implications for hydrologic modeling. Water Resources Research, 31(1): 173-184.

Shanley, J.B. and N.E. Peters, 1993. Variation in aqueous sulfate concentrations at Panola Mountain, Georgia. Journal of Hydrology, 146:361-382.

Sklash, M.G., 1990. Environmental isotope studies for storm and snowmelt runoff generation. Burt, T.P., M.G. Anderson. New York, John Wiley: 401-435.

Sklash, M.G. and R.N. Farvolden, 1979. The Role of Groundwater in Storm Runoff. Journal of Hydrology, 43: 45-65.

Swistock, B.R., D.R. DeWalle, and W.E. Sharpe, 1989. Sources of acidic storm flow in an Appalachian headwater stream. Water Resources Research, 25: 2139-2147.

Unnikrishna, P.V., J.J. McDonnell, D.G. Tarboton, C. Kendall, and G.N. Flerchinger, Unpublished. Hydrologic processes in a small semi-arid catchment, submitted to Journal of Hydrology.

USDA, 1997. Soil Survey of the Boise Front: Interim and Supplemental Report, Natural Resource Conservation Service, Boise, Idaho.

USDA, 1974. Soil-Hydrologic Reconnaissance Survey, Forest Service, Boise, Idaho.

Walling, D.E. and B.W. Webb, 1986. Solutes in river systems. In: S.T. Trudgill (Editor), Solute Processes. John Wiley, New York, pp. 251-327.

Wels, C., R. J. Cornett, and B.D. LaZerte, 1990. Groundwater and Wetland Contributions to Stream Acidification: An Isotopic Analysis. Water Resources Research, 26(12): 2993-3003.

Wilcox, B.P., B.D. Newman, D. Brandes, D.W. Davenport, and K. Reid, 1997. Runoff from a semiarid ponderosa pine hillslope in New Mexico. Water Resources Research, 33: 2301-2314.

APPENDIX A

Dry Creek Watershed Soil Series Description

APPENDIX A

Description of NRCS Soil Map Groups in the Upper Dry Creek Watershed. Excerpt from USDA NRCS - Soil Survey of the Boise Front Project, Idaho, Interim and Supplemental Report May 1997.

Soil Map Group – 300

Soil Map Unit: 358 – Qualridge-Fortbois Complex

Setting	
Landform:	Hill backslopes
Elevation:	2,750 to 3,850 feet
Average annual precipitation:	14 inches
Average annual air temperature:	52° F
Average frost free period:	150 days
Major use:	Wildlife and rangeland
Composition	
Quailridge and similar soils:	50%
Fortbois and similar soils:	30%
Contrasting inclusion:	20%
Major Components	
Quailridge coarse sandy loam	
Slopes:	35 to 65%
Position on landform:	South facing slightly convex backslopes
Vegetal climax association:	Antelope bitterbrush, basin big sagebrush, bluebunch wheatgrass, and Thurber needlegrass
Typical profile:	0 to 4 inches – grayish brown coarse sandy loam 4 to 19 inches – brown sandy clay loam 19 to 46 inches – pale brown coarse sandy loam with thin clay bands 46 to 60 inches – very pale brown fine gravelly loamy coarse sand
Drainage class:	Well drained
Surface runoff:	Rapid
Permeability:	Moderate
Available water capacity:	Low
Shrink-swell potential:	Moderate
Depth class:	Very Deep

Fortbois loamy sand	
Slopes:	50 to 90%
Position on landform:	South-facing convex upper backslopes
Vegetal climax association:	Antelope bitterbrush, Indian ricegrass and needleandthread grass
Typical profile:	0 to 7 inches – grayish brown and brown loamy sand 7 to 11 inches – light brownish gray sandy loam 11 to 17 inches – pale brown loamy sand 17 to 60 inches – very pale brown sand
Drainage class:	Somewhat excessively drained
Surface runoff:	Rapid
Permeability:	Moderately rapid
Available water capacity:	Low
Shrink-swell potential:	Low
Depth class:	Very Deep
Contrasting Inclusions	
10% - Shawmount soils on shoulders and upper backslopes under basin big sagebrush and bluebrunch wheatgrass 5% - Hullgulch soils on footslopes and lower backslopes under basin big sagebrush, bluebunch wheatgrass, and Thurber needlegrass 5% - Rock outcrop	

Soil Map Unit: 360 – Picketpin-Van Dusen Complex

Setting	
Landform:	Hill backslopes
Elevation:	2,800 to 3,950 feet
Average annual precipitation:	16 inches
Average annual air temperature:	47° F
Average frost free period:	110 days
Major use:	Rangeland
Composition	
Picketpin and similar soils:	50%
Van Dusen and similar soils:	35%
Contrasting inclusion:	15%
Major Components	
Picketpin loam	
Slopes:	25 to 65%
Position on landform:	North-facing slightly convex backslopes
Vegetal climax association:	Basin big sagebrush, bluebunch wheatgrass, and Idaho fescue

Picketpin loam continued	
Typical profile:	0 to 5 inches – grayish brown loam 5 to 11 inches – brown sandy clay loam 11 to 17 inches –brown clay loam 17 to 35 inches – yellowish brown sandy clay loam 35 to 60 inches – very pale brown fine gravelly coarse sandy loam with thin clay bands.
Drainage class:	Well drained
Surface runoff:	Rapid
Permeability:	Moderately slow
Available water capacity:	Medium
Shrink-swell potential:	Moderate
Depth class:	Very Deep

Van Dusen Loam	
Slopes:	35 to 65%
Position on landform:	North-facing slightly concave and lower backslopes
Vegetal climax association:	Xeric big sagebrush and Idaho Fescue
Typical profile:	0 to 7 inches – dark grayish brown loam 7 to 39 inches – grayish brown and brown loam 39 to 60 inches – yellowish brown and light yellowish brown clay loam
Drainage class:	Well drained
Surface runoff:	Rapid
Permeability:	Moderately slow
Available water capacity:	High
Shrink-swell potential:	Moderate
Depth class:	Very Deep

Contrasting Inclusions
10% - soils like Picketpin soils but with an accumulation of calcium carbonate in the lower subsoil on very steep north-facing backslopes under basin big sagebrush, bluebunch wheatgrass and Idaho fescue. 5% - Hullgulch soils on slightly convex shoulders and south-facing backslopes under basin big sagebrush, bluebrunch wheatgrass and Thurber needlegrass

Soil Map Unit: 361 – Quailridge-Hullsgulch-Cranegulch Complex

Setting	
Landform:	Backslopes and footslopes
Elevation:	2,700 to 3,850 feet
Average annual precipitation:	14 inches
Average annual air temperature:	51° F
Average frost free period:	150 days
Major use:	Rangeland

Composition	
Quailridge and similar soils:	35%
Hullsgulch and similar soils:	30%
Cranegulch and similar soils:	15%
Contrasting inclusion:	20%
Major Components	
Quailridge coarse sandy loam	
Slopes:	25 to 50%
Position on landform:	Shoulders and south-facing convex backslopes
Vegetal climax association:	Antelope bitterbrush, basin big sagebrush, bluebunch wheatgrass, and Thurber needlegrass
Typical profile:	0 to 4 inches – grayish brown coarse sandy loam 4 to 19 inches – brown sandy clay loam 19 to 46 inches – pale brown coarse sandy loam with thin clay bands 46 to 60 inches – very pale brown fine gravelly loamy coarse sand
Drainage class:	Well drained
Surface runoff:	Rapid
Permeability:	Moderate
Available water capacity:	Low
Shrink-swell potential:	Moderate
Depth class:	Very Deep
Hullsgulch coarse sandy loam	
Slopes:	15 to 50%
Position on landform:	Shoulders and slightly convex backslopes
Vegetal climax association:	Basin big sagebrush, bluebunch wheatgrass, and Thurber needlegrass
Typical profile:	0 to 12 inches – grayish brown coarse sandy loam 12 to 25 inches – yellowish brown and light yellowish brown sandy clay loam 25 to 38 inches – very pale brown sandy clay loam 38 to 53 inches – very pale brown gravelly coarse sandy loam and light yellowish brown gravelly sandy clay loam. 53 to 60 inches – very pale brown gravelly loamy coarse sand with thin clay bands
Drainage class:	Well drained
Surface runoff:	Medium to Rapid
Permeability:	Moderately slow
Available water capacity:	Medium
Shrink-swell potential:	Moderate

Hullsgulch coarse sandy loam continued	
Depth class:	Very Deep

Cranegulch loam	
Slopes:	15 to 50%
Position on landform:	Footslopes and lower backslopes
Vegetal climax association:	Basin big sagebrush and bluebunch wheatgrass
Typical profile:	0 to 10 inches – grayish brown loam 10 to 14 inches – yellowish brown sandy clay loam 14 to 33 inches – yellowish brown sandy clay loam and clay 33 to 60 inches – light yellowish brown sandy clay loam and clay
Drainage class:	Well drained
Surface runoff:	Rapid to very rapid
Permeability:	Slow
Available water capacity:	High
Shrink-swell potential:	High
Depth class:	Very Deep

Contrasting Inclusions
5% - Picketpin soils on north-facing backslopes under basin big sagebrush, bluebunch wheatgrass, and Idaho fescue. 5% - Piercepark soils on footslopes and concave backslopes under basin big sagebrush, bluebunch wheatgrass and Thurber needlegrass. 5% - Shawmount soils on summits under basin big sagebrush and bluebunch wheatgrass 3% - Flofeather soils on slightly convex footslopes under basin big sagebrush, Antelope bitterbrush, and needleandthread grass. 2% - Rock outcrop with hackberry occasionally rooted in fractures

Soil Map Unit: 371 – Quailridge-Fortbois-Rock Outcrop Complex

Setting	
Landform:	gulches
Elevation:	3,150 to 3,750 feet
Average annual precipitation:	14 inches
Average annual air temperature:	51° F
Average frost free period:	145 days
Major use:	Wildlife habitat and rangeland
Composition	
Quailridge and similar soils:	45%
Fortbois and similar soils:	20%
Rock Outcrop:	15%

Contrasting inclusion:	20%
Major Components	
Quailridge coarse sandy loam	
Slopes:	25 to 65%
Position on landform:	South-facing slightly convex slopes
Vegetal climax association:	Antelope bitterbrush, basin big sagebrush, bluebunch wheatgrass, and Thurber needlegrass
Typical profile:	0 to 10 inches – grayish brown gravelly coarse sandy loam 10 to 23inches – brown and pale brown gravelly sandy clay loam 23 to 37 inches – pale brown fine gravelly coarse sandy loam with thin clay bands 37 to 60 inches – very pale brown fine gravelly loamy coarse sand
Drainage class:	Well drained
Surface runoff:	Rapid
Permeability:	Moderate
Available water capacity:	Low
Shrink-swell potential:	Moderate
Depth class:	Very Deep
Fortbois loamy sand	
Slopes:	50 to 90%
Position on landform:	South-facing convex slopes
Vegetal climax association:	Antelope bitterbrush, Indian ricegrass, and needleandthread grass
Typical profile:	0 to 7 inches – grayish brown and brown loamy sand 7 to 11 inches – light brownish gray sandy loam 11 to 17 inches –pale brown loamy sand 17 to 60 inches – very pale brown sand
Drainage class:	Somewhat excessively drained
Surface runoff:	Rapid
Permeability:	Moderately rapid
Available water capacity:	Low
Shrink-swell potential:	Low
Depth class:	Very Deep
Rock Outcrop	
Position on landform:	Ledges and barren areas of exposed sandstone bedrock. Hackberry is commonly rooted in fractures.
Surface runoff:	Very rapid

Contrasting Inclusions
10% - Hullgulch soils on slightly concave slopes under basin big sagebrush, bluebunch wheatgrass, and Thurber needlegrass 5% - Polecat soils on slightly concave slopes under basin big sagebrush and bluebunch wheatgrass. 5% - Stu soils on south-facing slightly convex slopes under basin big sagebrush, bluebunch wheatgrass, and Thurber needlegrass

Soil Map Group – 500

Soil Map Unit: 506 – Brownlee-Robbscreek-Whisk Complex

Setting	
Landform:	Hill summits, shoulders and back slopes
Elevation:	3,500 to 5,000 feet
Average annual precipitation:	19 inches
Average annual air temperature:	47° F
Average frost free period:	110 days
Major use:	Rangeland
Composition	
Brownlee and similar soils:	50%
Robbscreek and similar soils:	20%
Whisk and similar soils:	15%
Contrasting inclusion:	15%
Major Components	
Brownlee loam	
Slopes:	8 to 35%
Position on landform:	Concave summits and backslopes
Vegetal climax association:	Xeric big sagebrush and bluebunch wheatgrass
Typical profile:	0 to 16 inches – brown loam 16 to 27 inches – brown and yellowish brown sandy clay loam 27 to 45 inches – yellowish brown fine gravelly sandy loam 45 to 50 inches – weathered bedrock 50 inches – bedrock
Drainage class:	Well drained
Surface runoff:	Medium to rapid
Permeability:	Moderately slow
Available water capacity:	Medium
Shrink-swell potential:	Moderate
Depth class:	Deep

Robbscreek fine gravelly coarse sandy loam	
Slopes:	8 to 25%
Position on landform:	Slightly convex summits and shoulders
Vegetal climax association:	Xeric big sagebrush, Antelope Bitterbrush, and bluebunch wheatgrass.
Typical profile:	0 to 13 inches – grayish brown and brown fine gravelly coarse sandy loam 13 to 19 inches – yellowish brown fine gravelly sandy clay loam 19 to 30 inches – yellowish brown and light yellowish brown fine gravelly sandy clay loam 30 inches – bedrock
Drainage class:	Well drained
Surface runoff:	Medium to Rapid
Permeability:	Moderately slow
Available water capacity:	Low
Shrink-swell potential:	Moderate
Depth class:	Moderately Deep
Whisk fine gravelly sandy loam	
Slopes:	8 to 35%
Position on landform:	Convex summits and shoulders
Vegetal climax association:	Xeric big sagebrush, Antelope Bitterbrush, and bluebunch wheatgrass.
Typical profile:	0 to 3 inches – brown fine gravelly sandy loam 3 to 14 inches – brown and yellowish brown fine gravelly sandy loam 14 inches - bedrock
Drainage class:	Somewhat excessively drained
Surface runoff:	Rapid to very rapid
Permeability:	Moderately Rapid
Available water capacity:	Very low
Shrink-swell potential:	Low
Depth class:	Shallow
Contrasting Inclusions	
10% - Aradan soils on concave backslopes under xeric big sagebrush, bluebunch wheatgrass, and Idaho fescue. 3% - Roney soils on slightly convex summits and backslopes under xeric big sagebrush, Antelope Bitterbruch, and bluebunch wheatgrass. 2% - Rock outcrop	

Soil Map Unit: 508 – Dobson-Roney-Rock Outcrop

Setting	
Landform:	Hill backslopes and canyon walls
Elevation:	3,000 to 5,100 feet
Average annual precipitation:	16 inches
Average annual air temperature:	49° F
Average frost free period:	130 days
Major use:	Rangeland
Composition	
Dobson and similar soils:	45%
Roney and similar soils:	25%
Rock Outcrop:	20%
Contrasting inclusion:	10%
Major Components	
Dobson fine gravelly coarse sandy loam	
Slopes:	35 to 90%
Position on landform:	Convex backslopes and walls
Vegetal climax association:	Antelope bitterbrush, basin big sagebrush, bluebunch wheatgrass, and Thurber needlegrass
Typical profile:	0 to 2 inches – grayish brown gravelly coarse sandy loam 2 to 12inches – brown and pale brown gravelly sandy clay loam 12 to 14 inches – very pale brown fine gravelly loamy coarse sand 14 inches – bedrock
Drainage class:	Somewhat excessively drained
Surface runoff:	Very Rapid
Permeability:	Moderately rapid
Available water capacity:	Very low
Shrink-swell potential:	Low
Depth class:	Shallow
Roney fine gravelly coarse sandy loam	
Slopes:	35 to 90%
Position on landform:	Concave backslopes and walls
Vegetal climax association:	Xeric big sagebrush, Antelope bitterbrush and bluebunch wheatgrass

Roney fine gravelly coarse sandy loam continued	
Typical profile:	0 to 10 inches – dark grayish brown fine gravelly coarse sandy loam 10 to 24 inches – brown fine gravelly coarse sandy loam 24 to 30 inches –brown fine gravelly loamy coarse sand 30 inches – bedrock
Drainage class:	Somewhat excessively drained
Surface runoff:	Very rapid
Permeability:	Moderately rapid
Available water capacity:	Very low
Shrink-swell potential:	Low
Depth class:	Moderately Deep
Rock Outcrop	
Position on landform:	Convex backslopes, walss and barren areas of exposed granite bedrock.
Surface runoff:	Very rapid
Contrasting Inclusions	
5% - Olation soils on concave toeslopes and drainage ways under xeric big sagebrush and blubunch wheatgrass 5% - Schiller soils on concave toeslopes and drainage ways under xeric big sagebrush, Anterlope bitterbrush and bluebunch wheatgrass	

Soil Map Unit: 511 – Olaton-Roney-Schiller Complex

Setting	
Landform:	Hill backslopes and canyon walls
Elevation:	4,200 to 5,700 feet
Average annual precipitation:	20 inches
Average annual air temperature:	46° F
Average frost free period:	100 days
Major use:	Rangeland
Composition	
Olaton and similar soils:	45%
Roney and similar soils:	25%
Schiller and similar soils:	20%
Contrasting inclusion:	15%

Major Components	
Olaton fine gravelly sandy loam, moist	
Slopes:	35 to 90%
Position on landform:	Concave backslopes and walls
Vegetal climax association:	Cherry and Idaho fescue
Typical profile:	0 to 24 inches – very dark gray and very dark grayish brown fine gravelly sandy loam 24 to 58 inches dark grayish brown fine gravelly sandy loam 58 to 60 inches – brown very gravelly sandy loam
Drainage class:	Somewhat excessively drained
Surface runoff:	Rapid
Permeability:	Moderately rapid
Available water capacity:	Low
Shrink-swell potential:	Low
Depth class:	Very deep
Roney fine gravelly coarse sandy loam,moist	
Slopes:	35 to 90%
Position on landform:	Slightly convex backslopes and walls
Vegetal climax association:	Xeric big sagebrush, bluebunch wheatgrass, and Idaho fescue
Typical profile:	0 to 17 inches – dark grayish brown fine gravelly coarse sandy loam 17 to 38 inches – brown fine gravelly sandy loam 38 inches – bedrock
Drainage class:	Somewhat excessively drained
Surface runoff:	Very rapid
Permeability:	Moderately rapid
Available water capacity:	Very low
Shrink-swell potential:	Low
Depth class:	Moderately Deep
Schiller gravelly coarse sandy loam, moist	
Slopes:	35 to 90%
Position on landform:	Concave backslopes and walls
Vegetal climax association:	Cherry and Idaho fescue

Schiller gravelly coarse sandy loam, moist continued	
Typical profile:	0 to 15 inches – very dark grayish brown gravelly coarse sandy loam 15 to 33 inches – very dark grayish brown very gravelly coarse sandy loam 33 to 60 inches – dark grayish brown extermely cobbly coarse sandy loam
Drainage class:	Somewhat excessively drained
Surface runoff:	Rapid
Permeability:	Moderately rapid
Available water capacity:	Low
Shrink-swell potential:	Low
Depth class:	Very Deep
Contrasting Inclusions	
10% - Whisk soils on summits and shoulders under xeric bid sagebrush, Antelope bitterbrush and bluebunch wheatgrass 5% - Rock outcrop	

Soil Map Unit: 525 – Robbscreek-Dobson-Brownlee Complex

Setting	
Landform:	Hill backslopes and shoulders
Elevation:	3,300 to 4,900 feet
Average annual precipitation:	16 inches
Average annual air temperature:	48° F
Average frost free period:	125 days
Major use:	Rangeland
Composition	
Robbscreek and similar soils:	35%
Dobson and similar soils:	30%
Brownlee and similar soils:	20%
Contrasting inclusion:	15%
Major Components	
Robbscreek fine gravelly coarse sandy loam	
Slopes:	25 to 65%
Position on landform:	Convex backslopes
Vegetal climax association:	Xeric big sagebrush, Antelope bitterbrush and bluebunch wheatgrass

Robbscreek fine gravelly coarse sandy loam continued	
Typical profile:	0 to 13 inches – grayish brown and brown fine gravelly coarse sandy loam 13 to 19 inches – yellowish brown gravelly sandy clay loam 19 to 30 inches – yellowish brown and light yellowish brown fine gravelly sandy clay 30 inches – bedrock
Drainage class:	Well drained
Surface runoff:	Very rapid
Permeability:	Moderately slow
Available water capacity:	Low
Shrink-swell potential:	Moderate
Depth class:	deep
Roney fine gravelly coarse sandy loam,moist	
Slopes:	35 to 90%
Position on landform:	Slightly convex backslopes and walls
Vegetal climax association:	Xeric big sagebrush, bluebunch wheatgrass, and Idaho fescue
Typical profile:	0 to 17 inches – dark grayish brown fine gravelly coarse sandy loam 17 to 38 inches – brown fine gravelly sandy loam 38 inches – bedrock
Drainage class:	Somewhat excessively drained
Surface runoff:	Very rapid
Permeability:	Moderately rapid
Available water capacity:	Very low
Shrink-swell potential:	Low
Depth class:	Moderately Deep
Schiller gravelly coarse sandy loam, moist	
Slopes:	35 to 90%
Position on landform:	Concave backslopes and walls
Vegetal climax association:	Cherry and Idaho fescue
Typical profile:	0 to 15 inches – very dark grayish brown gravelly coarse sandy loam 15 to 33 inches – very dark grayish brown very gravelly coarse sandy loam 33 to 60 inches – dark grayish brown extermely cobbly coarse sandy loam
Drainage class:	Somewhat excessively drained
Surface runoff:	Rapid
Permeability:	Moderately rapid
Available water capacity:	Low

Schiller gravelly coarse sandy loam, moist continued	
Shrink-swell potential:	Low
Depth class:	Very Deep
Contrasting Inclusions	
10% - Whisk soils on summits and shoulders under xeric bid sagebrush, Antelope bitterbrush and bluebunch wheatgrass 5% - Rock outcrop	

APPENDIX B

Dry Creek Water Chemistry Data Set

APPENDIX C

Snowmelt 1 Principal Component Analysis

APPENDIX D

Snowmelt 2 Principal Component Analysis